NASA TM X-62,265 I

NASA TECHNICAL
MEMORANDUM

NASA TM X-62,265

A SIMULATOR INVESTIGATION OF THE INFLUENCE OF ENGINE RESPONSE CHARACTERISTICS ON THE APPROACH AND LANDING FOR AN EXTERNALLY BLOWN FLAP AIRCRAFT

Part 1: Description of the Simulation and Discussion of Results

James A. Franklin and Robert W. Koenig

Ames Research Center
Moffett Field, Calif. 94035
and
Lewis Research Center
Cleveland, Ohio 44135

May 1973

A SIMULATOR INVESTIGATION OF THE INFLUENCE OF ENGINE RESPONSE CHARACTERISTICS ON THE APPROACH AND LANDING FOR AN EXTERNALLY BLOWN FLAP AIRCRAFT

Part 1: Description of the Simulation and Discussion of Results

James A. Franklin
Ames Research Center

and

Robert W. Koenig
Lewis Research Center

SUMMARY

Investigation of the influence of engine response characteristics on approach and landing operations of a powered lift aircraft were carried out in a piloted ground-based simulation at the Ames Research Center. The aircraft simulated was a four engine, externally-blown jet-flap configuration having an 80 pound wing loading and .56 thrust to weight ratio. Normal four-engine approaches and landings as well as wave-offs and landings following a single outboard engine failure were evaluated. Three engine models were investigated, ranging from a rapid responding variable pitch fan or variable inlet guide vane configuration to a more slowly responding fixed geometry configuration. Results indicate that for ideal operating conditions and minimal pilot reaction delay, substantial reductions in engine-out wave-off altitude increment and touchdown sink rate for engine-out landings can be achieved with the fast engine compared to the slow engine response. However, delays in pilot reaction of one to two seconds diminish the advantage of rapid thrust response. A need exists for some form of automatic cueing of the pilot or automatic engine control to enable the potential of rapid thrust response to be realized in improving safety in the event of an engine failure.

NOTATION

ALPHA, (α)	angle of attack, degrees
b	wing span, feet
$\bar{c}$	mean aerodynamic chord, feet
C_D	drag coefficient, D/qS
$C_{D_{GE}}$	drag coefficient in ground effect
$C_{D_{\delta_{SP}}}$	rate of change of drag coefficient with spoiler deflection, per degree
CDDE, ($C_{D_{\delta_H}}$)	rate of change of drag coefficient with stabilizer deflection, per degree
CDD7, ($C_{D_{\Delta f_3}}$)	rate of change of drag coefficient with deflection of aft element of inboard segment of trailing edge flaps, per degree
C_j	engine gross thrust coefficient, T/qS
C_L	lift coefficient, L/qS
$C_{L_{GE}}$	lift coefficient in ground effect
$C_{L_{MAX_{3E}}}$	engine out maximum lift coefficient
$C_{L_{\delta_{SP}}}$	rate of change of lift coefficient with spoiler deflection, per degree
CLB, (C_{l_β})	rate of change of rolling moment coefficient with side slip angle, per degree
CLDR, ($C_{l_{\delta_r}}$)	rate of change of rolling moment coefficient with rudder deflection, per degree
CLD3, ($C_{l_{\Delta\delta f_3}}$)	rate of change of rolling moment coefficient with differential deflection of aft element of outboard segment of trailing edge flaps, per degree

CLD4, $(\Delta C_{l_{EO}})$	increment of rolling moment coefficient due to outboard engine inoperative
CLIFT	see C_L
CLIFTDE, $(C_{L_{\delta_H}})$	rate of change of lift coefficient with stabilizer deflection, per degree
CLIFTD7, $(C_{L_{\Delta f_3}})$	rate of change of lift coefficient with deflection of aft element of inboard segment of trailing edge flaps, per degree
CLP, (C_{l_p})	damping in roll, per radian
CLR, (C_{l_R})	rolling moment due to yaw, per radian
C_l	rolling moment coefficient, M_R/qSb
$C_{l_{\dot{\beta}}}$	$\partial C_{l_\beta}/\partial\dot{\beta}$, per radian
$C_{l_{\delta_A}}$	rate of change of rolling moment coefficient with aileron deflection, per degree
$C_{l_{\delta_{SP}}}$	rate of change of rolling moment coefficient with spoiler deflection, per degree
$C_{m_{GE}}$	pitching moment coefficient in ground effect
CM, (C_m)	pitching moment coefficient, $M/qS\bar{c}$
CMDE, $(C_{m_{\delta_H}})$	rate of change of pitching moment coefficient with stabilizer deflection, per degree
CMD7, $(C_{m_{\Delta f_3}})$	rate of change of pitching moment coefficient with deflection of aft element of inboard segment of trailing edge flaps, per degree
CMQ, (C_{m_Q})	damping in pitch, per radian
C_n	yawing moment coefficient M_Y/qSb
$C_{n_{\dot{\beta}}}$	$\partial C_n/\partial\dot{\beta}$, per radian

$C_{n_{\delta_A}}$	rate of change of yawing moment coefficient with aileron deflection, per degree
$C_{n_{\delta_{SP}}}$	rate of change of yawing moment coefficient with spoiler deflection, per degree
C_{N_Q}	rate of change of normal force with pitch, per radian
CNB, (C_{n_β})	rate of change of yawing moment coefficient with side slip angle, per degree
CNDR, $(C_{n_{\delta_r}})$	rate of change of yawing moment coefficient with rudder deflection, per degree
CND3, $(C_{n_{\Delta\delta f_3}})$	rate of change of yawing moment coefficient with differential deflection of aft element of outboard segment of trailing edge flaps, per degree
CND4, $(\Delta C_{n_{EO}})$	increment of yawing moment coefficient due to outboard engine inoperative
CNP, (C_{n_p})	yawing moment due to roll, per radian
CNR, (C_{n_R})	damping in yaw, per radian
C_Y	side force coefficient, F_Y/qS
C_{Y_P}	side force due to roll, per radian
C_{Y_R}	side force due to yaw, per radian
$C_{Y_{\dot\beta}}$	$\partial C_Y/\partial\dot\beta$, per radian
$C_{Y_{\delta_{SP}}}$	rate of change of side force coefficient with spoiler deflection, per degree
CYB, (C_{Y_β})	rate of change of side force coefficient with side slip angle, per degree
CYDR, $(C_{Y_{\delta_r}})$	rate of change of side force coefficient with rudder deflection, per degree

CYD3, $(C_{Y_{\Delta\delta f_3}})$	rate of change of side force coefficient with differential deflection of aft element of outboard segment of trailing edge flaps, per degree
D	drag force, pounds
EBF	externally blown flap
F_Y	side force, pounds
GAMMA	flight path angle, degrees
$G_{C_{l_\beta}}$	gain for C_{l_β}
h	height of wing quarter chord above ground, feet
h_{fail}	altitude at instant of engine failure, feet
h_{min}	minimum altitude during wave-off, feet
δ_H	horizontal-tail incidence angle, degrees
KEAS	equivalent air speed, knots
K_1	engine model scaling parameter
L	lift force, pounds
M	pitching moment, foot-pounds
M_R	rolling moment, foot-pounds
M_Y	yawing moment, foot-pounds
P_b, p_B	roll rate, radians/second, degrees/second
q	free-stream dynamic pressure, pounds/feet^2
Q_b, q_B	pitch rate, radians/second, degrees/second
R_b, r_B	yaw rate, radians/second, degrees/second
S, (S_w)	wing area, feet^2
S_H	horizontal-tail area, feet^2
s	Laplace operator

T (T_1, T_2, T_3, T_4)	thrust, pounds (for engines 1,2,3,4)
T_c	commanded thrust, pounds
$\dot{T}_1$,$\dot{T}_2$	rates of change of thrust for second order engine model components, pounds/second
t	time, seconds
$t_{95\%}$	time for engine to accelerate to 95 percent thrust, second
V	airspeed, knots
$V_{Reference}$	reference airspeed, knots
V_T	true airspeed, feet/second
V_{wo}	airspeed at wave-off ($\dot{h} = 0$), knots
W	gross weight, pounds
Z_α	vertical velocity damping, feet per second^2 per radian
β	side slip angle, degrees
$\dot{\beta}$	$\partial\beta/\partial t$, radians/sec
δ_A	aileron deflection ($\delta_{A_L} - \delta_{A_R}$), degrees
δ_c	column position, inches
δ_e	elevator deflection, trailing edge down is positive, degrees
δf_1	deflection of forward element of trailing edge flap, degrees
δf_2	deflection of middle element of trailing edge flap, degrees
δf_3, (δ_F)	deflection of aft element of trailing edge flap, degrees
δ_p	rudder pedal position, inches

δ_r	rudder deflection, trailing edge left is positive, degrees
δ_{SP}	spoiler deflection, trailing edge up is positive, degrees
δ_T	throttle position, percent
δ_w	wheel position, degrees
$\Delta C_{D_{GE}}$	increment in drag coefficient due to ground effect
$\Delta C_{m_{GE}}$	increment in pitching moment coefficient due to ground effect
Δf_3	deflection of inboard aft element of trailing edge flap, degrees
$\Delta \delta_{f_3}$	deflection of outboard aft element of trailing edge flap, degrees
Δt_T	time delay from instant of engine failure to throttle advance, seconds
Δt_f	time delay from instant of throttle advance to autospeed disengage, seconds
θ	pitch attitude, degrees
ϕ	bank angle,degrees
τ	engine deceleration time constant, seconds
ζ_1, w_1	damping ratio and natural frequency of washed-out second order engine acceleration model component
ζ_2, w_2	damping ratio and natural frequency of second order engine acceleration model component

INTRODUCTION

Short-haul aircraft which use propulsive lift for short takeoffs and landings, depend on engine thrust to provide lift at low airspeeds. As a consequence of this reliance on engine thrust, control of the aircraft becomes critical particularly in the event of an engine failure during the landing approach. In particular, the vertical departure from the flight path must be corrected by restoring the aircraft lift as quickly as possible. This can be done either by increasing engine thrust or aircraft flight speed or both. Speed increases are undesirable because of the marginal altitude available for gaining speed in the latter stages of the approach and the inability to quickly change speed to make the flight path recovery. Therefore, engine thrust must be increased as rapidly as possible to restore the aircraft to a safe operating condition for continuing the approach or for conducting a wave-off.

Rapid thrust variations are restricted by engine mechanical and aeronautical designs and physical limits. A typical mechanical design limit is a turbine inlet temperature overshoot limit which results from a large fuel surge as the throttle is advanced very rapidly while the engine is at reduced thrust. Exceeding this limit can severly shorten turbine lift expectancy. Compressor surge is an aeronautical limit while large inertia changes of the rotating machinery (fan, compressor and turbines) impose a physical limit when very fast thrust increases are attempted. Conventional turbofan engine thrust response rate is primarily limited by rotating machinery inertia changes. Most inertia limitations can be reduced by operating the rotating machinery at or near design rotational speeds over a range of thrust levels. Recent engine studies by Detroit Diesel Allison, Division of General Motors and The General Electric Company (contracts NAS3-16727 and NAS3-16726) and STOL short-haul aircraft system studies by Mc Donnell-Douglas and Lockheed (NAS2-6994 and NAS2-6995) have shown that an engine with variable pitch fan blades has economic and other advantages

for short-haul transportation. Reference 1 points out that a variable-pitch fan engine can nearly eliminate the large inertial effects that compromise engine thrust response. This is done by running the fan at high rpm with low blade pitch (and corresponding low thrust), and then increasing blade pitch to initiate thrust response. Large changes in engine thrust can thus be achieved very rapidly.

To evaluate the influence of engine thrust response on operation of a powered lift aircraft, a piloted simulation of such a vehicle was conducted. The operating procedures investigated were the following:

- Normal landing approaches (6 degree glide paths) using either aircraft rotation or engine power for flare
- Wave-offs with and without an outboard engine failure
- Engine out landings

Representative engines were selected for simulation from the recent NASA engine study contracts. Figure 1 shows some response rates as a function of maximum thrust. Only response rates from 50 percent to maximum thrust are shown as an example. Other initial starting values of percent thrust with corresponding differences in response time were used in the simulation. Engine (1) response is thought to be achievable with a variable pitch fan or an engine with variable inlet guide vanes. Engine (2) represents a NASA preliminary design requirement based on Reference 2. Engine (2) could also be representative of a variable pitch fan with a slightly slower response rate due to lower temperature overshoot limits than Engine (1). Engine (3) response is typical for a fixed pitch fan. All these engine response rates (1, 2, and 3) are representative of what preliminary studies have shown to be achievable.

EXPERIMENTAL PROGRAM

Evaluation Task and Procedure

Pilot evaluations of the effects of engine response characteristics on aircraft handling began with familiarization with the aircraft under normal operating conditions, then progressed to engine-out situations. The sequence of the evaluations consisted of

- normal (all engines operating) approaches and landings to acquaint the pilots with the aircraft and to explore different flare techniques,
- four engine wave-off maneuvers to explore operational techniques and to establish a baseline wave-off altitude increment
- engine-out wave-offs to establish the altitude increment for wave-off for each of the subject engine response characteristics,
- engine-out landings after engine failures at various altitudes to determine the pilot's ability to safely land the aircraft for each of the engine response characteristics, and
- normal approaches and landings for evaluation of artificial augmentation of Z_{α} as a means of improving flight path and flare control.

Landing Approach and Flare

The pilots assumed control of the aircraft with it trimmed and configured for descent on the glideslope and aligned with the localizer. The approach was made at 75 knots on a 6 degree glideslope. The runway was 1500 feet long with touchdown zone markings as indicated in Figure 2. All approaches were made under VFR conditions. No turbulence or wind shear conditions were evaluated nor were recoveries from offsets from the localizer purposely included in the program. The intent was to

achieve a relative comparison of the aircraft's engine out performance for the various engine response characteristics with as few additional confusing factors as possible. It was felt that the increase in difficulty of the task imposed by turbulence, shears, or alignment maneuvering might obscure the contributions of engine response which were sought in these experiments.

Two flare techniques were utilized in the landing evaluations. For one technique, the aircraft was trimmed at a slight nose down attitude for the approach, and the pilot performed the flare by rotating the aircraft to touchdown attitude and advancing the throttles if necessary to further reduce the sink rate to an acceptable level. In the alternate technique, the aircraft was trimmed to a slight nose up attitude on the approach, flown down the glideslope at constant attitude, and flared by advancing the throttles to check the sink rate. The latter technique was the most demanding of engine response during the flare and provided the best indication of the influence of engine response on normal landings.

Waveoff

Following familiarization runs, engine-out wave-offs were conducted for an engine failure at 200 feet altitude. The preferred technique for performing the wave-off required the pilot to (1) identify the engine failure through whatever cues were available to him, (2) immediately advance throttles for maximum thrust and simultaneously disengage the autospeed control, and (3) allow the aircraft to accelerate to 80 but not beyond 85 knots for the recovery. Disengagement of the autospeed system (described subsequently) was accomplished through a button on the left hand throttle which also automatically reconfigured the flaps for wave-off. With the autospeed system off the aircraft could quickly accelerate to the desired wave-off speed. The pilot was then required to briskly raise the aircraft's nose to hold the speed in the 80-85 knot region. Wave-offs were continued until a rate of climb of 200 to 500 ft/min was established and then the run was terminated.

Engine-Out Landings

Once the minimum wave-off altitude was established for each engine response characteristic, engine-out landings were conducted for engine failures below the minimum wave-off altitude. Engine failures at altitudes of approximately 100, 75, 50, and 35 feet were performed. The pilot again was required to identify the failure, to advance throttles for power required to continue the approach and if possible to land the aircraft within the landing zone at an acceptable sink rate. The autospeed system was left on and the aircraft was not reconfigured.

Abused Approaches

A few approaches were made at higher than nominal sink rates and lower power settings in an attempt to determine the effect of this specific abuse on engine-out wave-off capability. Rates of descent were in the 1000-1200 ft/min range, corresponding to flight paths of 7.5 to 9.0 degrees. Power settings were reduced to less than 50 percent of maximum for these conditions.

Description of the Simulation

Aircraft

The airplane simulated in this study was a high-wing four-engine STOL transport, with high-bypass-ratio turbofan engines and externally-blown jet-flaps. A three view schematic of the airplane is presented in Figure 3. Its general configuration and aerodynamic characteristics were based on an externally blown flap aircraft which had previously undergone extensive development and simulator evaluation at the Langley Research Center (Reference 4) and Flight Research Center (Reference 5). The wing loading was 80 pounds per square foot and the maximum thrust to weight ratio for the approach condition was .56. A more detailed description of the aerodynamic configuration is given in Reference 3.

The wing incorporated a blown leading-edge flap and triple-slotted trailing-edge flaps. Figure 4 illustrates the engine-flap system arrangement. Flaps were deflected 60 degrees in the landing

configuration. Drooped ailerons and spoilers with maximum deflections of 60° were used for roll control. Deflections of the inboard trailing edge aft flap elements (Δf_3) provided direct drag control for speed stabilization. The horizontal stabilizer was used for longitudinal control and incorporated a leading edge Kruger flap and a geared elevator. Stabilizer authority was $\pm$10 degrees. Elevator gearing provided elevator deflections of +10 to -50 degrees corresponding to + and -10 degrees of stabilizer deflection. The vertical stabilizer employed a 0.57 chord double-hinged rudder for directional control. Maximum rudder deflection was $\pm$45 degrees.

The mass and dimensional characteristics of the airplane are presented in Table I. Aerodynamic data and characteristics are presented in Part 2 of this report. The basic data source was Reference 3 with the following exceptions:

dynamic stability derivatives - Reference 6

longitudinal and lateral-directional spoiler data - Reference 7

lateral-directional aileron data - Reference 8

longitudinal ground effect data - Unpublished Langley data

Block diagrams of the aerodynamic simulation are shown in Figures 5 through 10. An indication of the aircraft's performance is provided in Figure 11 for the approach flap setting of 60 degrees. Static thrust to weight ratio at 100 percent thrust is .69 which reduced to .56 at the approach speed due to thrust lapse characteristics (thrust variation with airspeed) of the high bypass ratio engines. It may be seen from the figure that four-engine operation in the approach configuration offers adequate climb and descent capability at the nominal approach speed of 75 knots. Margins of 16.7 degrees angle of attack and 1.26 V_S from the stall are available at the approach power setting of 61 percent. Operation is on the back side of the drag curve corresponding to $d\gamma/dV$= .18 deg/knot. Loss of one engine seriously degrades the aircraft's performance. As is shown in Figure 12, a positive rate of climb cannot be established at the nominal approach speed of 75 knots even with the flaps configured for wave off. Adequate climb becomes available above

80 knots and is the basis for the speed range of 80 to 85 knots selected for engine-out waveoffs.

Control System

The longitudinal flight control and command augmentation system is shown in Figure 13. Pitch attitude control was accomplished using an attitude command augmentation system which provided an incremental attitude change in proportion to column position and suppression of pitch disturbances through the attitude stabilization function. The control law and gains are shown in Figure 13. Airspeed command and stabilization were provided by the autospeed control system shown in Figure 13. This system functioned by driving the inboard aft flap segment (Δf_3) in proportion to speed error. The commanded airspeed was selected by the pilot by positioning the reference indicator on his airspeed instrument. Disengagement of the autospeed system was accomplished by depressing the autospeed disengage button located on the left hand throttle. Autospeed disengage automatically commanded the inboard aft segment flap to retract to the wave-off setting of 35 degrees. The flap drive rate was 20 deg/sec. Sample time histories of the aircraft's response to a step column input with the augmentation system off and on are shown in Figure 14.

The lateral-directional command augmentation system is shown in Figure 15. Roll control was accomplished using the ailerons and spoilers. A roll rate command/bank angle hold system was utilized whereby wheel position commanded roll rate and a centered wheel allowed the system to stabilize bank angle at the desired value. Improved roll control precision, and suppression of both the spiral divergence and response to external disturbances were thereby provided. The aileron-spoiler schedule produced only aileron deflection for the first 30 degrees of wheel travel (commanded by the pilot or augmentation system). From 30 degrees to full wheel, maximum aileron deflection and spoiler deflection in a 2:1 ratio to wheel deflection are commanded. Dutch roll damping and turn coordination were provided using the double hinged rudder. As shown in Figure 15 damping was achieved through a pseudo sideslip rate

control law and turn coordination was provided by commanding rudder deflection in proportion to roll rate and wheel position. Sample time histories of the aircraft's response to wheel and pedal doublet inputs with the augmentation system off and on are shown in Figures 16a and b respectively.

Engine Model

The range of engine acceleration-deceleration characteristics to be evaluated were shown previously in Figure 1. Simulation was accomplished with a dynamic model which is conceptually represented in the block diagram of Figure 17. The computer was required to sense whether the throttle had commanded a thrust increase or decrease. Thrust increases were computed by the two upper blocks and were composed of the sum of a rate limited second order response and a washed out, rate limited second order response. The second order block provides the basic acceleration characteristic, rate limited as required to match the characteristics of Figure 1. The washed out second order block provided the rapidly peaking, overshooting response typical of the variable pitch fan or variable inlet geometry engine. Otherwise, this element of the engine simulation was not required to match the response characteristics of the other engine models. Thrust decreases were computed by the lower block and were represented by a first order lag.

Figure 18 illustrates the response characteristics of the three engine models evaluated in the simulation. Acceleration curves for step thrust commands of 20, 35, and 50 percent are shown. The character of these curves was not made dependent on the value of the initial thrust setting. The same deceleration curve was used for each of the engine models. Throttle commands for a thrust decrease and thrust decay at engine failure both followed this deceleration curve. A listing of the parameters used in each engine model is provided in Table II.

Simulator

The simulation facility utilized was the Ames Research Center Moving Cab Transport Simulator with a high resolution visual display. The simulator provided motion in the pitch, roll and heave axes. Motion response was commanded in each axes through a fourth order washout filter described by the relationship

$$X_{response} = \left(\frac{K\, s^4}{(s^2+2\zeta\omega s + \omega^2)^2} \right) X_{command}$$

where for the respective cases the gain, damping ratio and natural frequency were

	K	ζ	ω	
pitch	.25	1.0	.17	rad/sec
roll	.25	1.0	.33	rad/sec
heave	.25	2.0	.7	rad/sec

Displacement, velocity, and acceleration limitations for each axis were

	displacement	velcoity	acceleration
pitch	+14 deg -6 deg	.22 rad/sec	4.7 rad/sec^2
roll	$\pm$9 deg	.22 rad/sec	4.7 rad/sec^2
heave	$\pm$12 inches	------	32.2 ft/sec^2

A full flight instrument panel was available to the pilot, including an ADI, a sensitive airspeed indicator, barometric and radio altitude, instantaneous vertical speed, angles of attack and sideslip, compass heading, glideslope and localizer error. Percent of maximum thrust was presented as the reference for engine power setting. A conventional control column and wheel arrangement was used, with a pitch trim toggle switch located on the left hand grip. Control force characteristics are listed in Table III. Four conventional throttles were arrayed on a floor mounted center pedestal. A linear gearing was provided for thrust command as a function of throttle position. The flap lever was mounted to the right of the throttles on the pedestal and a separate lever to the left of the throttles gave the pilot independent

control of the third flap segment if he so desired. Engage switches and indicator lights were provided for the pitch, roll, yaw, and autospeed command augmentation functions.

Data Acquisition

Three Ames experimental test pilots and two contractor pilots participated in the program. Time histories of the aircraft's response and the pilot's control activity were recorded. Touchdown status information was recorded for

pitch attitude	touchdown position	column position
angle of attack	sink rate	throttle position
airspeed		engine thrust

These data were used to determine the altitude required to perform a wave-off following an engine failure as well as touchdown sink rate and landing dispersion for normal and three engine landings. Nominal sink rate prior to engine failure, wave-off airspeed, and time delays related to pilot reaction to the engine failure were extracted from the data and used to assess the effect of abuses of the approach, wave-off and landing on engine out wave-off and landing performance.

RESULTS AND DISCUSSION

In the discussion which follows, the effect of variations in engine response characteristics on (1) landing precision for normal operation, (2) the altitude loss experienced during a wave-off following an engine failure, (3) the sink rate at touchdown following an engine failure at low altitude, and (4) augmentation of vertical velocity damping are presented. These contributions are shown for ideal operating conditions and pilot reaction to the engine failure. An indication is also provided of the penalties on engine-out wave-off and landing performance resulting from delays in recognition and action on the engine failure and from abuses of the established wave-off or landing procedure.

Normal Landing Performance

A brief investigation of the influence of engine response on flight path control for the approach and landing flare was made during the simulator program. For the landing approach, the pilots indicated that precise flight path control could be achieved with either the fast or slow engine response. Examples of large flight path corrections following step thrust commands are shown in Figure 19. Attitude was held essentially constant during the maneuver. The differences in flight path response were not sufficient to alter the pilots' impressions of their ability to make glideslope corrections down to altitudes of 200 to 300 feet.

Evaluation of the use of thrust to control the landing flare proved to be difficult for the pilots. One factor contributing to this difficulty was the flare technique. Normally, the approach was made in a 3.5 degree nose down attitude and the flare was conducted by rotating the aircraft to a nose up attitude of approximately 5 to 6 degrees. An example of such a flare maneuver is shown in the time history of Figure 20. The attitude change served to check the sink rate reasonably well and to afford some control during the flare itself. As a consequence, thrust was used sparingly and in an open loop manner if it was used at all. Data on landing precision for this flare technique are presented in Figure 21 and represent reasonable performance.

To provide more demands for use of thrust during the flare, the aircraft was trimmed at a 2 to 3 degree nose high attitude on the approach and was flared at essentially constant attitude with thrust alone. Under these circumstances, the pilots commented that the flare was quite difficult to perform with the slow responding engine. While they conceded that some improvement in landing precision might be possible with the fast engine, they found it difficult to assess the degree of this improvement. The pilots noted that precise control of sink rate during the flare was difficult due to their inability to detect small changes in sink rate and to quickly assess the effect of their corrections. Contributing factors were the limited vertical

acceleration cues from the motion drive system and the difficulty in deriving vertical velocity cues from the visual display. The low level of vertical velocity damping inherent in the basic airframe $\left(\frac{Z_\alpha}{V_o} = -.4/\text{sec}\right)$ also inhibited precise control of sink rate.

Engine-Out Wave-Off

Data from a series of engine-out wave-off maneuvers are presented in Figure 23. These data were obtained under conditions of ideal operation in that no turbulence, winds, or shears were present. A straight-in approach was made to the STOL runway under VFR conditions and the wave-off was executed immediately upon recognizing the engine failure. Furthermore, the pilots' wave-off techniques in these particular instances were among the best observed during the simulation program as regards reaction time, aircraft reconfiguration, and establishment of the wave-off speed. Typical values for reaction time are indicated in the figure. These data were selected from the total data set so as to isolate the contributions of the engine response characteristics from other factors which might influence wave-off performance. The figure shows the loss in altitude from the point of engine failure to the minimum altitude reached during the wave-off as a function of the nominal approach sink rate for each of the three engine response characteristics. Most of the data were collected for the nominal approach condition ($\gamma \triangleq -6$ deg); however, data from a few higher sink rate conditions are shown to illustrate the effect of approach angle (e.g. engine failure encountered in the process of a correction from an offset above the glideslope) on the altitude loss increment. At the nominal approach condition the altitude lost during wave-off for the fastest engine was, on the average, 45 feet less than for the slowest engine. Relative comparisons of the influences of the various engines are more meaningful than absolute performance values for each engine since the particular aircraft model, thrust to weight ratio, wave-off technique, and fidelity of the simulation environment

all contributed to the wave-off characteristics associated with each particular engine. Specific contributions of such factors as pilot delay in recognizing and acting on the engine failure are considered subsequently. Representative time histories of the wave-off for the fast and slow engines are shown in Figures 24 and 25. Pilot reaction times for throttle advance and autospeed cutoff were on the order of 1.5 seconds. Waveoff airspeed was approximately 85 knots. These values represented typical pilot reaction and wave-off technique for the data of Figure 23.

Variations in the nominal approach sink rate can be seen in Figure 23 to have a strong influence on the altitude lost during waveoff. Increasing the approach path angle by 1.5 to 2 degrees appears to increase the altitude loss increment for the fast engine to values representative of the slow engine at the nominal approach condition.

A reasonable correlation of the wave-off performance for the various engines and approach conditions was obtained by relating altitude loss to maximum sink rate encountered during the wave-off. This correlation is illustrated in Figure 26. Notwithstanding the data scatter, a reasonable straight line relationship between the altitude loss increment and maximum sink rate is apparent. Scatter is on the order of $\pm$14 feet. As is noted in the inset diagram, the increase in rate of sink from the nominal approach condition was on the order of 200 to 250 ft/min for the fast engine while for the slower engine this increase was approximately 500 ft/min. Corresponding altitude increments to the point of maximum rate of sink were 40 and 70 feet respectively. As can be noted from Figures 24 and 25, by the time the aircraft reached its maximum sink rate full thrust had nearly been reached on the remaining engines. Beyond that point the recovery from the engine failure was independent of engine response and was primarily dependent on the sink rate at that point.

As a means of correlating wave-off performance with engine response, the time required for the engine to reach 95 percent of maximum thrust from its approach thrust setting was plotted against altitude loss.

Figure 27 illustrates these results. Nominal differences between engines appear to be

25 feet	comparing engines 1 and 2
45 feet	comparing engines 1 and 3

with scatter on the order of $\pm$12 to 20 feet over the range of data shown. The range of time response characteristics shown can be expected to include penalties imposed for bleed requirements and power extraction for accessory drives. The best wave off capability shown for the fast engine response was an altitude increment of 75 feet. In comparison, an altitude loss of 25 to 30 feet was experienced for a normal four engine maximum performance wave-off. This comparison provides a feeling for the minimum penalty of an engine failure on wave-off performance for this particular aircraft. Even if engine response was instantaneous the minimum time required for pilot recognition of the engine failure would dictate an additional altitude loss of 40 to 50 feet to wave-off.

In summary, under ideal operating conditions and for quick pilot response to an engine failure, the altitude loss for an engine-out wave-off in excess of that required to perform a normal wave-off with all engines operating is approximately 60 feet for the fast engine and 105 feet for the slow engine. Hence, the fast engine offers a 43 percent reduction over the slow engine in altitude required to wave-off, and thus provides a substantial improvement for engine-out operation. However, degradation in operating conditions and pilot performance impose significant penalties on wave-off performance as will be noted in the subsequent discussion.

Delay in pilot recognition and reaction to the engine failure increased the altitude required for wave-off. Figure 28 illustrates the effect of a delay in throttle advance for nominal wave-off airspeeds of 80-85 knots and for essentially no delay in autospeed system disengage (Δt_f < .3 sec). The quickest reaction times under ideal conditions were in the order of 1.2 to 1.5 seconds. The most readily detectable cue of engine failure to which the pilot could respond was

the bank angle excursion induced by the roll asymmetry when the engine failed. Normal acceleration cues from the simulator motion were not of sufficient magnitude to be felt by the pilot. The increase in vertical velocity did not become visually apparent to the pilot until a sizeable sink rate had already built up. Engine instruments were located on the center instrument panel and were not included in the pilot's continuous scan pattern. An example of the aircraft's lateral-directional response to an engine failure with the lateral-directional SAS on is shown in Figure 29. The combined effects of SAS and the pilots recovery action limited the maximum bank angle excursion to approximately 5 degrees. It is quite possible that turbulence or normal pilot maneuvering could obscure this cue and increase the delay in pilot corrective action for engine-out recovery. It is apparent from Figure 28 that delays on the order of two seconds in advancing throttles increased the altitude loss for the fast engine to values representative of the slower engines under ideal reaction conditions. Thus, pilot reaction delays diminish the significance of the reduction in altitude increment afforded by the fast engine over its slowest counterpart.

The effect of delay in autospeed disengagement over and above the delay for throttle advance is shown in Figure 30. Throttle reaction delays were less than 1.7 seconds and wave-off airspeeds were 80 to 85 knots. Autospeed disengage is indicated by the point at which the third flap segment begins to retract. Effects of delay in the autospeed disengage were somewhat less than those associated with throttle advance. A one second delay increased the altitude increment on the order of 15 to 20 feet.

Abuse of speed control for the wave-off had some influence on wave-off performance. A limited amount of data is presented in Figure 31 for speeds over the range 80 to 88 knots which indicate an increase in altitude increment at the higher wave-off airspeeds. Note on the figure that wave-off airspeed is defined as the airspeed at which zero rate-of-climb is reached. Data which were uncontaminated by other effects such as recognition delays were not sufficient to define these

curves adequately for each of those engines. However, the penalty in altitude loss for wave-off airspeeds in excess of 80 knots appears to be about 3 to 4 feet per knot. It should be noted that the wave-off airspeed for minimum altitude loss is somewhat lower than the speed for maximum climb angle indicated in Figure 12.

Engine-Out Landing

Evaluations of continued approach and landings were conducted for engine failures occuring at approximately 100, 75, 50 and 35 feet. Touchdown sink rates for selected landings for each of these engine failure altitudes are presented in Figure 32. These data were obtained under ideal operating conditions and pilot performance. Nominal approach sink rates prior to engine failure were 800 ft/min. All touchdowns shown were between the runway threshold and the far end of the touchdown zone. The cross-hatched band, which reflects the range of results obtained for landings with all engines operating, serves as a baseline from which to evaluate the engine out data. For engine failures at 100 feet, no differences in landing performance appear for the fast and slow engine response. For engine failures below 100 feet, disparities in touchdown sink rate between the two engine models became pronounced. The limited data obtained for failures below 50 feet indicate similar performance for the fast and slow engines.

A clearer indication of the sensitivity of landing performance to engine response is provided in Figure 33. In this figure, sink rate data of Figure 32 are separated into four groups corresponding to the nominal altitudes for engine failure and are plotted against the time required for the engine to accelerate to 95 percent of maximum thrust. While the amount of data presented is insufficient to warrant a high degree of confidence in the quantitative results for each engine, the trends of the data give an indication of the sensitivity of landing precision to engine response. For engine failures at 100 feet or above, engine response appears to have little effect

on the pilot's ability to land the aircraft at sink rates comparable to normal four engine landings. For engine failures below 100 feet, the pilot's ability to arrest the sink rate became increasingly sensitive to engine response down to a critical failure altitude. Below this altitude, the effect of engine response diminished in significance. The critical altitude is likely to be of the order of the increment required for the pilot to recognize the failure and to begin to arrest the sink rate. For engine failures below this altitude, the pilot does not have time to recognize and act on the failure. At very low altitudes, the consequences of the failure itself have insufficient time to affect touchdown performance significantly.

Some typical time histories of engine failures at various altitudes for the fast and slow engines are presented in Figures 34 and 35. These time histories help to illustrate the pilot's technique for recovery from the failure and for performing the flare. They also give a perspective of the time required for engine response compared to the time encompasses by the landing.

Landing time histories for Engine 1 are shown in Figure 34 a through d for engine failures at 100, 75, 48, and 33 feet respectively. For the 100 and 75 foot cases, the pilot had adequate time to get the remaining engines up to a nominal desired level of thrust and even to modulate thrust for control during the flare. At the same time he advanced the throttles, the pilot also initiated a nose-up attitude change to assist in checking the sink rate. A final flare rotation occurred at approximately 40 feet. In both cases, it is apparent that the pilot had time for reasonable closed loop control during the flare. For engine failure at 50 feet, the pilot still had time to get thrust up to maximum (though barely) but he also executed an appreciably more rapid flare rotation beginning at about 50 feet. Although the outcome was a very low touchdown sink rate (1.6 ft/sec) the pilot's control of the flare had become essentially an open loop procedure consisting of large, rapid, step like inputs to the column and throttles. While excellent landing performance was obtained in this case, the pilots' commentary indicate that they had little confidence in repeatedly

achieving acceptable performance when an engine was lost at this altitude. Finally, for the example of an engine failure at 33 feet, the pilot did not recognize the failure in time to advance the throttles. The flare had already been initiated at approximately 50 feet and was performed solely by rotating the aircraft. A hard touchdown (7.8 ft/sec) was experienced since no thrust was increased on the good engines and thrust on the failed engine had decayed to nearly a third of its approach setting at touchdown.

Time histories for the slow engine are shown in Figure 35 a through c for failures at 100, 73, and 50 feet respectively. For these landings, in contrast to the landings with the fast engine, the pilot's only choice for thrust management was to advance the throttles to 100 percent. All control of the flare depended on rotation of the aircraft, whereas the fast engine provided some capability for flare control for engine failures at 100 and 75 feet as shown in Figure 34 a and b. For the case of engine failure at 100 feet, maximum thrust was achieved prior to touchdown and the pilot exercised some closed loop control over the flare. For engine failures at lower altitudes, control of the landing was strictly an open loop maneuver. Maximum thrust was not achieved for failures at 73 or 50 feet and despite large, rapid rotations hard touchdowns were experienced in both cases. The severity of the landing related to the level of thrust achieved prior to landing. For engine failures at either of these altitudes, the pilots had little confidence in being able to control the landing with acceptable precision.

An attempt is made in Figure 36 to summarize the engine-out landing data presented initially in Figure 32. Averages for data in each altitude grouping for the fast and slow engines are indicated by the solid points. The truncated bars show the range the data encompassed in each group. As has been commented previously, a high degree of confidence cannot be given to quantitative results such as averages obtained from such a small data sample. Although these data have been

faired through the average of each group, the absolute value of the fairing at each point should be viewed with some reservation. Two specific comments regarding the fairing of the fast engine data are in order. First, the fairing suggests that landings could be accomplished at lower sink rates under engine out conditions (for failures down to 50 feet) than for normal landings. This may or may not actually be the case. The engine failure caused the aircraft to sink below the glideslope somewhat before the sink rate could be checked. If the landing was continued from that point along a shallower path to the landing zone the touchdown sink rate would be expected to be lower than for a landing from the nominal glideslope. However, sufficient evidence does not exist from the data at hand to conclusively support this hypothesis. Second, the peak in the fairings was made on the strength of a single failure at 33 feet. While one data point would not ordinarily deserve such heavy weighting, it was supported by results obtained for the slow engine under nearly the same conditions. For all of these cases, the pilot did not recognize the failure in time to advance the throttles, thus the landings were all made through rotation of the aircraft.

The relative shapes of the curves for the fast and slow engines in Figure 36 provide the best interpretation of the data. The peaked areas of the two curves provide a comparison of the range of altitude for engine failure over which the aircraft was susceptible to hard landings while the peaks themselves indicate the relative touchdown sink rates. It appears that over an altitude band from approximately 40 to 80 feet, the slow engine made the aircraft substantially more susceptible to hard landings than did the fast engine.

The foregoing results are indicative of the potential landing performance attainable under ideal operating conditions and piloting technique. As was the case for engine out wave-off performance, engine out landings can be expected to be more severe in situations which the pilot does not immediately recognize the engine failure or which he misuses thrust in the recovery. In Figure 37, data from all of

the engine out landings made during the program are presented. Compared to the selected landing performance data summarized in the previous figure (and shown here as solid symbols), many more hard landings occurred for both the fast and slow engines (shown as open symbols), particularly for failures at 100 feet. These additional data tend to obscure differences in landing performance between the two engine response characteristics.

The cause of these hard landings can largely be attributed to delays for pilot recognition and to mismanagement of thrust on the remaining engines prior to and during the flare. The net result of either of these abuses of the landing was an insufficient level of thrust on the remaining engines prior to touchdown to check the sink rate. Thrust had to be increased from 4100 to approximately 6100 pounds per engine (a total thrust increase of 6000 pounds) to compensate for the failed engine and the spoiler required for lateral trim. Delays in commanding this thrust or commands for less than this amount were likely to produce hard landings. Figure 38 provides a feeling for the penalty in increased touchdown sink rate due to thrust mismanagement. Values on the abcissa represent average thrust values attained for the flare and as such include effects of pilot reaction delay, thrust command, and engine acceleration characteristics. For failures at 100 feet, misuse of thrust, to the point where only half of the required increment was achieved at touchdown, produced landings as severe as those experienced for engine failures at low altitude for the slower engine. For failures at 50 feet, similar misuse of thrust for the fast engine eliminated its advantage over the slow engine in reducing the landing impact.

In summary, while substantial improvements in engine out landing performance appear to be provided by reducing engine acceleration time, misuse of thrust can erode all of the advantages of the rapid thrust response. Even instantaneous response is of no value if the pilot delays appreciably in commanding increased thrust or if he does not command sufficient thrust to arrest the sink rate. Operation in turbulence, wind shears, and under IFR conditions provide distractions

which can prevent the pilot from recognizing an engine failure and responding properly to achieve acceptable landing precision. If the potential for engine out control inherent in an engine with rapid acceleration capability is to be realized, it is likely that some automatic means of alerting the pilot to an engine failure will be required.

Vertical Velocity Damping Augmentation

As a means for increasing the vertical velocity damping (Z_α) and possibly improving path control, a simple feedback of angle of attack to thrust command was implemented. This augmentation scheme effectively increased Z_α / V_o from -.4 to -1.0/sec. Typical response characteristics of the aircraft attitude and thrust changes with Z_α augmentation on and off are illustrated in Figures 39 and 40. The improvement in path following of attitude and quickened response to thrust is evident. Pilot commentary favorably reflected the improved path response. They were particularly impressed with the control of flight path with attitude due to the nearly simultaneous response of flight path to changes in attitude. These results agree with similar experience reported in Reference 9. Very limited data was available for normal STOL landings with Z_α augmentation. Much of the time for evaluation of this control scheme was spent flying at low altitude (10 to 20 feet) along a 10,000 foot conventional runway to allow the pilot to compare his ability to make small changes in vertical velocity with the Z_α augmentation on and off. The few STOL landings which were documented are shown in Figure 41. Since the flare technique required only an attitude change, the augmentation off data of Figure 21 are shown for comparison. For similar points of touchdown, some reduction in touchdown sink rate is evident for increased Z_α. Evaluations were made for both the fast and slow engine and differences in performance between the two cases were not readily apparent to the pilot. Time histories of the augmented aircraft's response to a change in attitude for the fast and slow engines are shown in Figure 42.

CONCLUSIONS

This simulation program was conducted to gain an initial impression of the significant contribution of engine transient response to normal and engine out operation for the STOL approach and landing. The conclusionswhich are based on these results are dependent, at least to some degree, on the thrust to weight ratio, aerodynamic characteristics, and control system of the simulated aircraft, and on the capability of the simulator itself.With these qualifications, the results indicate that, under ideal operational conditions and for quick pilot response to an engine failure, reducing engine acceleration times (from $t_{95\%}$ = 3.0 to .3 sec) provide

- substantial reduction in the altitude loss required for an engine out wave-off
- reduction in both the altitude range over which the aircraft is susceptible to hard touchdowns for engine out landings, and in the touchdown sink rate.

It can be expected that operation in turbulence, wind shears, IFR situations and other non-ideal conditions will tend to obscure the cues required for timely recognition of the engine failure. Penalties for delay in recognition of the engine failure and in reconfiguring the aircraft for wave-off can be particularly severe on wave-off performance. Similarly, delay in reaction to engine failure and mismanagement of thrust for the flare can severely penalize engine out landing performance. For either the wave-off or landing, these penalties for operational abuses can overshadow the favorable influence of rapid engine response. Hence, to adequately realize the potential for fast engine response to reduce wave-off altitude loss or to reduce landing sink rates following an engine failure, some means of reducing the pilot reaction time must be devised. Either automatic cueing to immediately alert the pilot to the engine failure or automatic thrust control to compensate for the effects of the engine failure offer potential solutions.

Augmentation of vertical velocity damping through a simple feedback of angle of attack to thrust command was considered favorable by the pilots. The pilots commented that this augmentation scheme considerably improved flight path control with attitude on the approach and through the flare.

REFERENCES

1. Rulis, R. J.: Status of Current Development Activity Related to STOL Propulsion Noise Reduction. NASA TM X-68195, 1973.
2. Anderson, S. B.; and Schroers, L. G.: Recommendations for V/STOL Handling Qualities. North Atlantic Treaty Organization, Advisory Group for Aeronautical Research and Development Report 408, 1962.
3. Parlett, L. P.; Greer, H. D.; Henderson, R. L.; and Carter, C. R.: Wind-Tunnel Investigation of an External-Flow Jet-Flap Transport Configuration Having Full-Span Triple-Slotted Flaps. NASA TN D-6391, 1971.
4. Grantham, W. D.; Nguyen, L. T.; Patton, J. M.; Deal, P. L.; Champine, R. A.; and Carter, C. R.: Fixed Base Simulator Study of an Externally Blown Flap STOL Transport Airplane During Approach and Landing. NASA TN D-6898, October 1972.
5. Kier, D. A.; Granthan, W. D.; Powers, B. G.; and Nguyen, L. T.: Simulation Evaluation of Externally Blown Flap and Augmentor Wing Transport Configurations. NASA SP-320, Paper 12, 1973.
6. Grafton, S. B.; Parlett, L. P.; and Smith, C. C., Jr.; Dynamic Stability Derivatives of a Jet Transport Configuration with High Thrust-Weight Ratio and an Externally Blown Jet Flap. NASA TN D-6440, 1971.
7. Parlett, L. P.; Freeman, D. C., Jr.; and Smith, C. C., Jr.: Wind-Tunnel Investigation of a Jet Transport Airplane Configuration with High Thrust-Weight Ratio and an External-Flow Jet Flap. NASA TN D-6058, 1970.
8. Freeman, D. C.; Parlett, L. P.; and Henderson, R. L.: Wind-Tunnel Investigation of a Jet Transport Airplane Configuration with an External-Flap Jet Flap and Inboard Pod-Mounted Engines. NASA TN D-7004, 1970.
9. Allison, R. L.; Mack, M.; and Rumsey, P. C.: Design Evaluation Criteria for Commercial STOL Transports. NASA CR-114454, June, 1972.

TABLE I

AIRPLANE CHARACTERISTICS

Wing	
area, $ft.^2$	600.0
aspect ratio	7.3
span, ft.	66.2
taper ratio	0.34
sweep @ ¼ chord line, deg.	27.5
dihedral @ ¼ chord line, deg.	- 3.5
incidence @ MAC, deg.	4.5
root thickness, % chord	14.0
tip thickness, % chord	11.0
mean aerodynamic chord (MAC), ft.	9.8
airfoil section	
root	NACA 63_2-A214
tip	NACA 63_2-A211
flap span, % semispan	61.7
flap hinge axis, % chord	78.0
Ailerons (plain flap down-rigged 30°)	
span, % semispan	28.1
hinge axis, % chord	78.0
deflection, deg.	0-60
Spoilers	
span, % semispan	57.0
hinge axis, % chord	10.0
deflection, deg.	0, + 60

Horizontal tail	
area, $ft.^2$	205.0
aspect ratio	5.3
span, ft.	33.0
sweep @ leading edge, deg.	29.0
elevator hinge axis, % chord	73.0
elevator travel, deg.	+10, -50
incidence, deg.	$\pm$ 10
volume coefficient	1.0
tail arm length, ft.	28.7
Vertical tail	
area, $ft.^2$	120.0
aspect ratio	1.66
sweep, deg.	37.0
volume coefficient	0.09
rudder hinge axis, % chord	57.0
rudder travel, deg.	$\pm$45.0
Engine placement	
inboard, % semispan	22.0
outboard, % semispan	42.0
Center of gravity location, % MAC	40.0
Moment of inertias, $slug\text{-}ft.^2$	
Ixx	213,000.
Iyy	242,500.
Izz	402,500.
Ixz	31,150.

Weight, lbs.	48,000.
Inboard, 3rd element flaps for flight path controls; deflection, degs.	$\pm$25.0 about the nominal δ_{f_3} deflection

TABLE II

ENGINE DYNAMIC RESPONSE PARAMTERS

Engine	K_1	ζ_1	ω_1 rad/sec	ζ_2	ω_2 rad/sec	τ sec	$\dot{T}_{max_2}$ % per sec
1	.8	.95	3.5	.9	8.0	.85	40.
2	0	---	---	.9	3.0	.85	∞
3.	0	---	---	.8	1.0	.85	∞

Engine 1

$\dot{T}_{max_1}$ % per sec	$T_c - T$ %
140.	$\leq$ 20.
200.	35.
260.	>50.

TABLE III

CONTROL FORCE AND DISPLACEMENT CHARACTERISTICS

Control	Breakout lbs	Gradient	Max Force lbs	Throw
Column	3	5 lb/inch	pull 40 push 20	aft 8 inches fwd 4 inches
Wheel	2	.3 lb/deg	20	± 60 deg
Pedals	8	21 lb/inch	70	± 3 1/2 inches

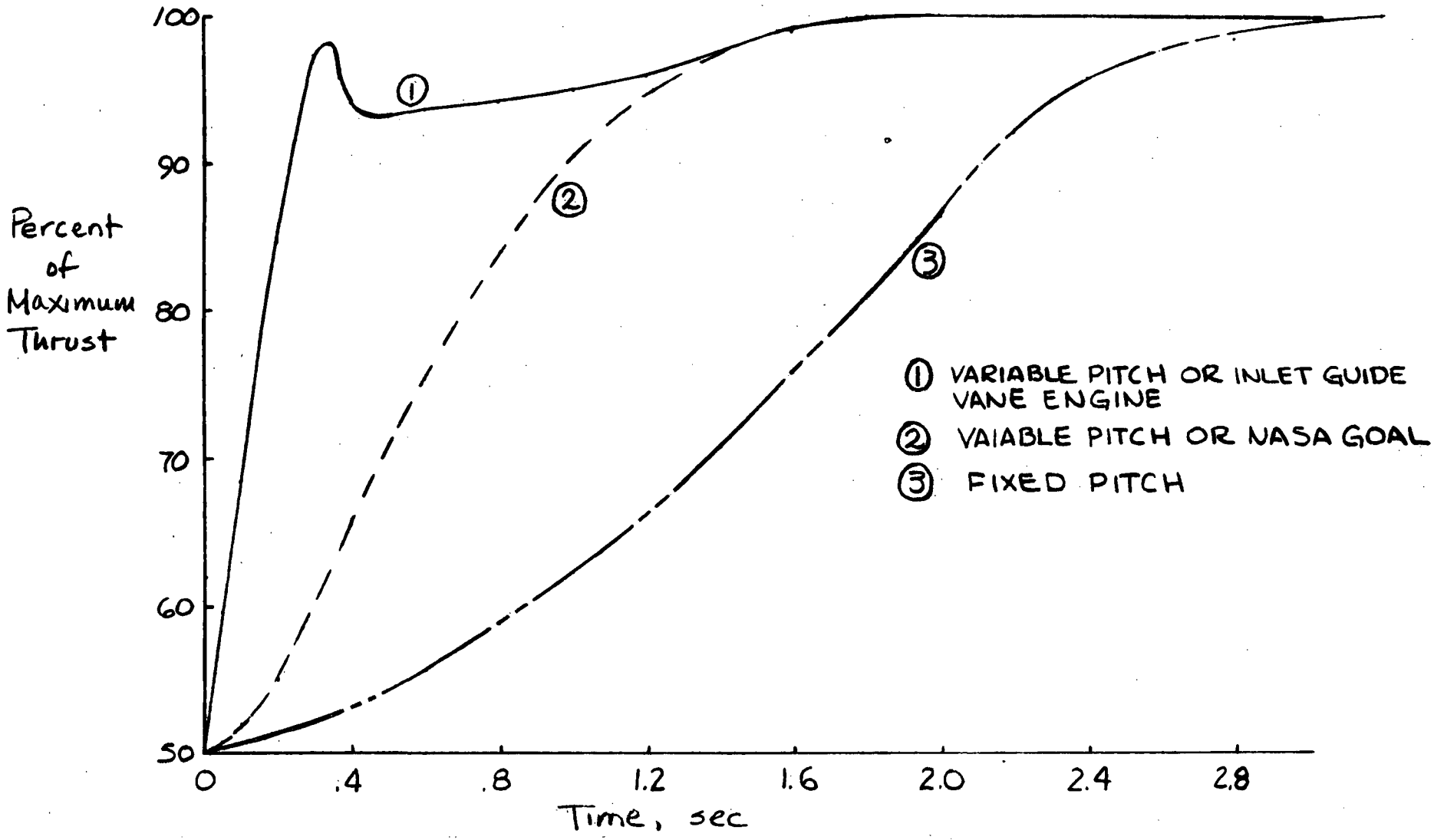

Figure 1. Engine Response Rates

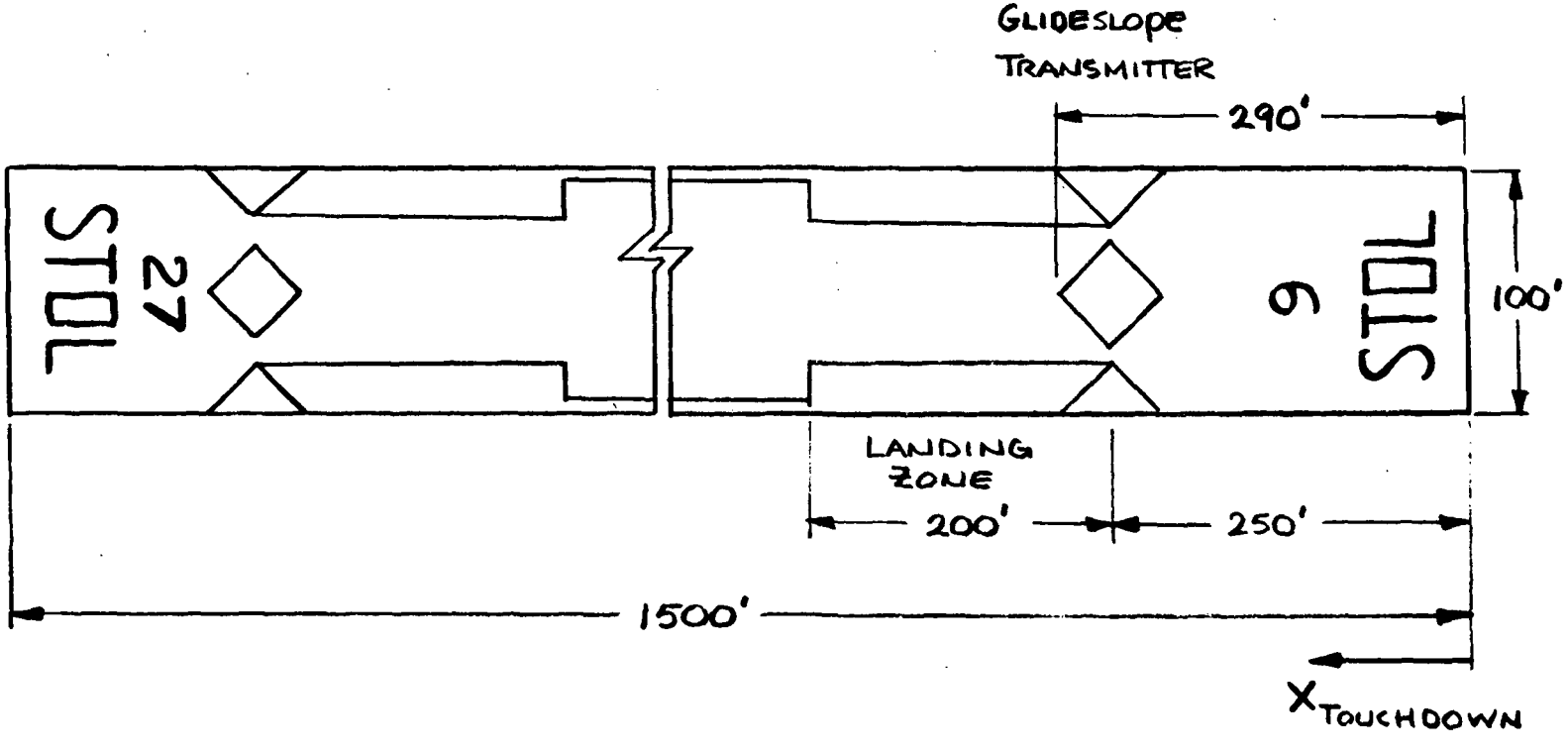

Figure 2 STOLPORT Layout

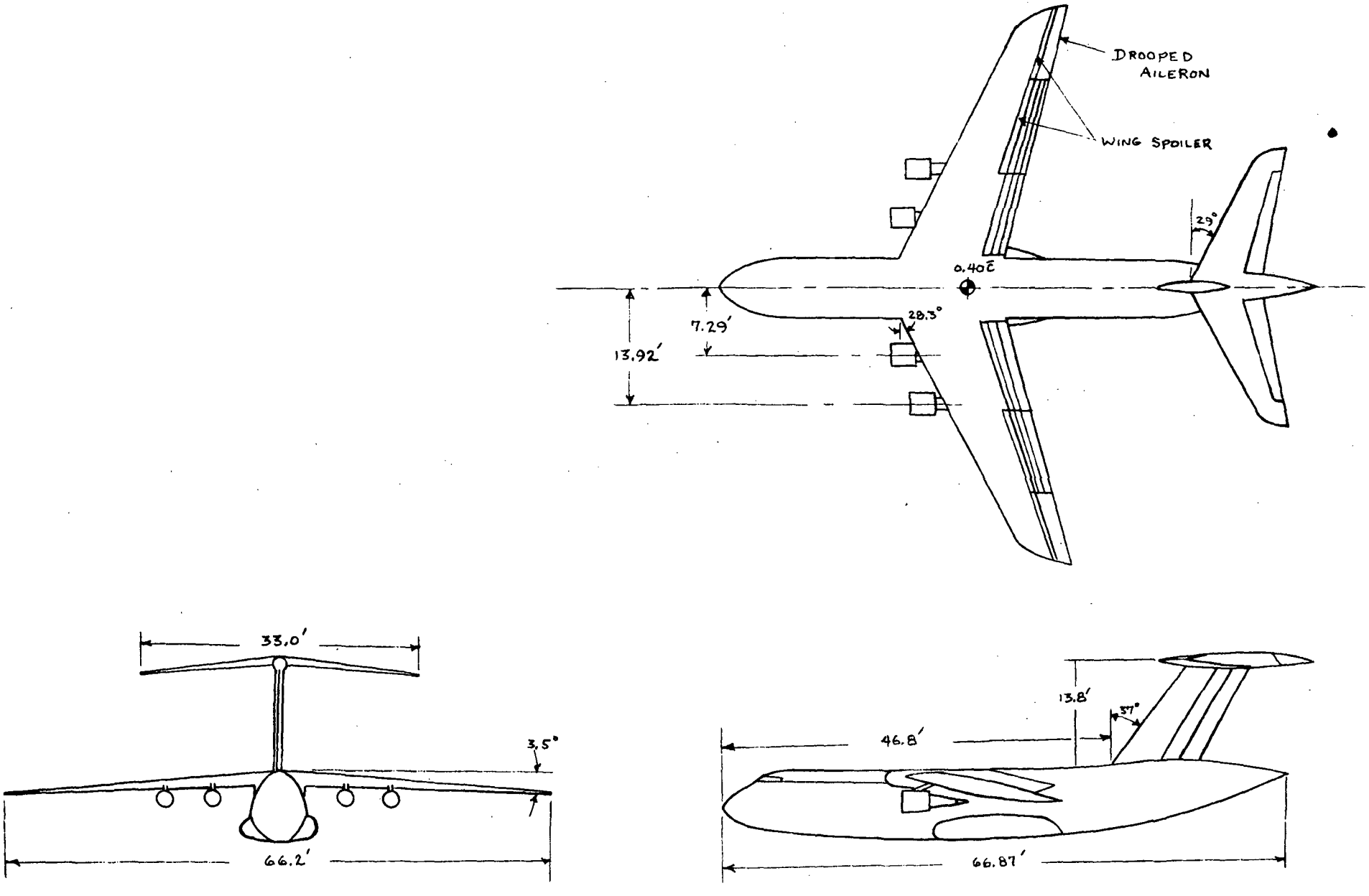

Figure 3 Three View Schematic of Simulated Aircraft

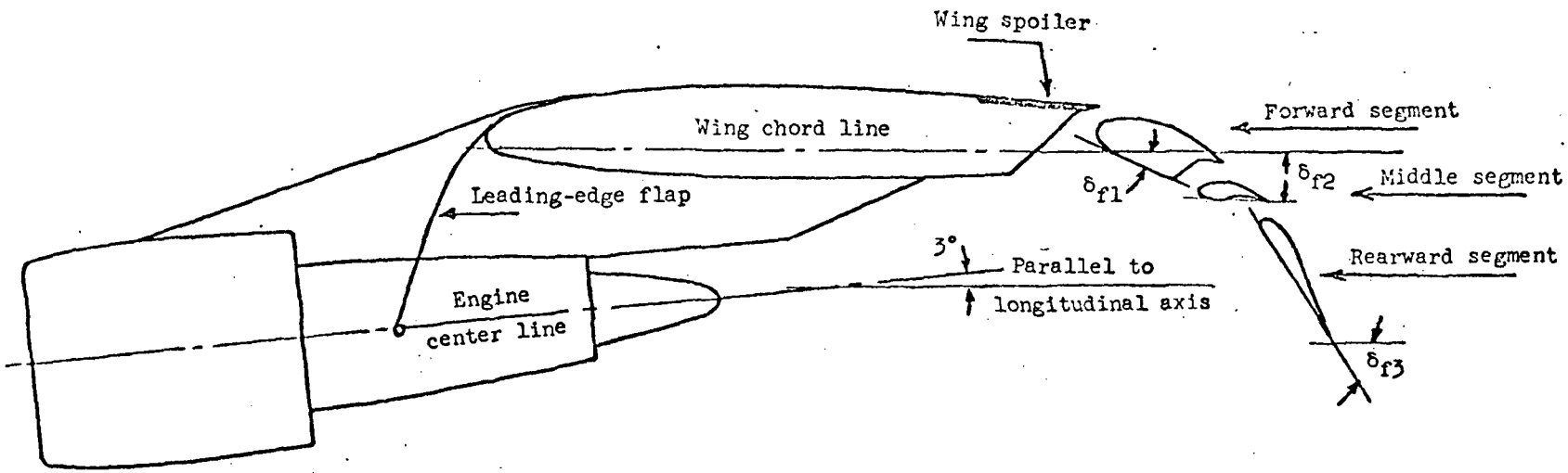

Figure 4 Flap Assembly and Engine Pylon Detail

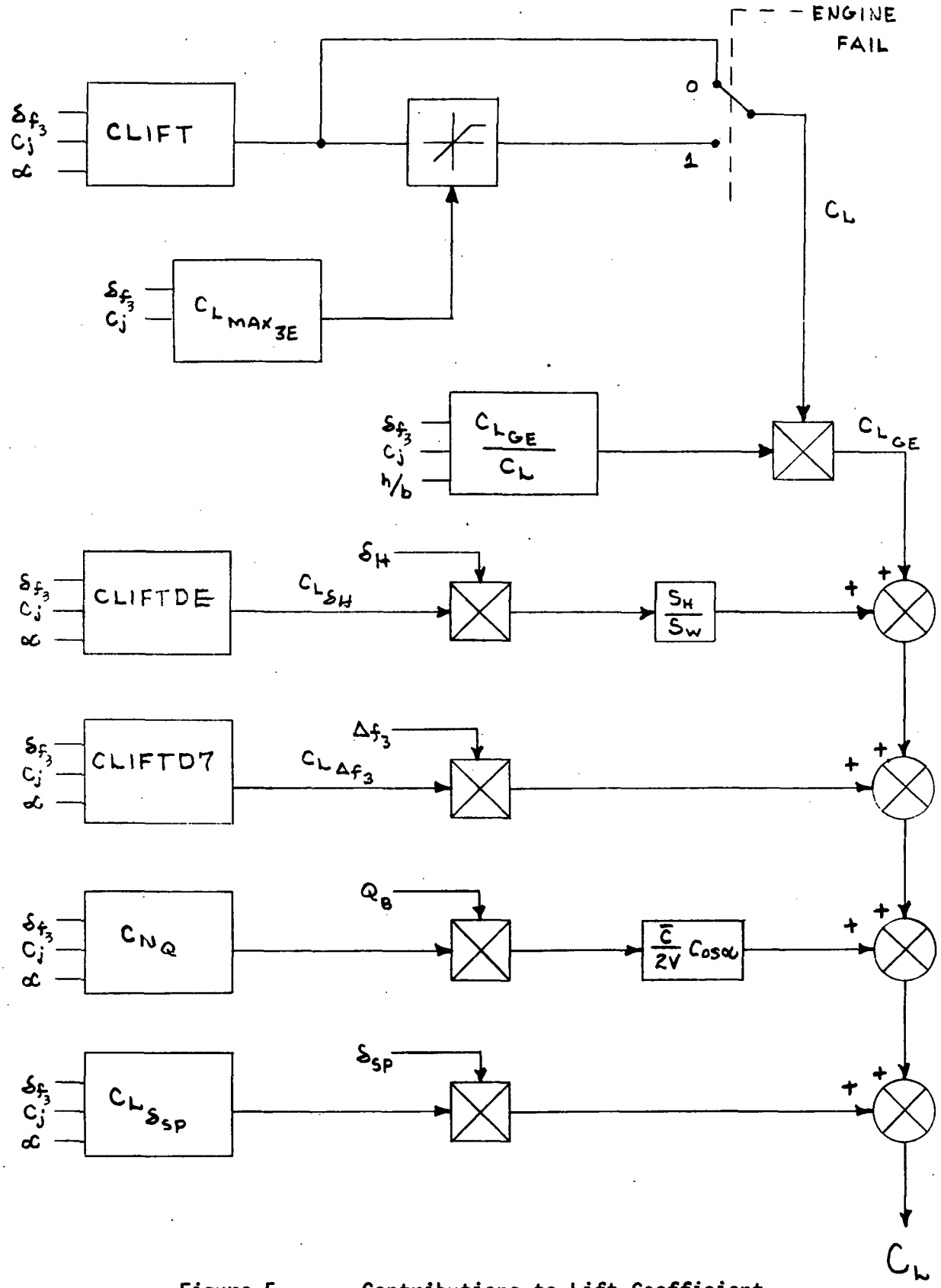

Figure 5 Contributions to Lift Coefficient

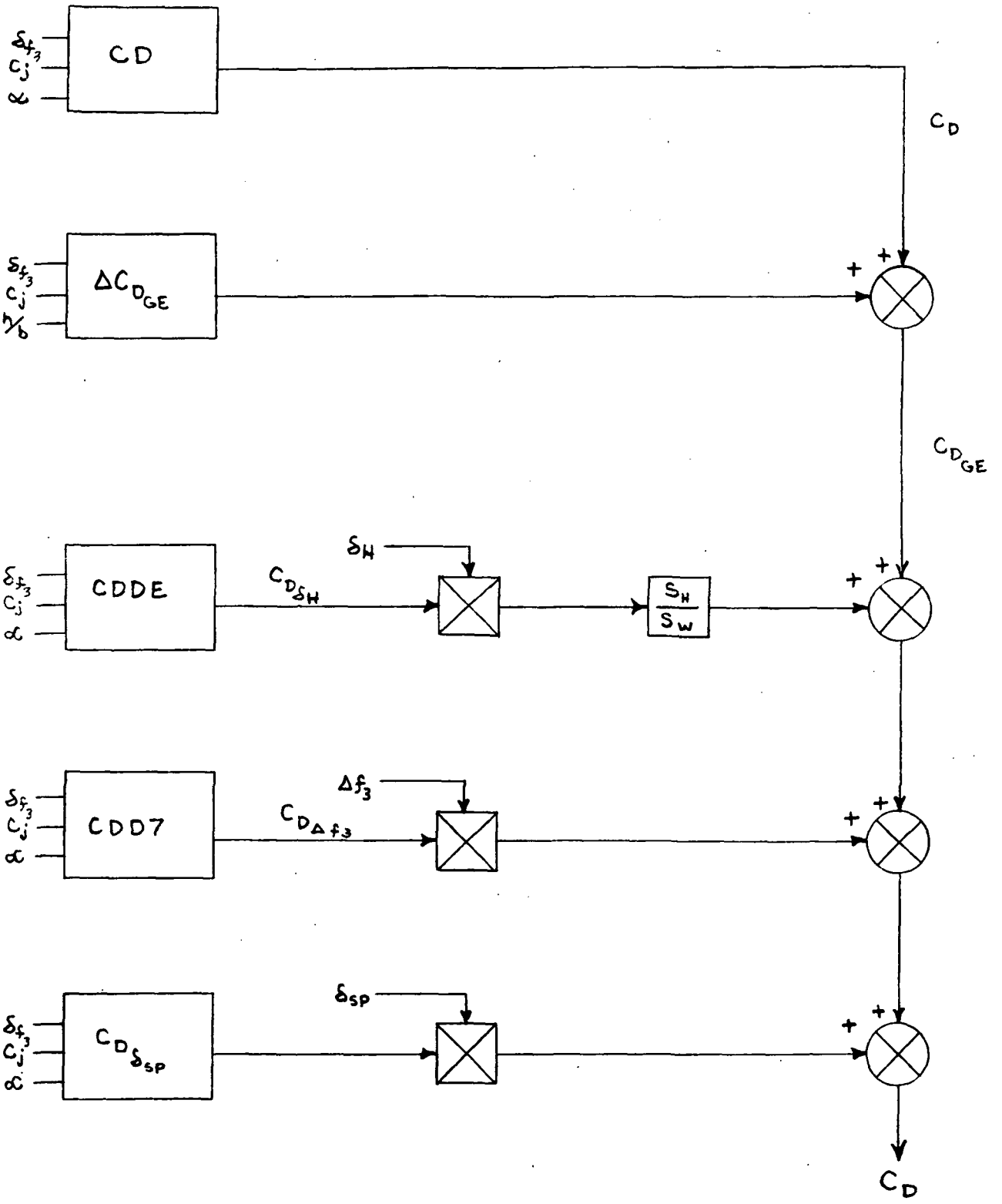

Figure 6 Contributions to Drag Coefficient

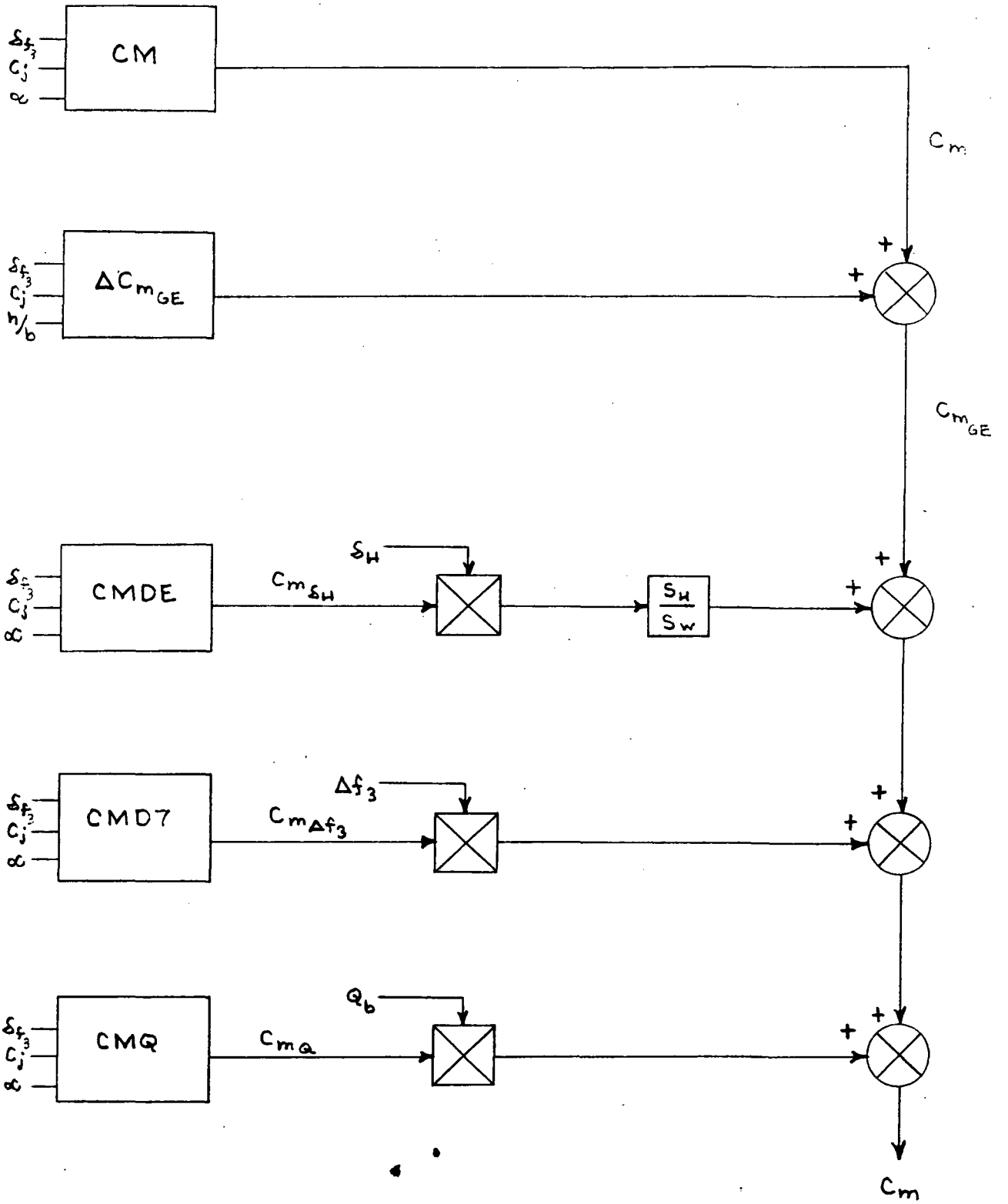

Figure 7 Contributions to Pitching Moment Coefficient

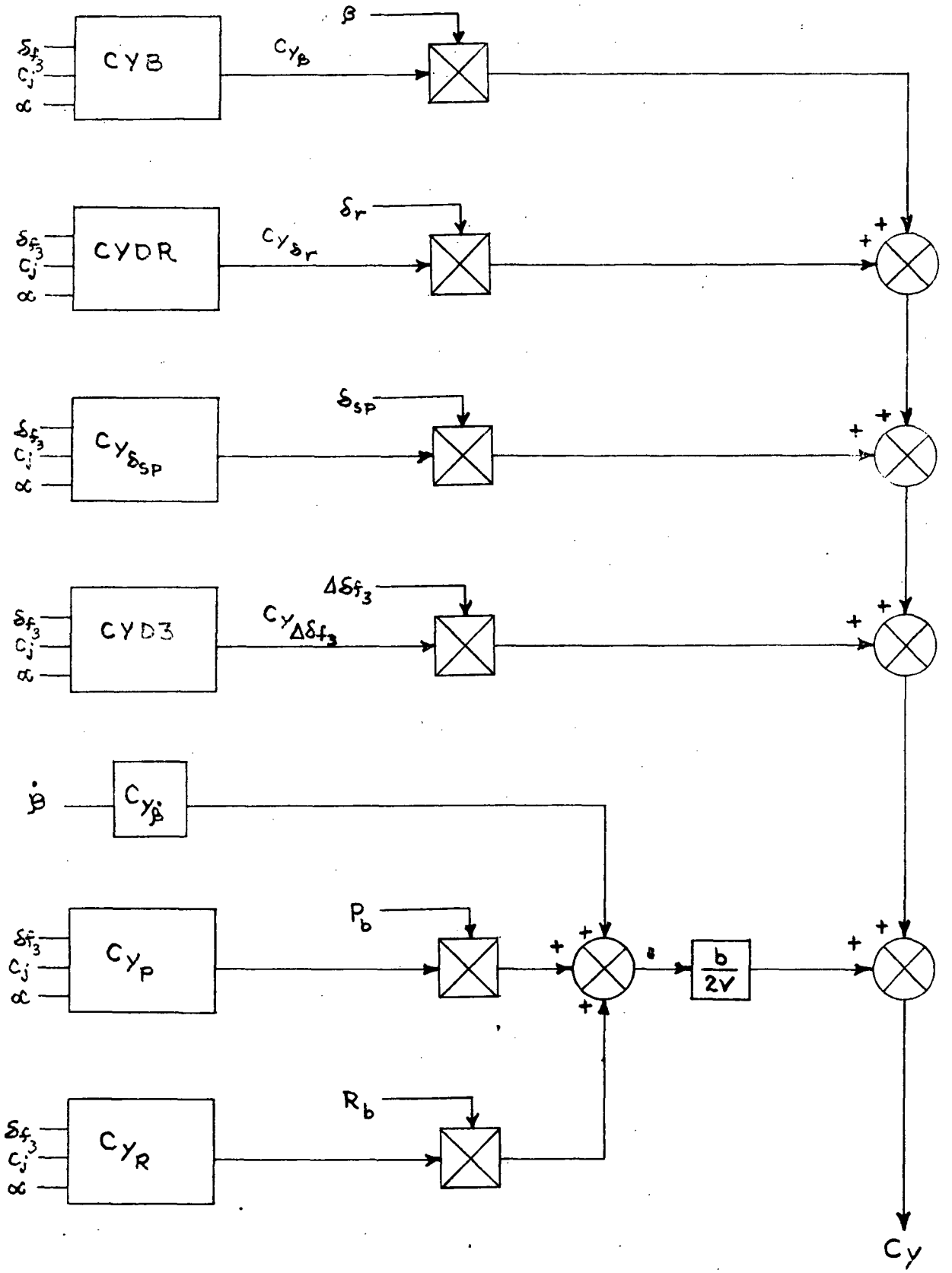

Figure 8 Contributions to Side Force Coefficient.

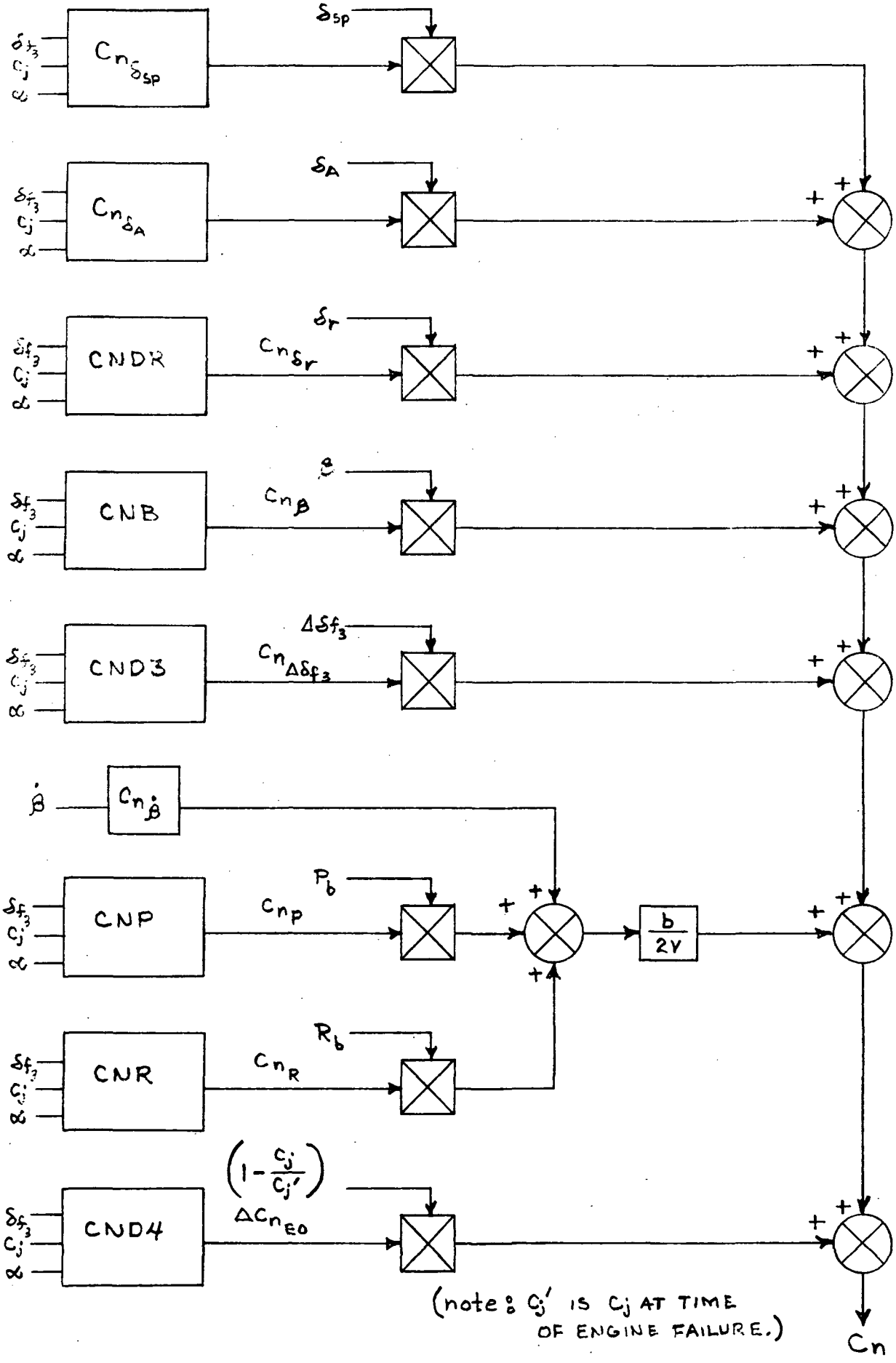

Figure 9 Contributions to Yawing Moment Coefficient

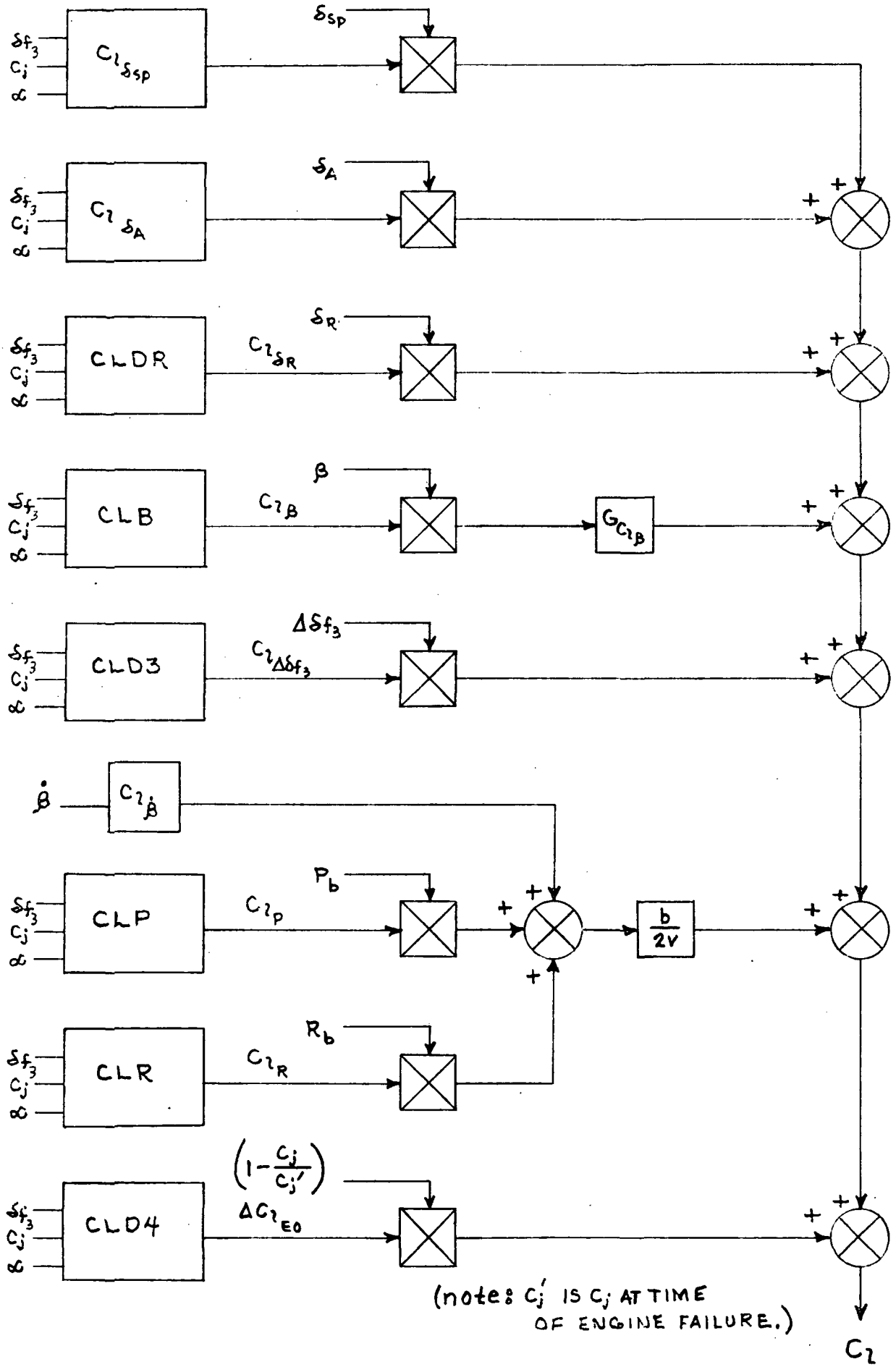

Figure 10 Contributions to Rolling Moment Coefficient .

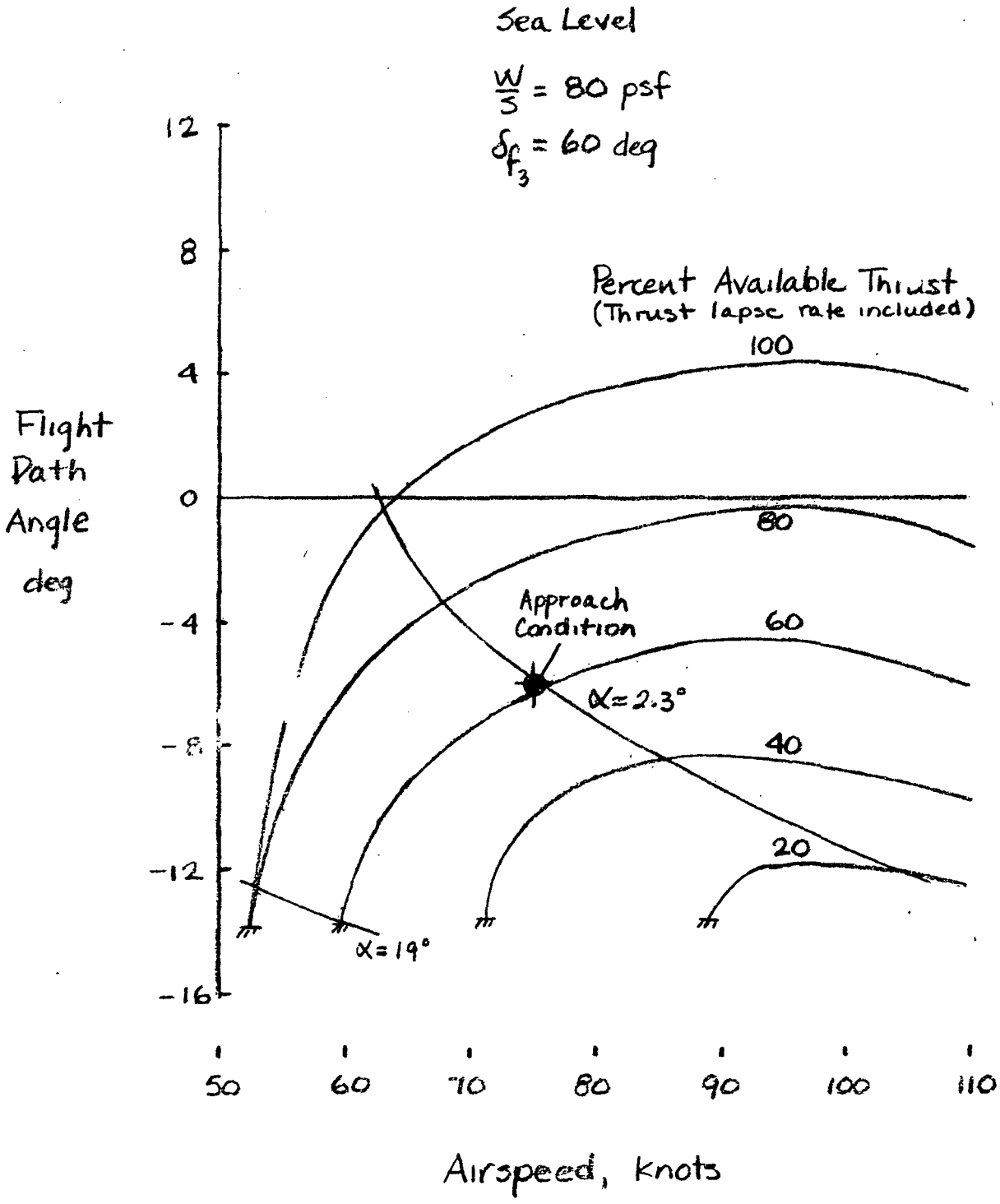

Figure 11 Performance Characteristics of Approach Configuration - All Engines Operating

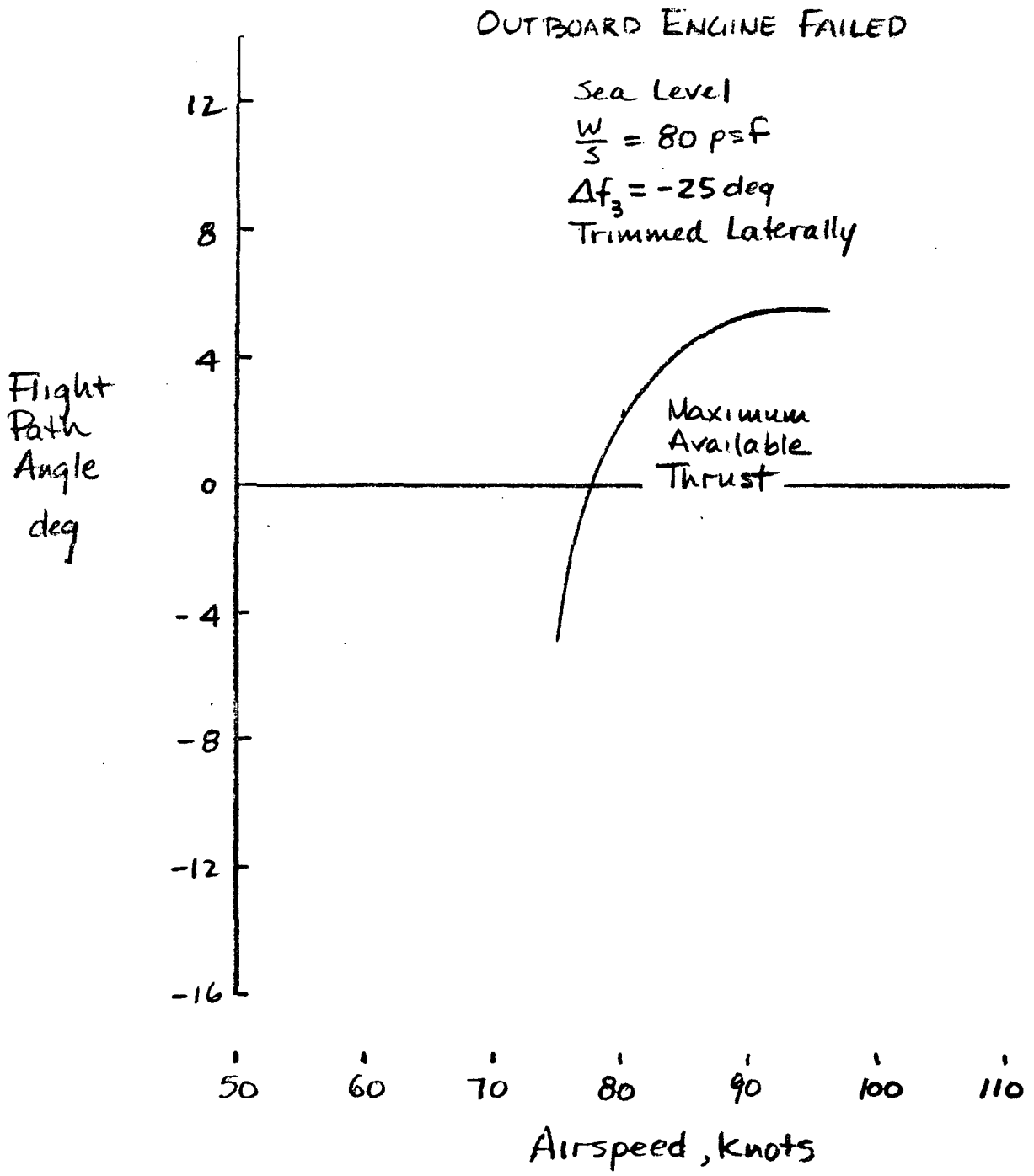

Figure 12 Performance Characteristics of Approach Configuration - Outboard Engine Failed

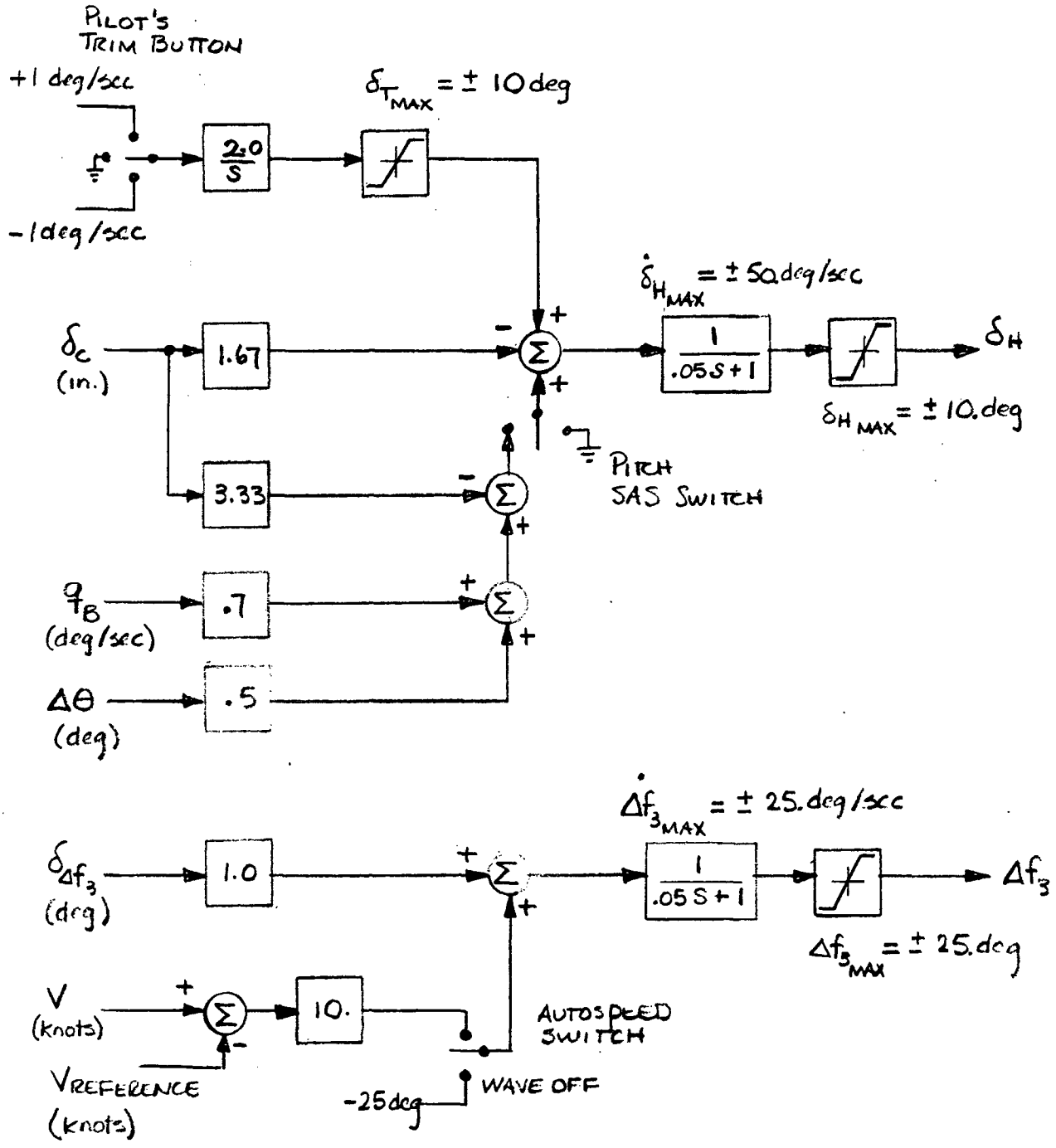

Figure 13 Longitudinal Stability and Command Augmentation System

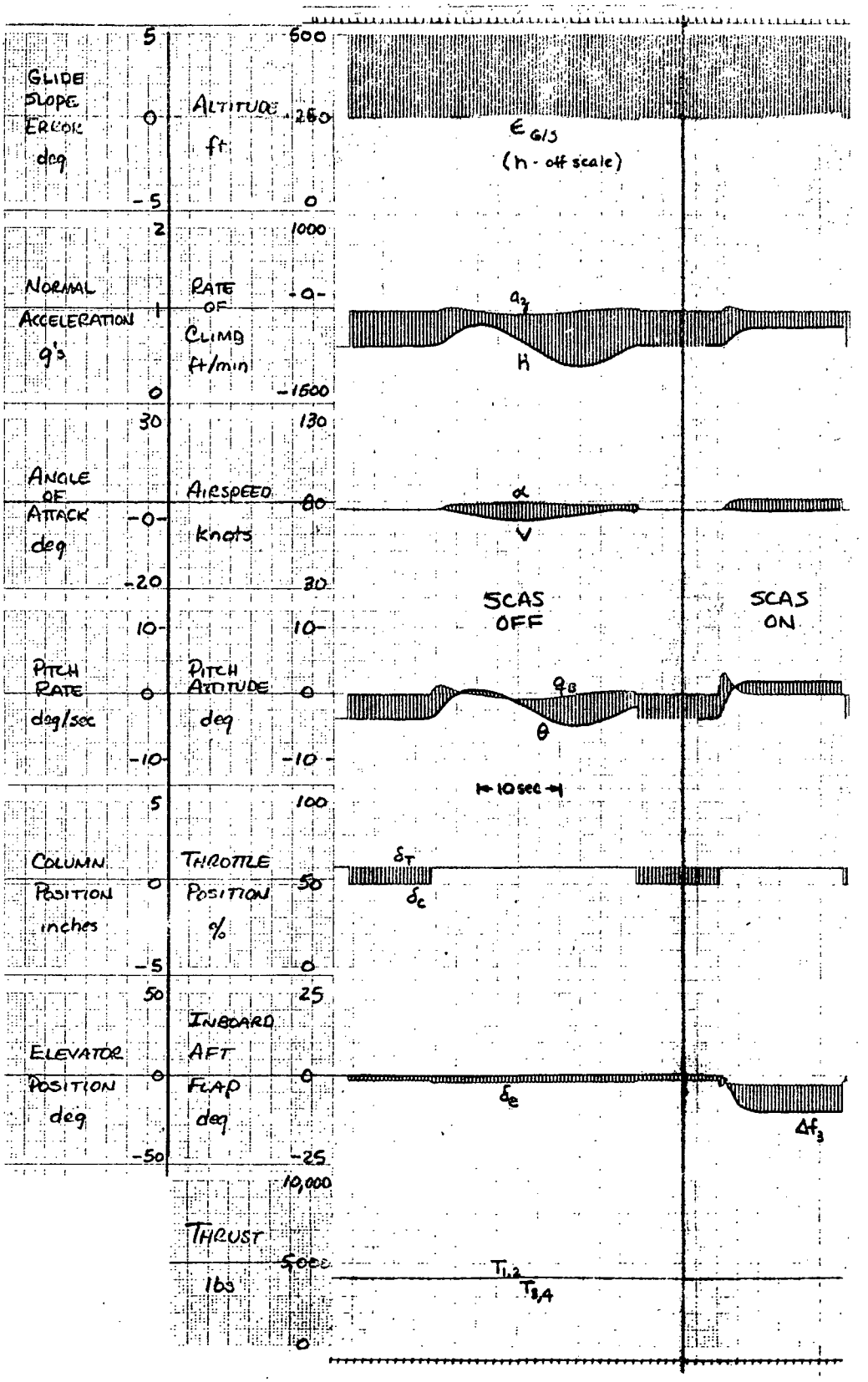

Figure 14 Longitudinal Response to a Step Column Input - SCAS Off and On

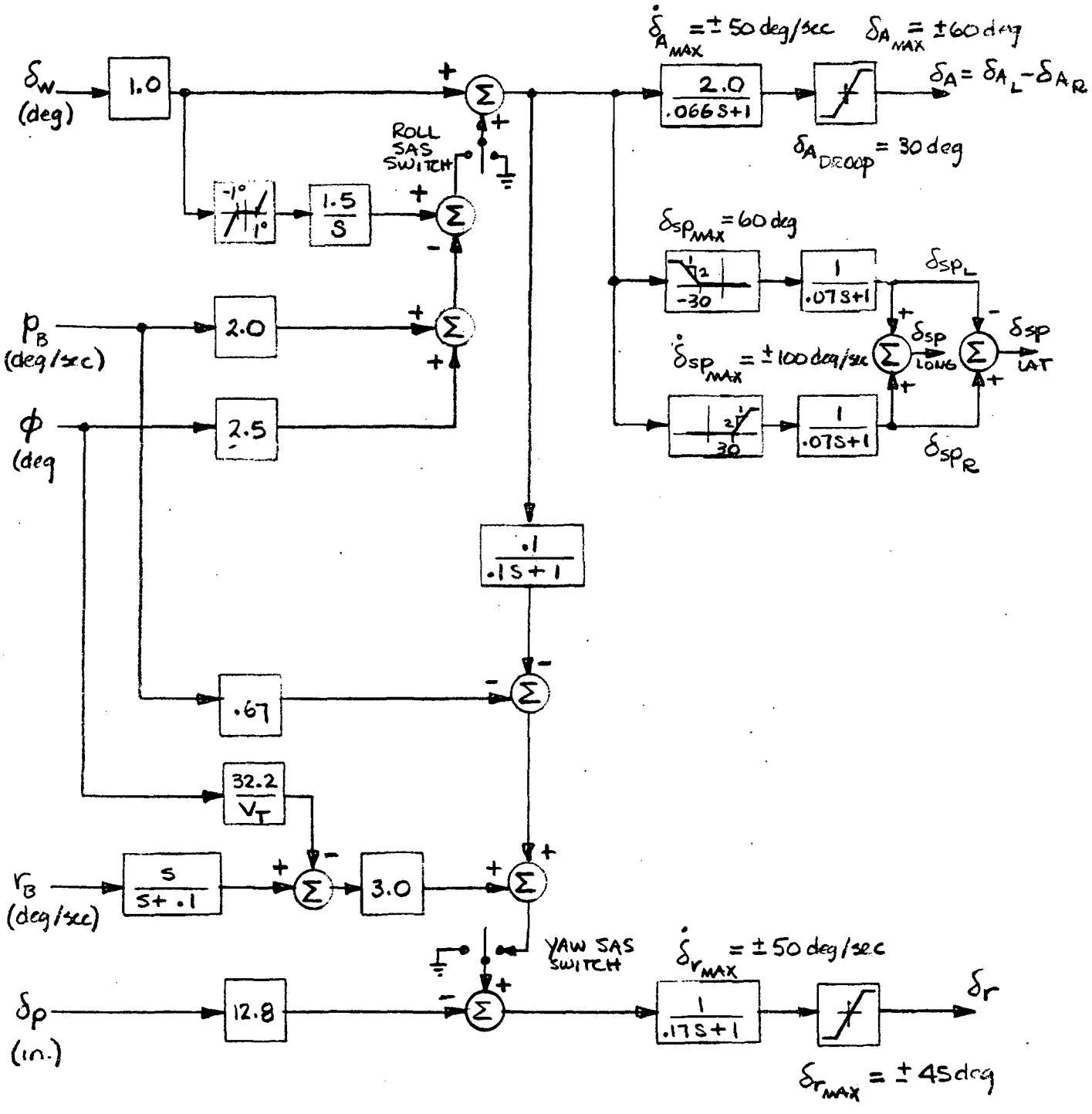

Figure 15 Lateral-Directional Stability and Command Augmentation System

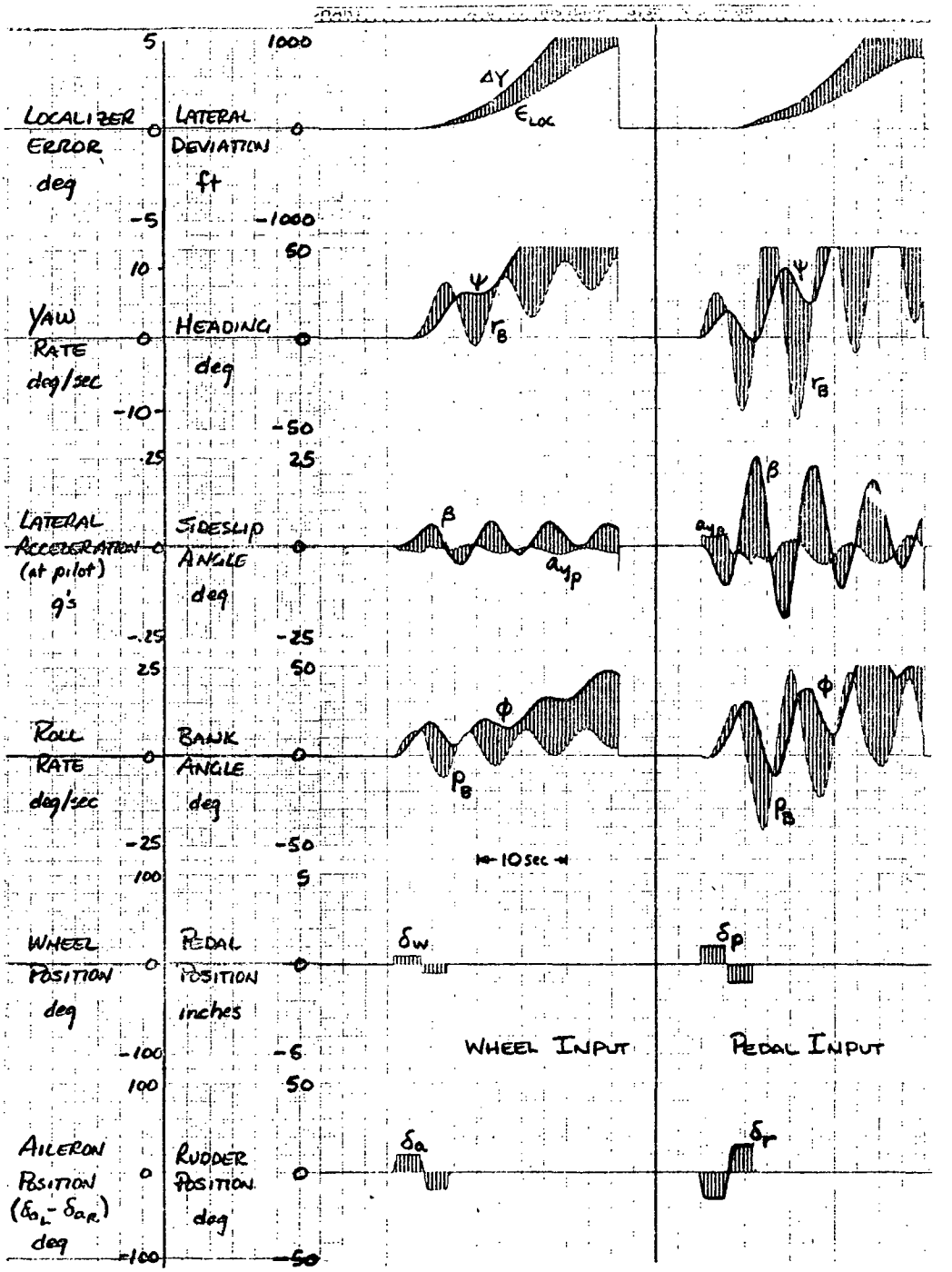

Figure 16a Lateral-Directional Response to Wheel and Pedal Doublet Inputs - SCAS Off

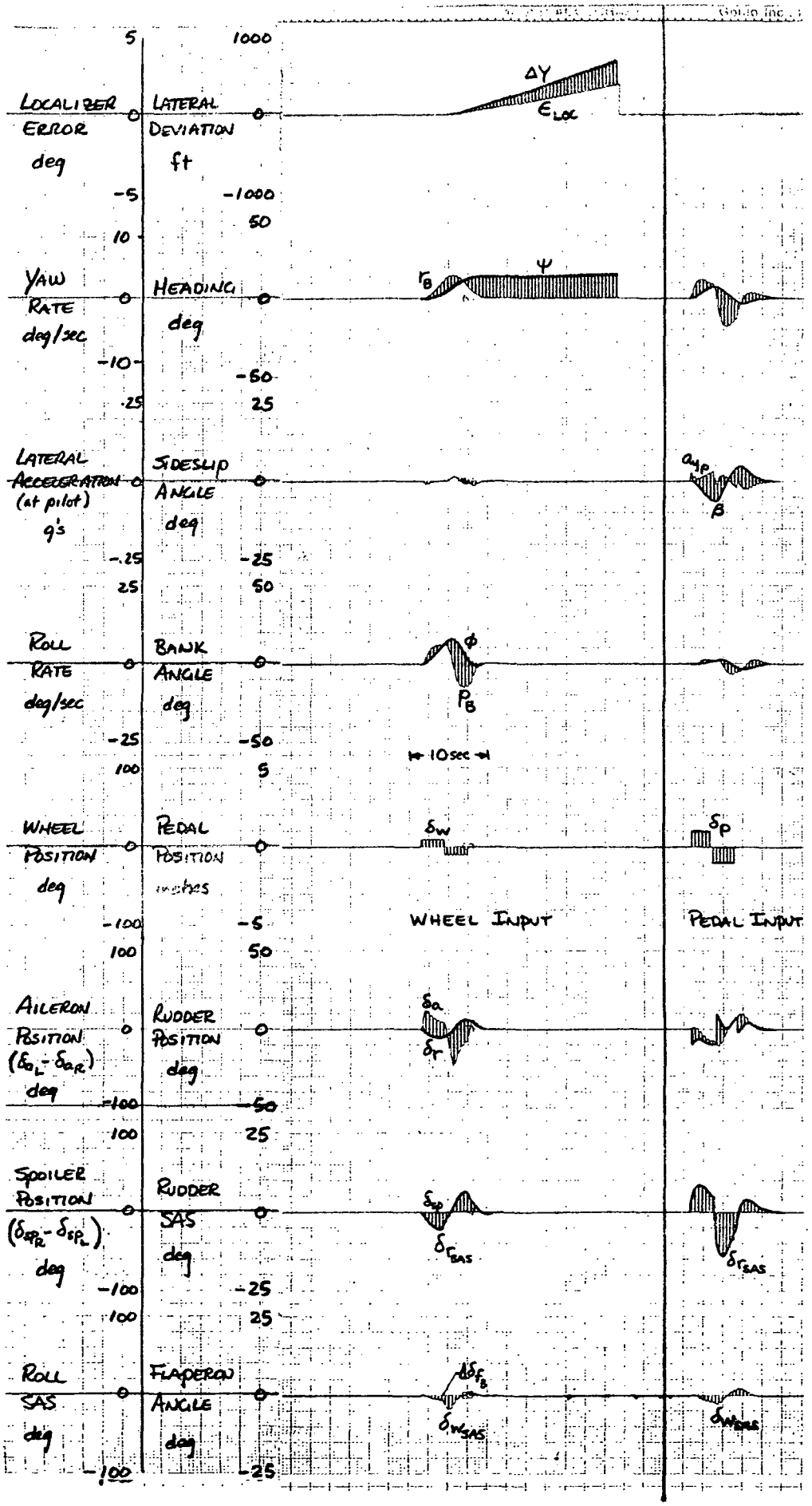

Figure 16b Lateral-Directional Response to Wheel and Pedal Doublet Inputs - SCAS On

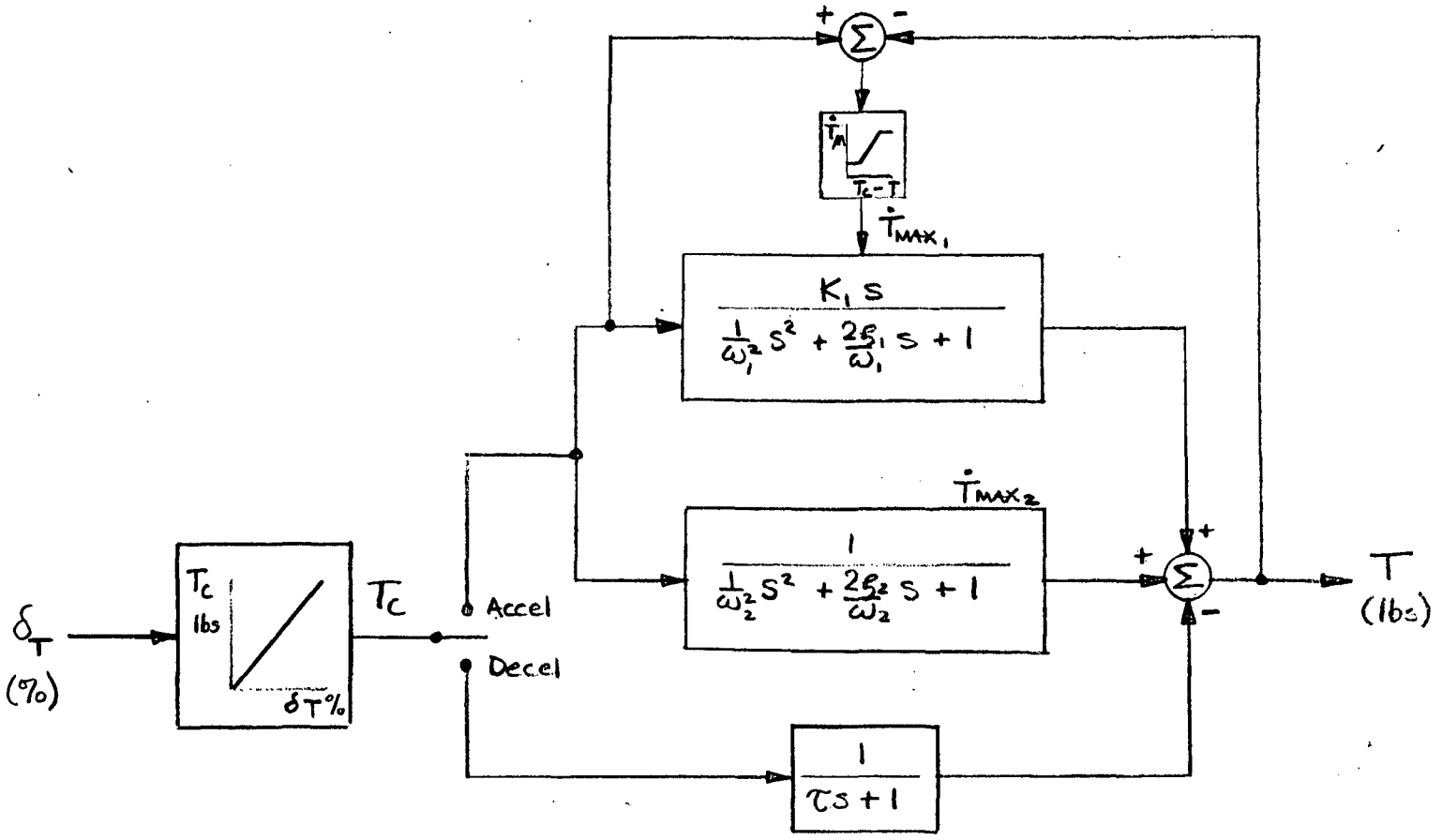

Figure 17 Block Diagram of Engine Dynamic Model

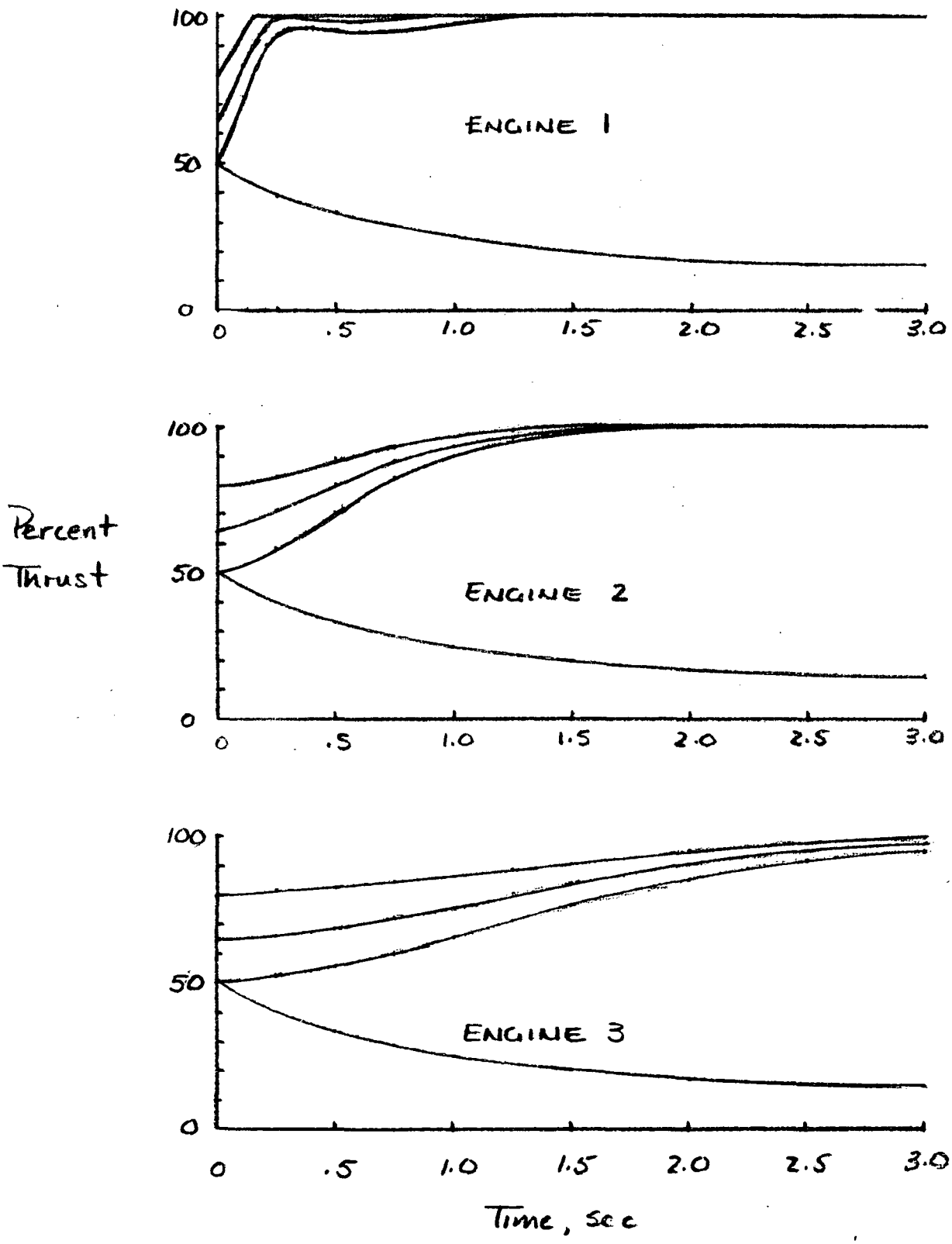

Figure 18a Response of Engine Models to a Step Command for Maximum Thrust - Initial Thrust Settings of 50, 65, and 80 Percent

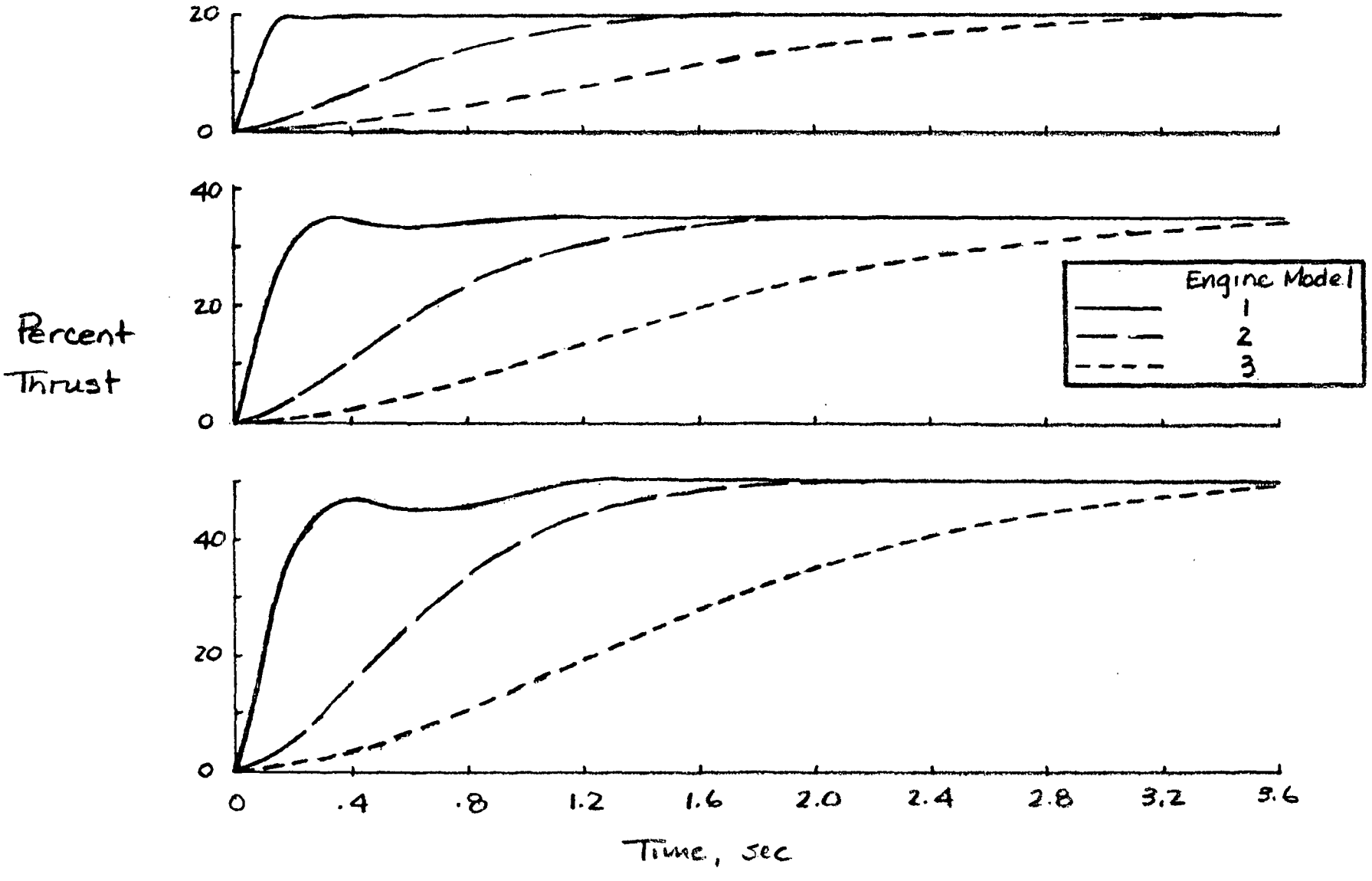

Figure 18b Comparison of Response of Engine Models to Step Thrust Commands of 20, 35, and 50 Percent

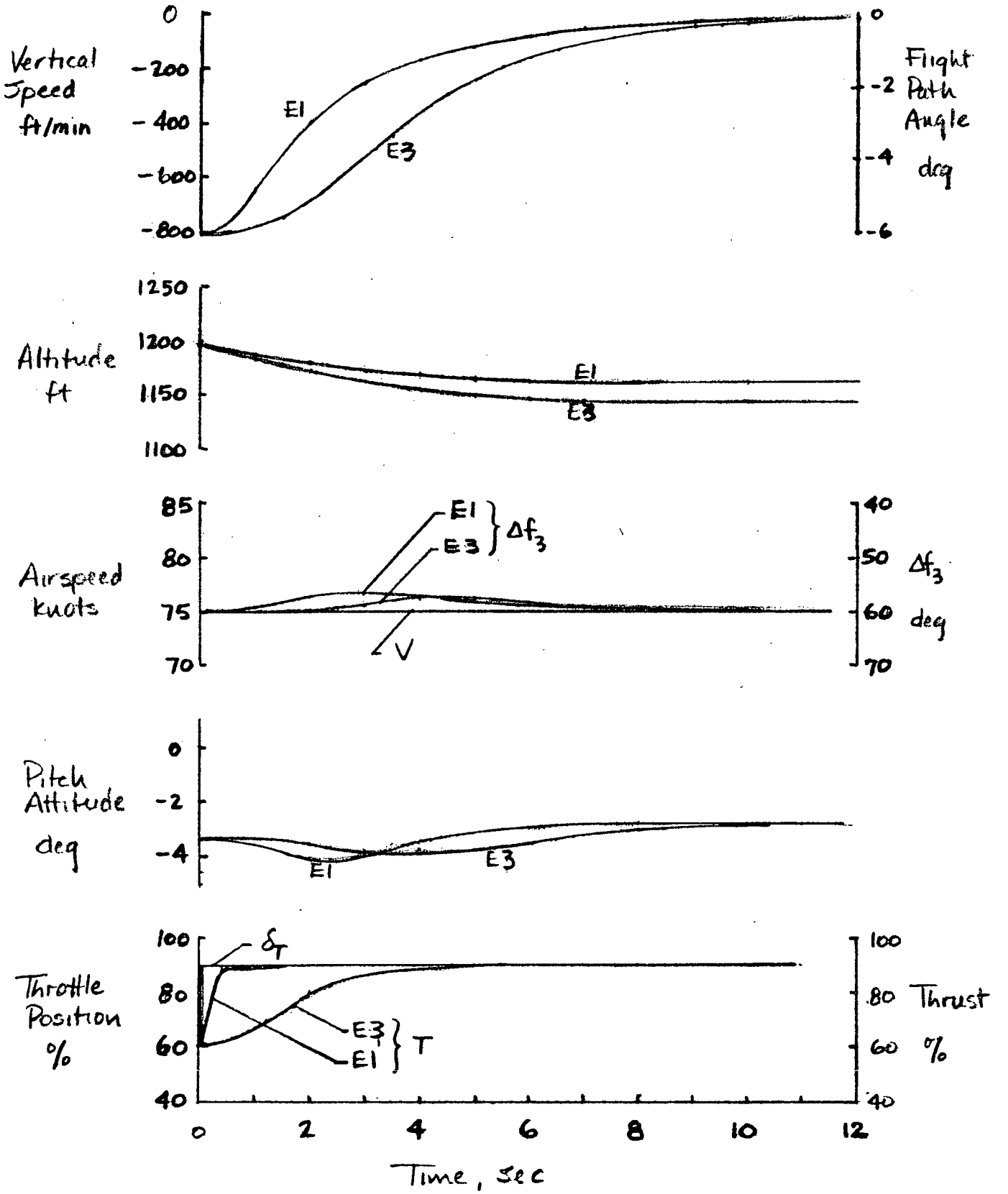

Figure 19 Comparison of Aircraft Response to a Step Throttle Input for the Fast and Slow Engine Response Characteristics

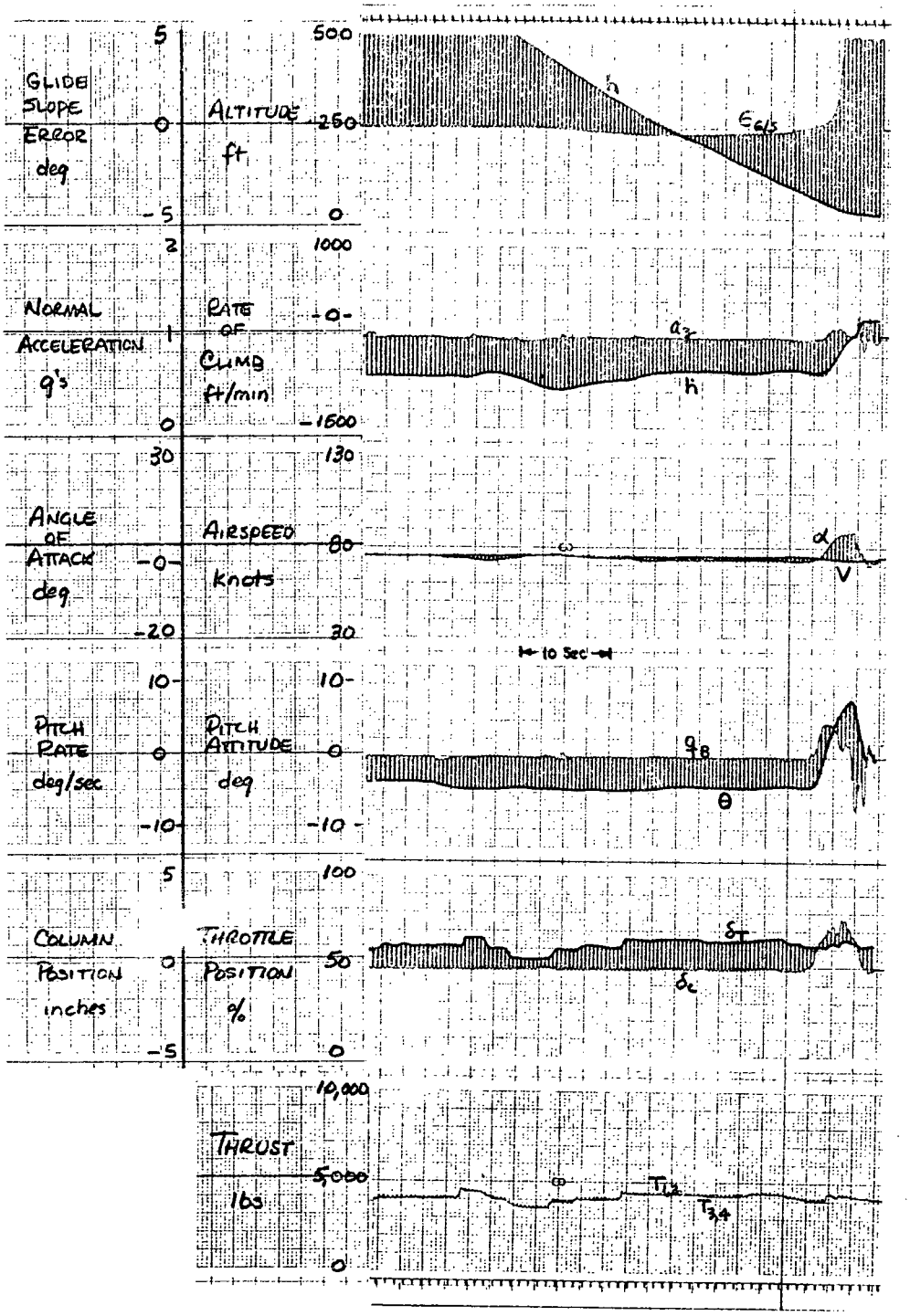

Figure 20 Typical Time History of a Landing Flare Performed with Aircraft Rotation

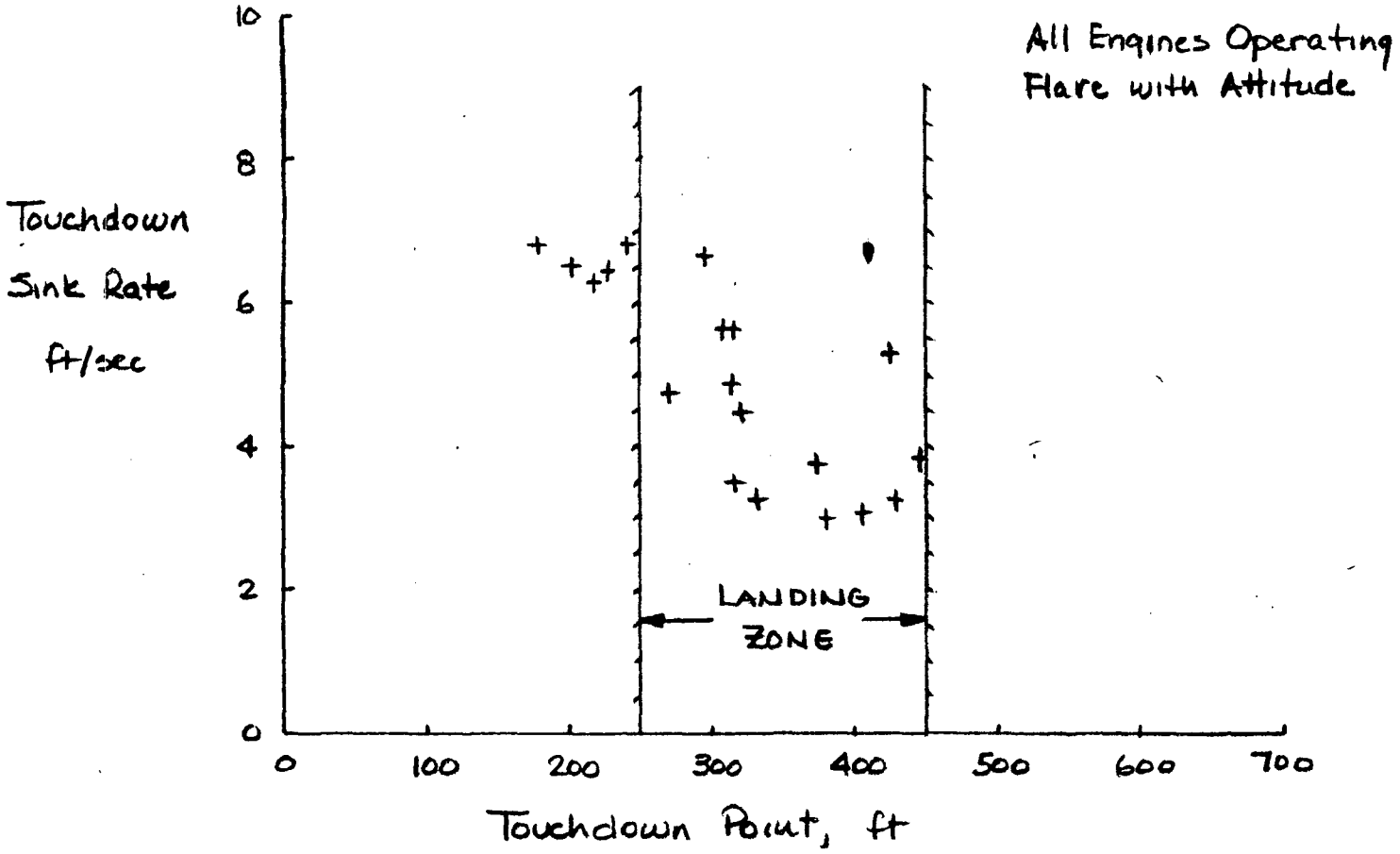

Figure 21 Landing Precision for Four Engine Operation - Flare by Aircraft Rotation

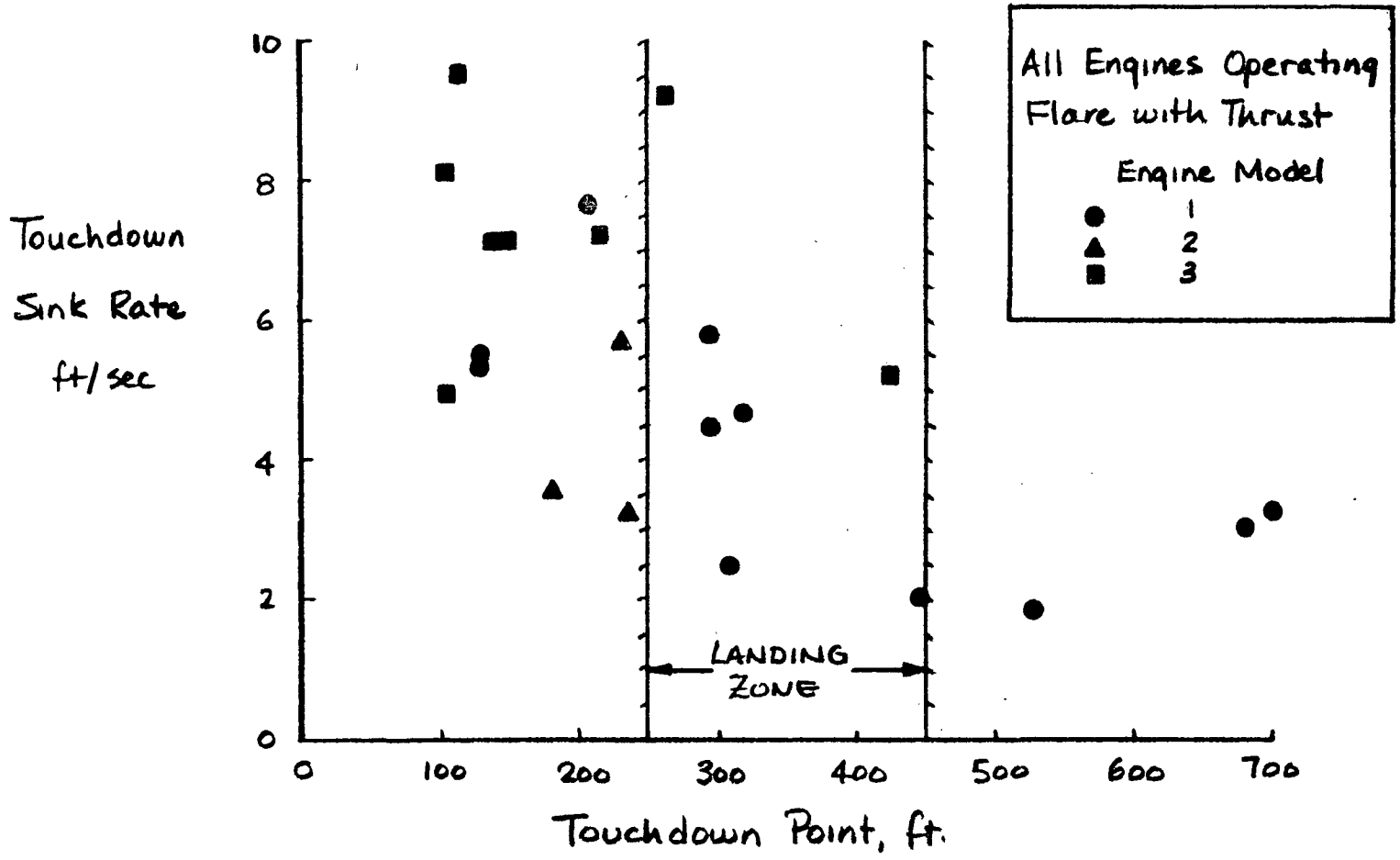

Figure 22 Landing Precision for Four Engine Operation - Flare by Thrust Increase

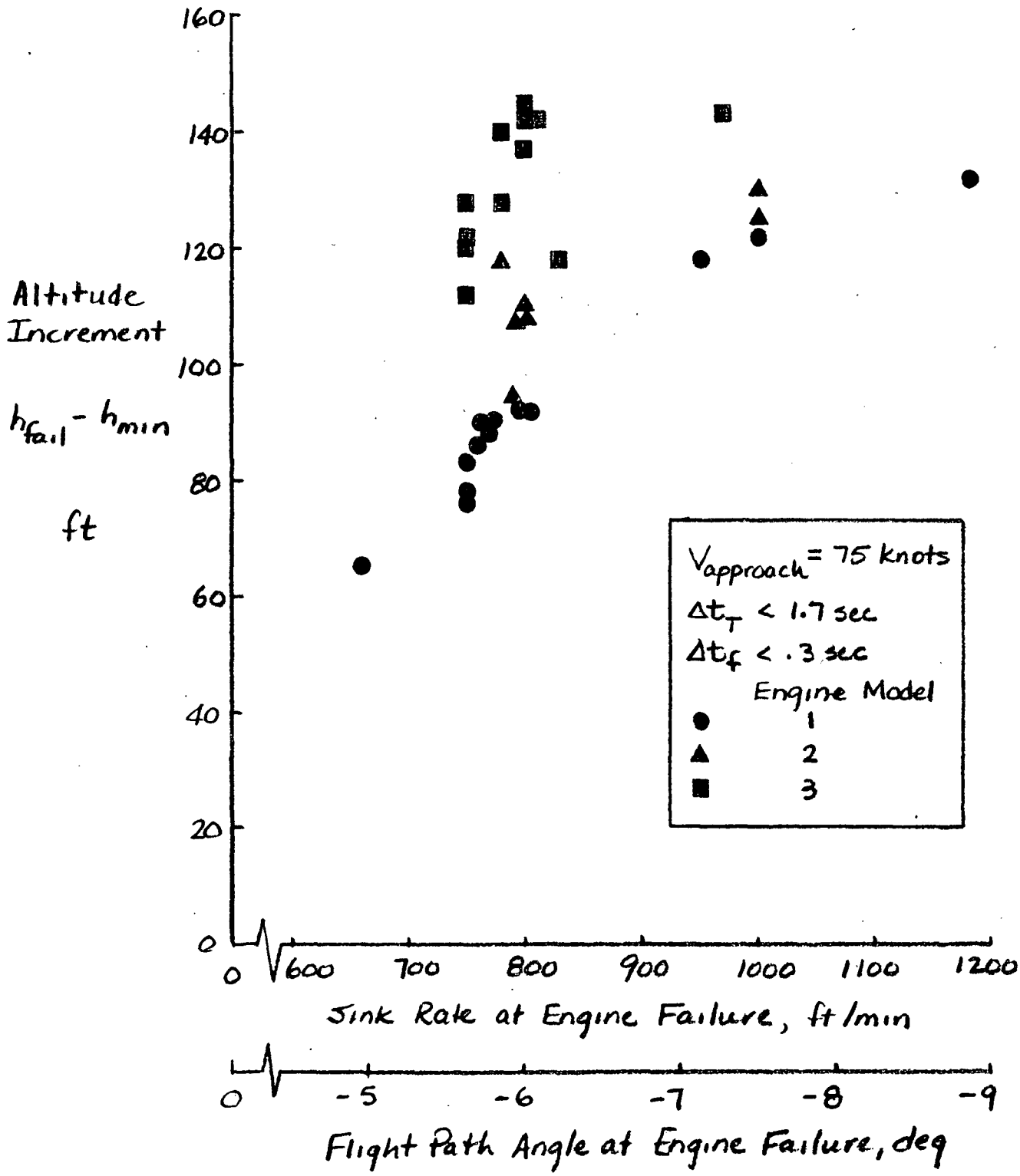

Figure 23 Engine-Out Wave-Off Performance for Variations in Engine Response and Approach Sink Rate - Selected Data

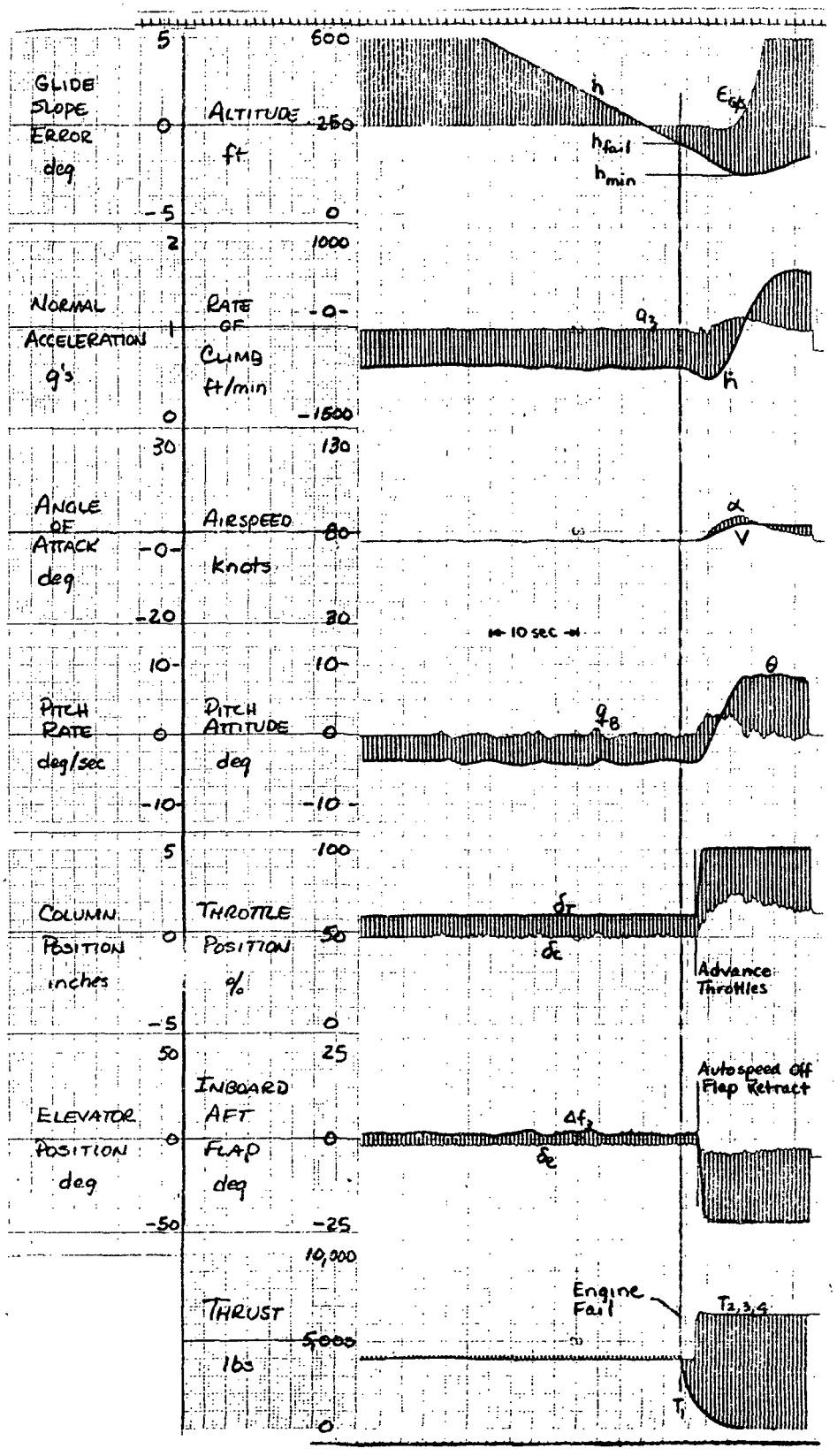

Figure 24 Time History of an Engine-Out Wave-Off - Fast Engine Response

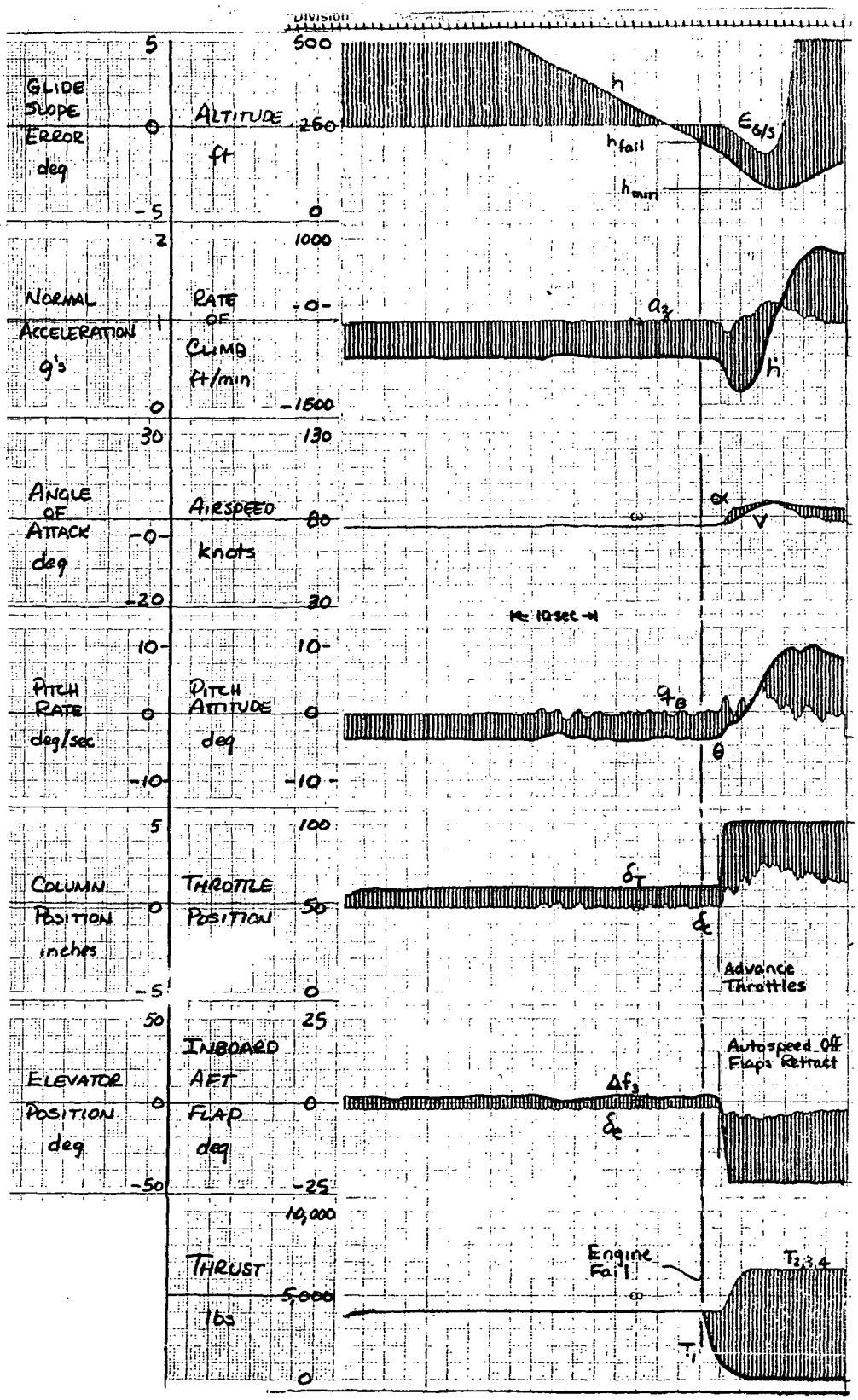

Figure 25 Time History of an Engine-Out Wave-Off - Slow Engine Response

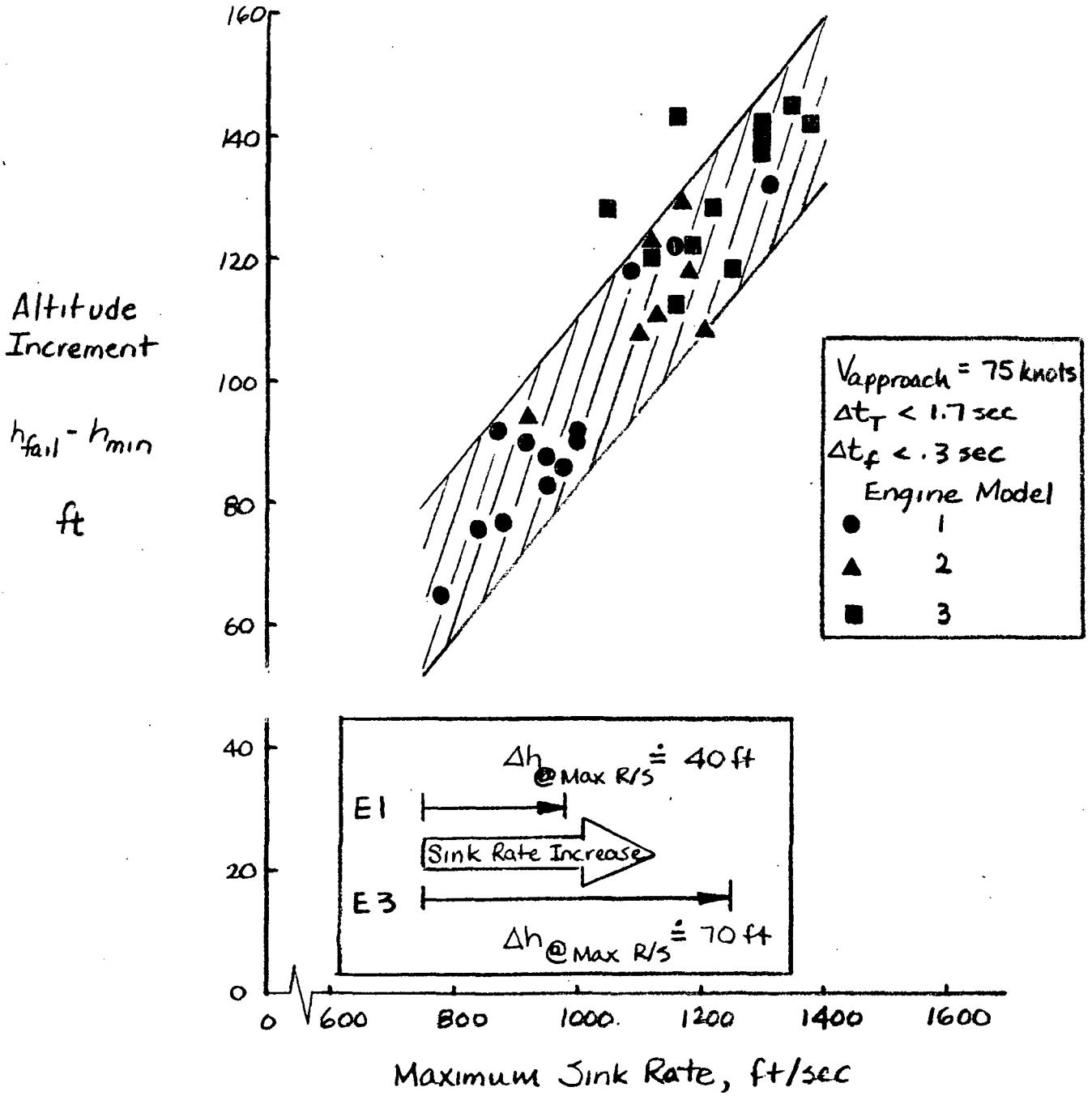

Figure 26 Trends of Engine-Out Wave-Off Performance with Maximum Sink Rate Following Engine Failure - Selected Data

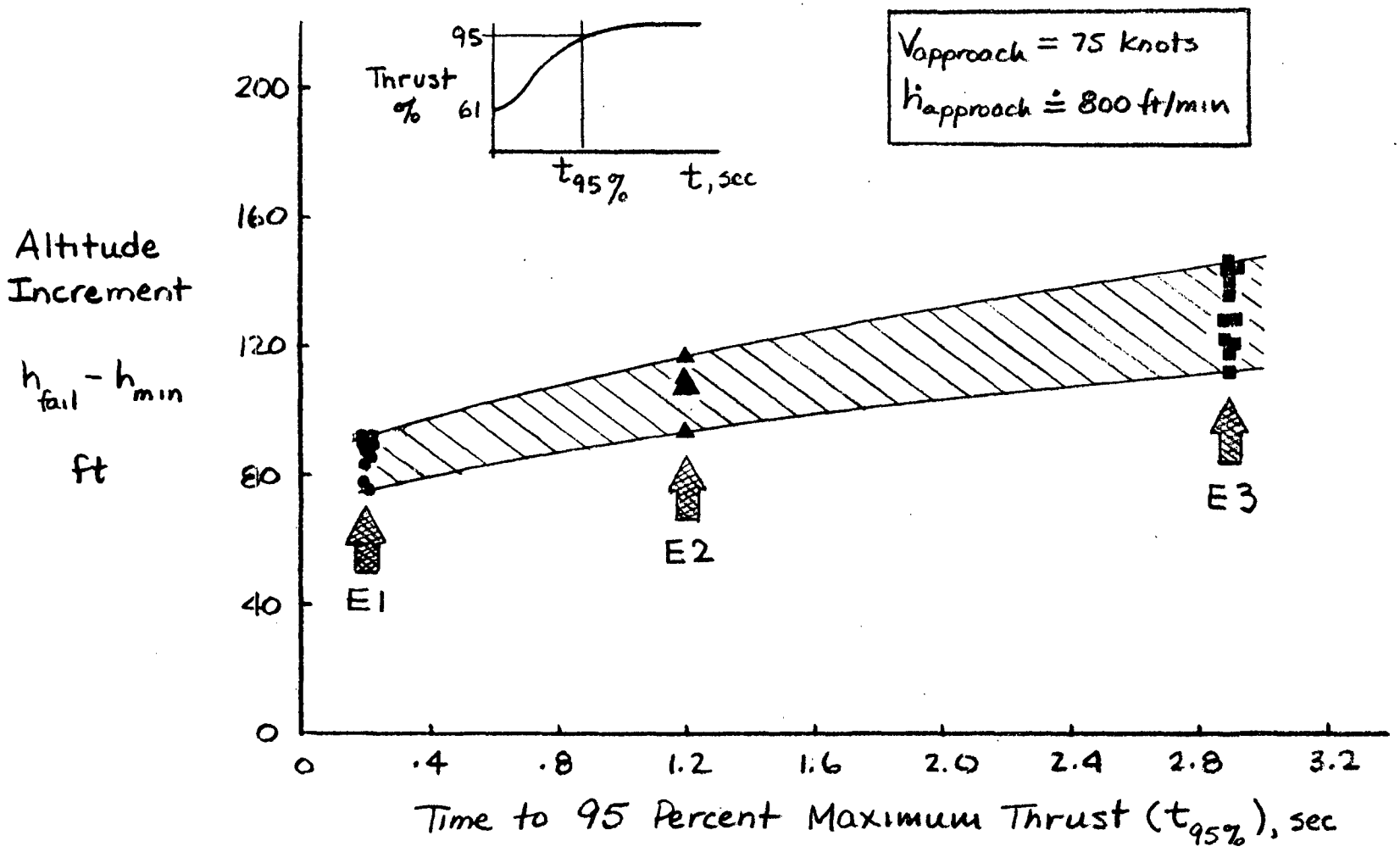

Figure 27 Trends of Engine-Out Wave-Off Performance with Time to 95 Percent Thrust - $\gamma \doteq$ -6 deg

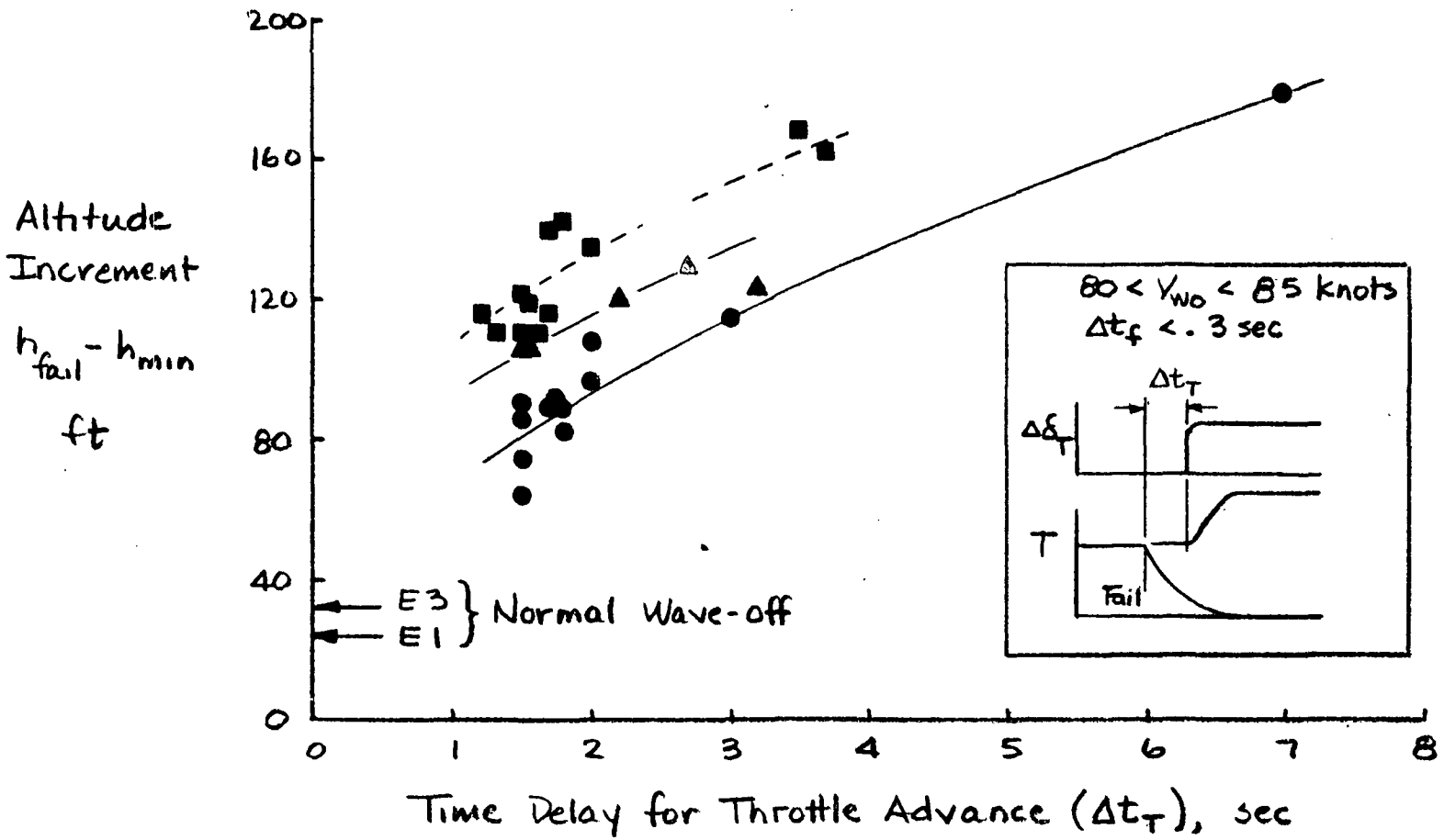

Figure 28 Effect of Delay in Throttle Advance on Engine-Out Wave-Off Performance

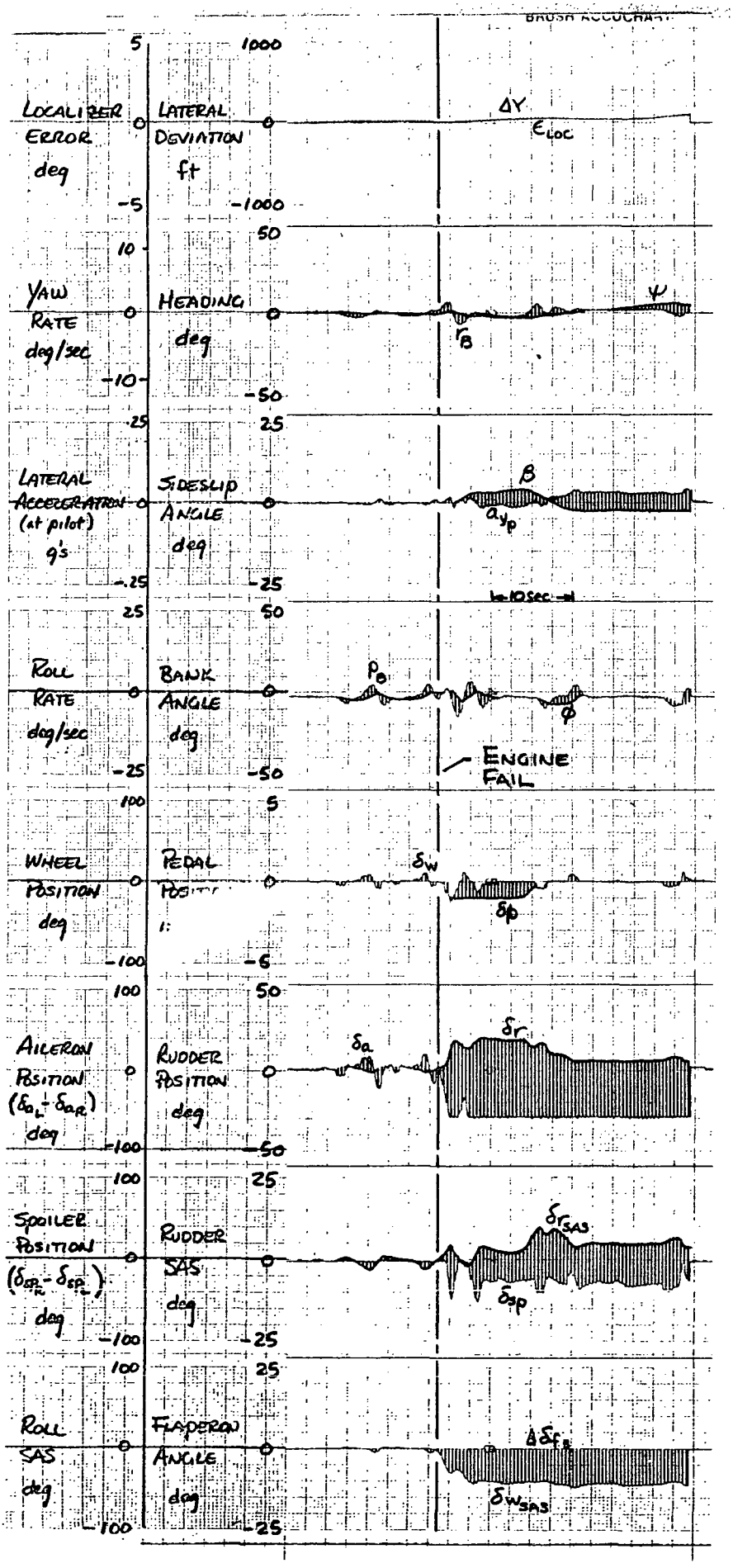

Figure 29 Lateral-Directional Response to Engine Failure - SCAS On

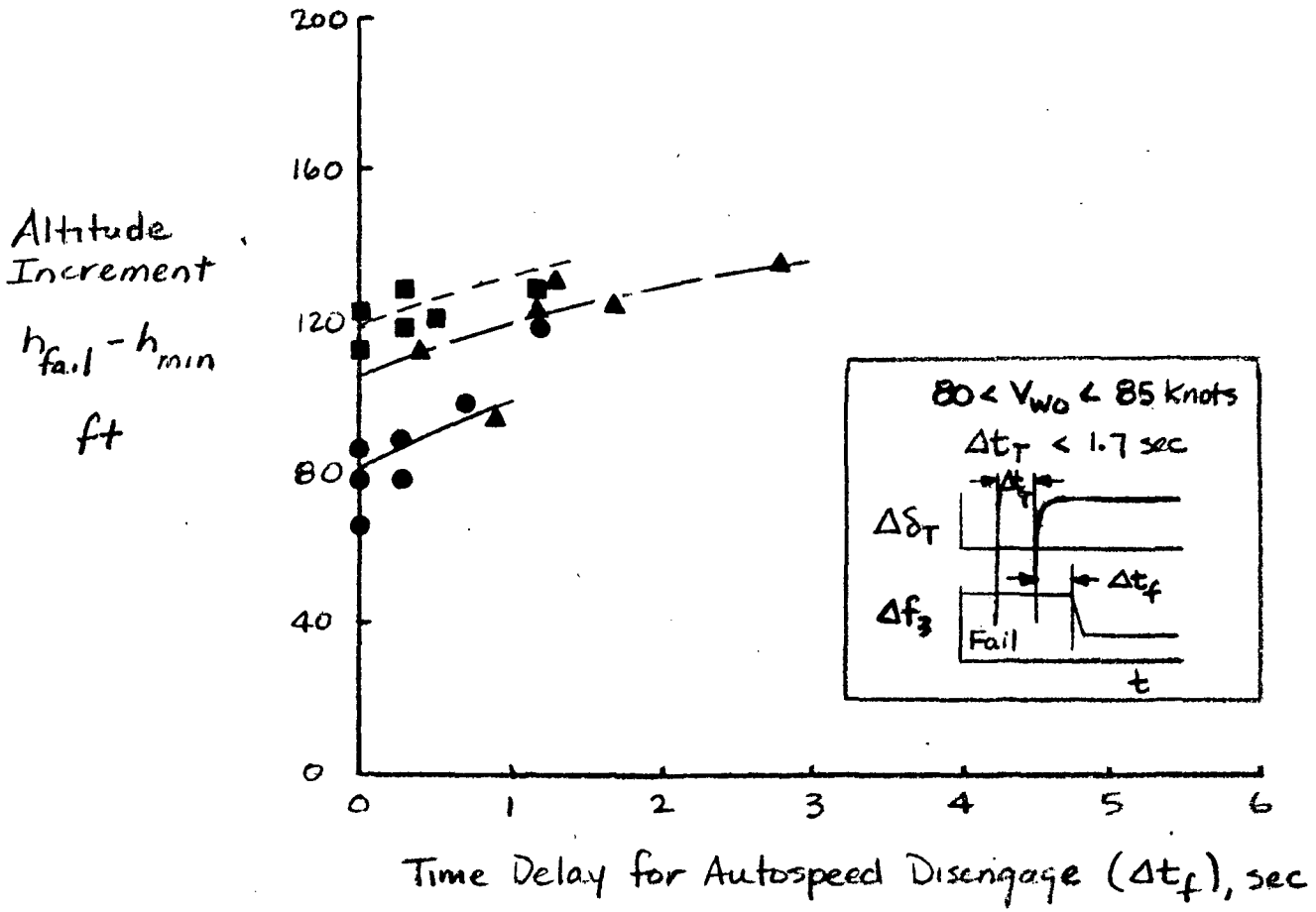

Figure 30 Effect of Delay in Autospeed Disengage on Engine-Out Wave-Off Performance

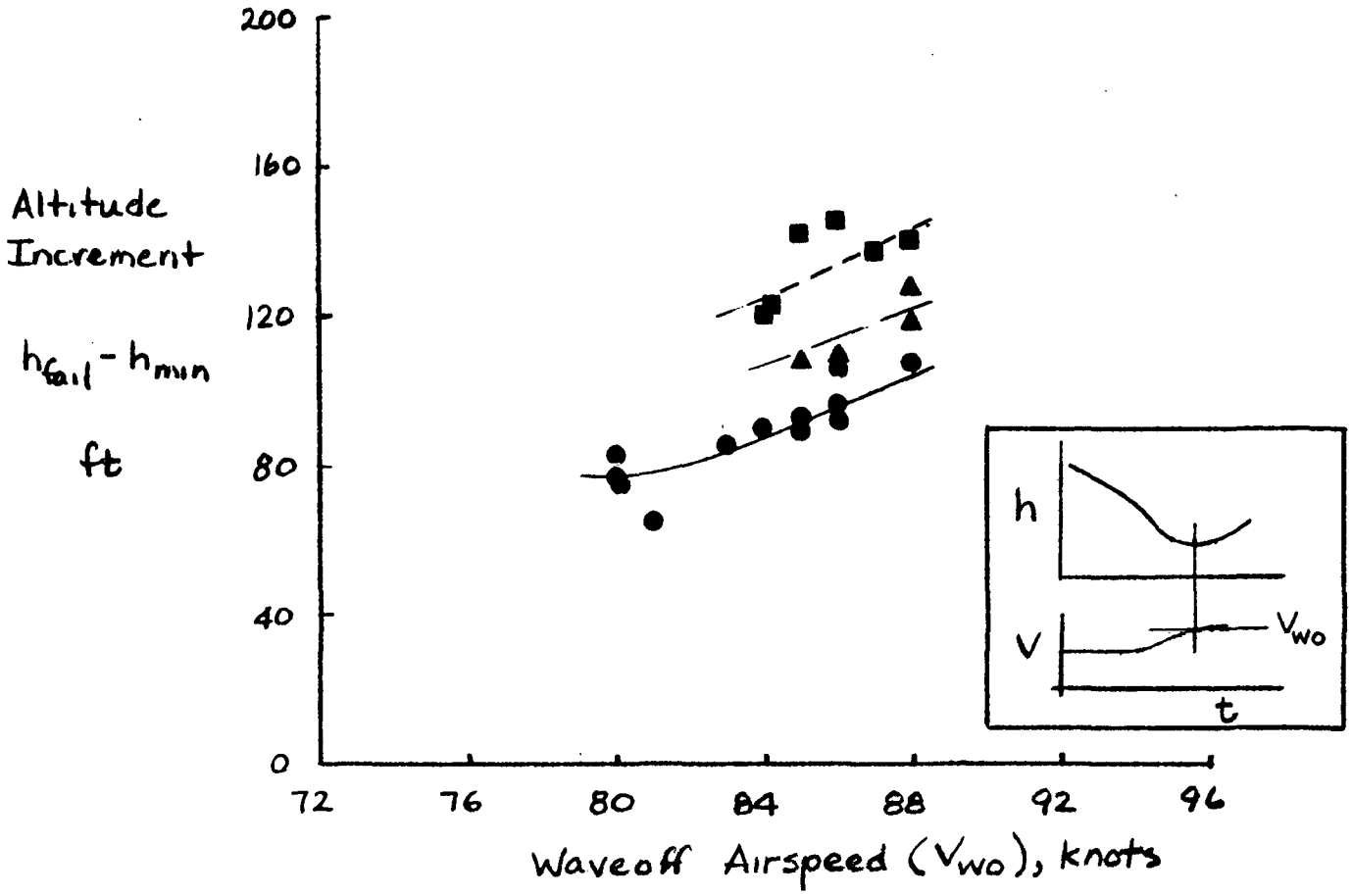

Figure 31 Effect of Wave-Off Airspeed on Engine-Out Wave-Off Performance

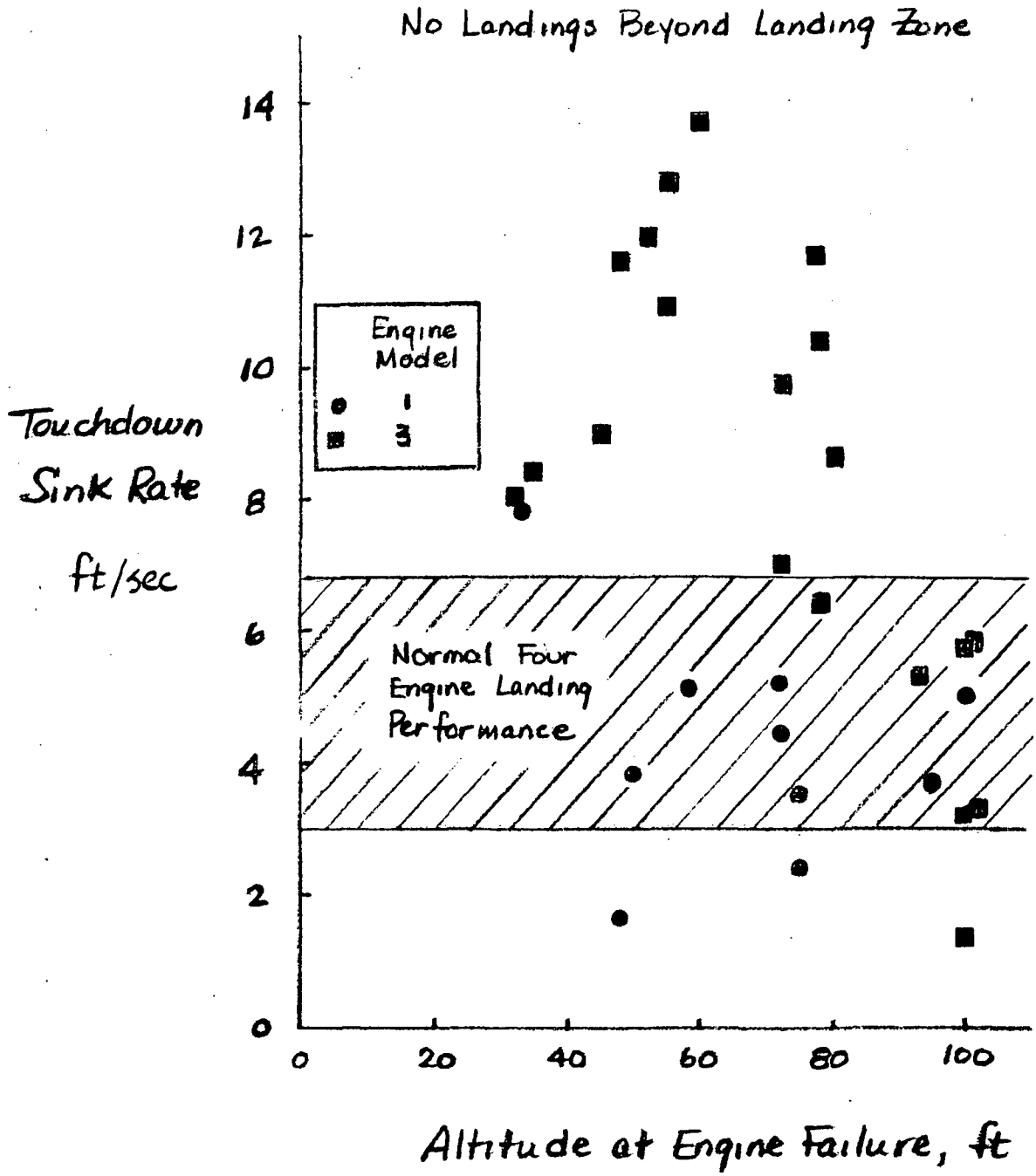

Figure 32 Selected Data for Engine-Out Touchdown Sink Rate for Variation in Altitude at Engine Failure - Fast and Slow Engine Response

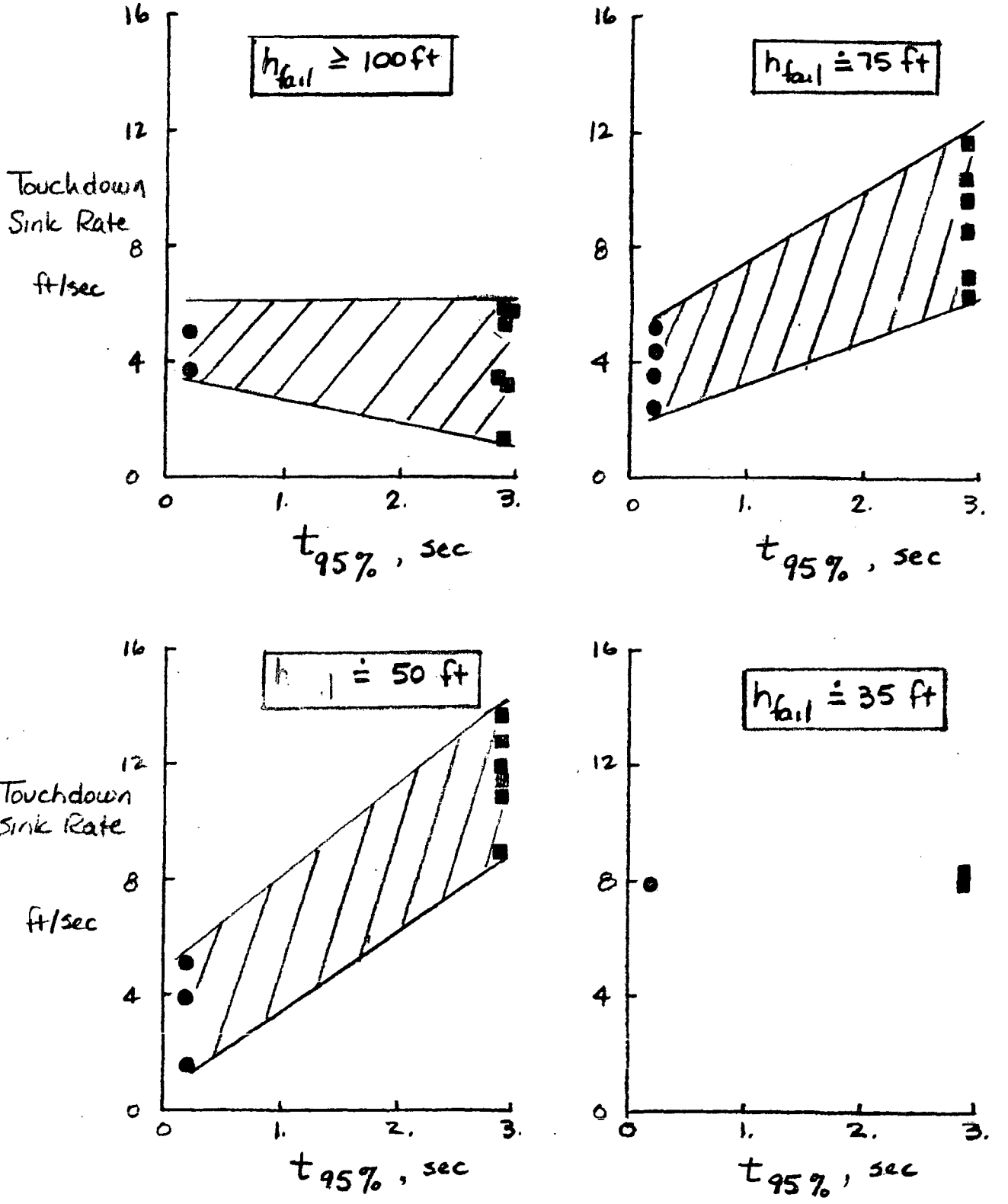

Figure 33 Trends of Engine-Out Touchdown Sink Rate with Time to 95 Percent Thrust - Various Altitudes for Engine Failure

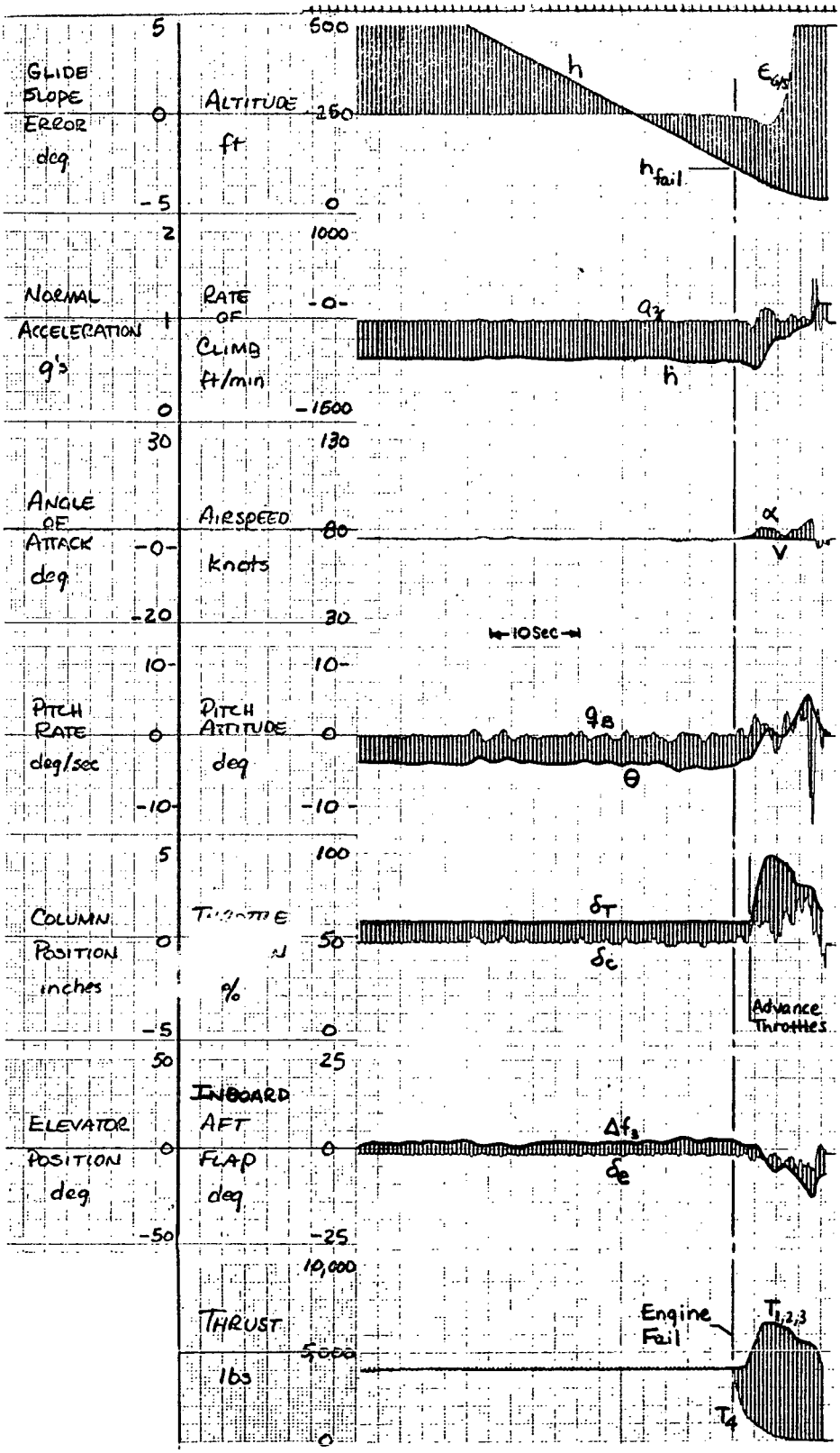

(a)

Figure 34 Typical Time History of an Engine-Out Landing for the Fast Responding Engine - Engine Failed at 100 Feet

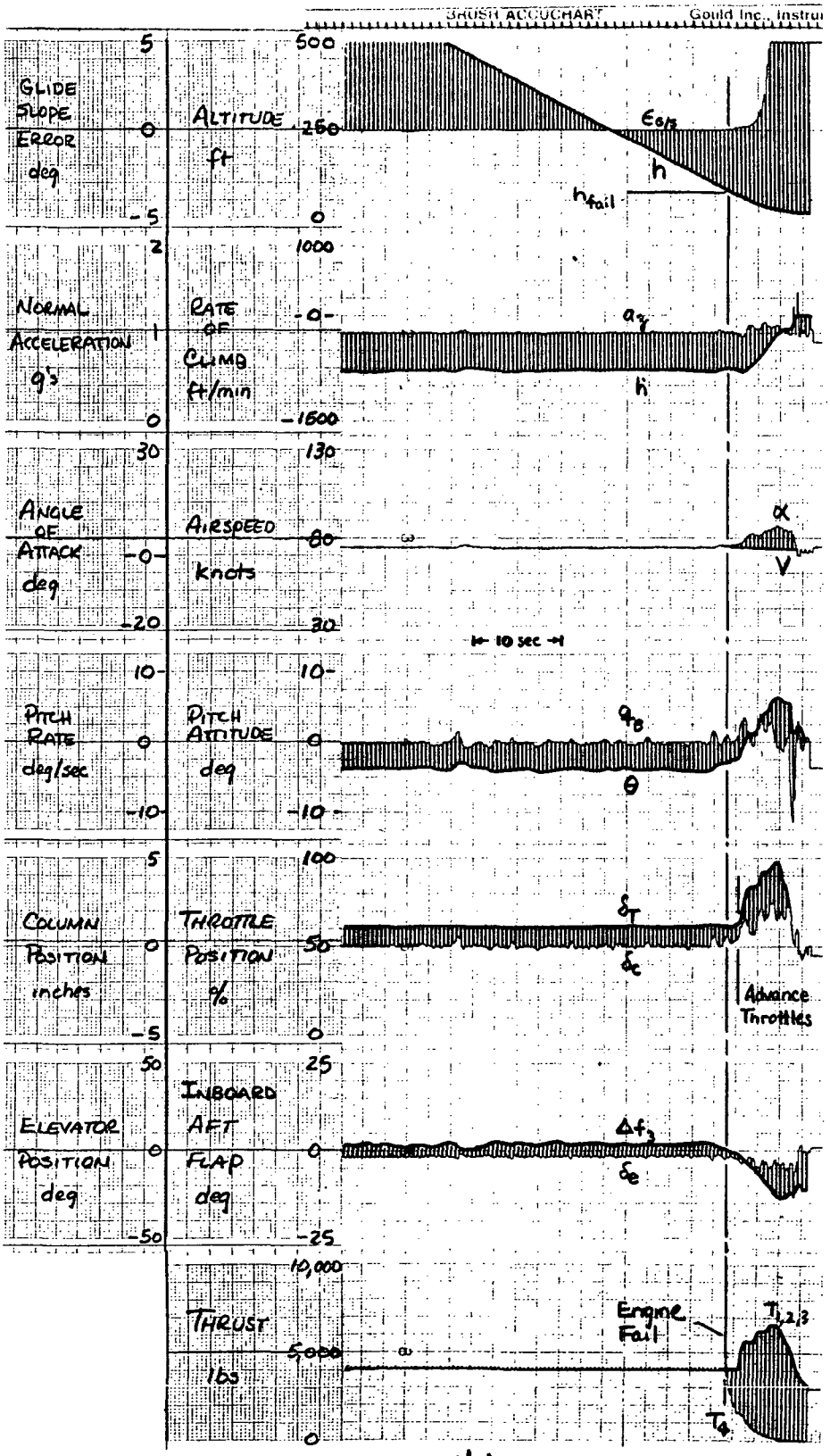

(b)

Figure 34 Continued - Engine Failed at 75 Feet

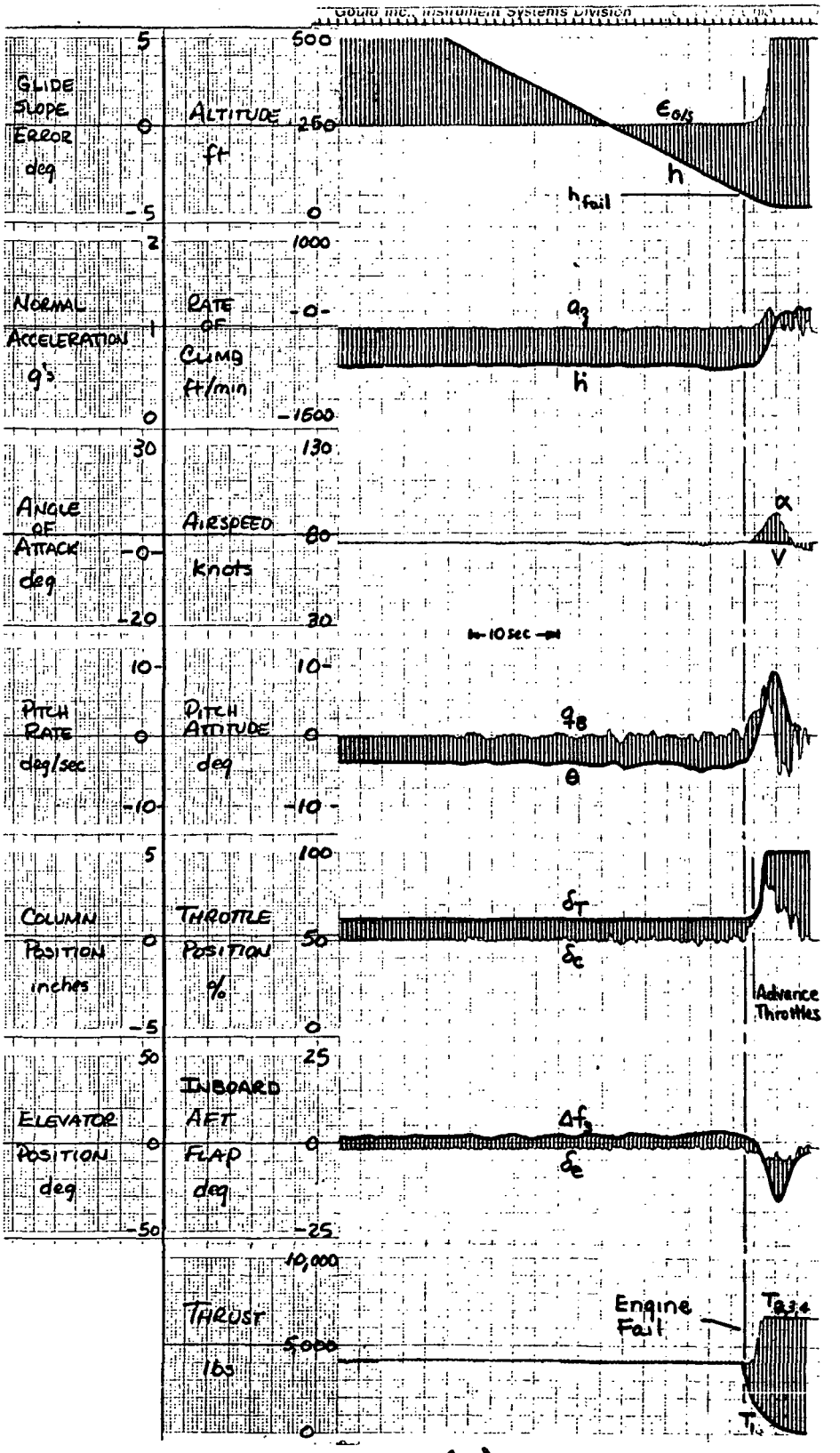

(c)

Figure 34 Continued - Engine Failed at 48 Feet

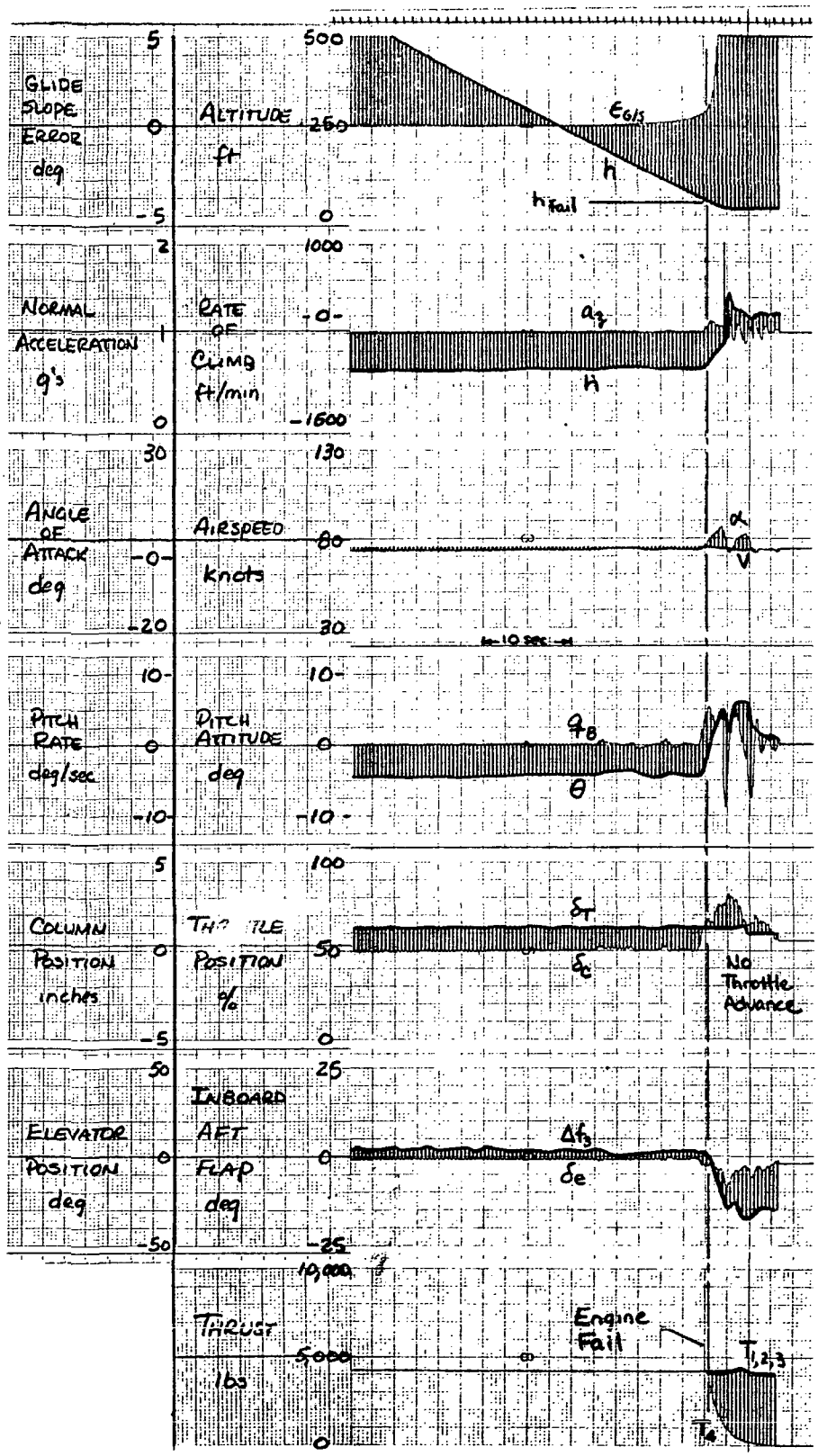

(d)

Figure 34 Continued - Engine Failed at 33 Feet

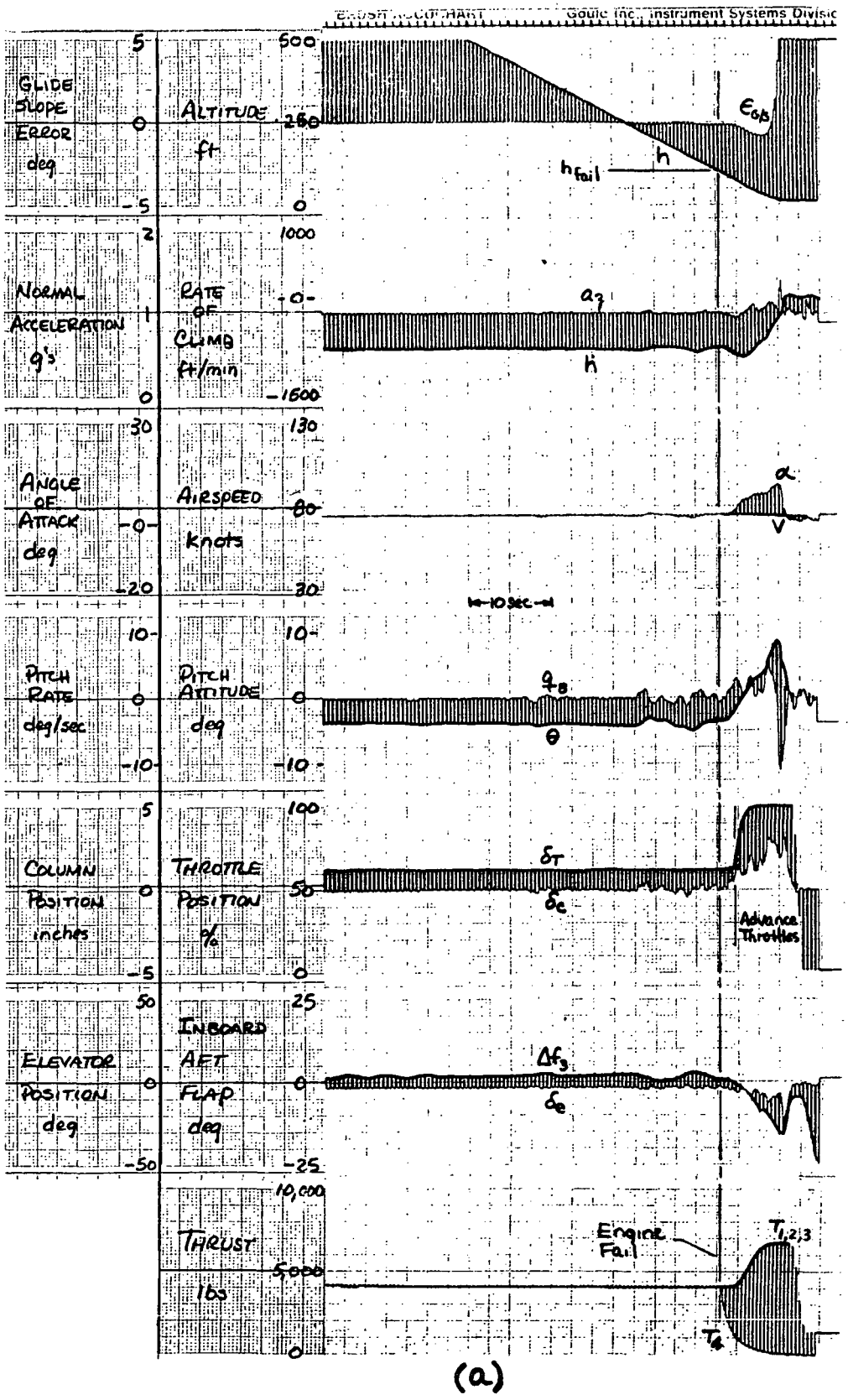

(a)

Figure 35 Typical Time History of an Engine-Out Landing for the Slow Responding Engine - Engine Failed at 100 Feet

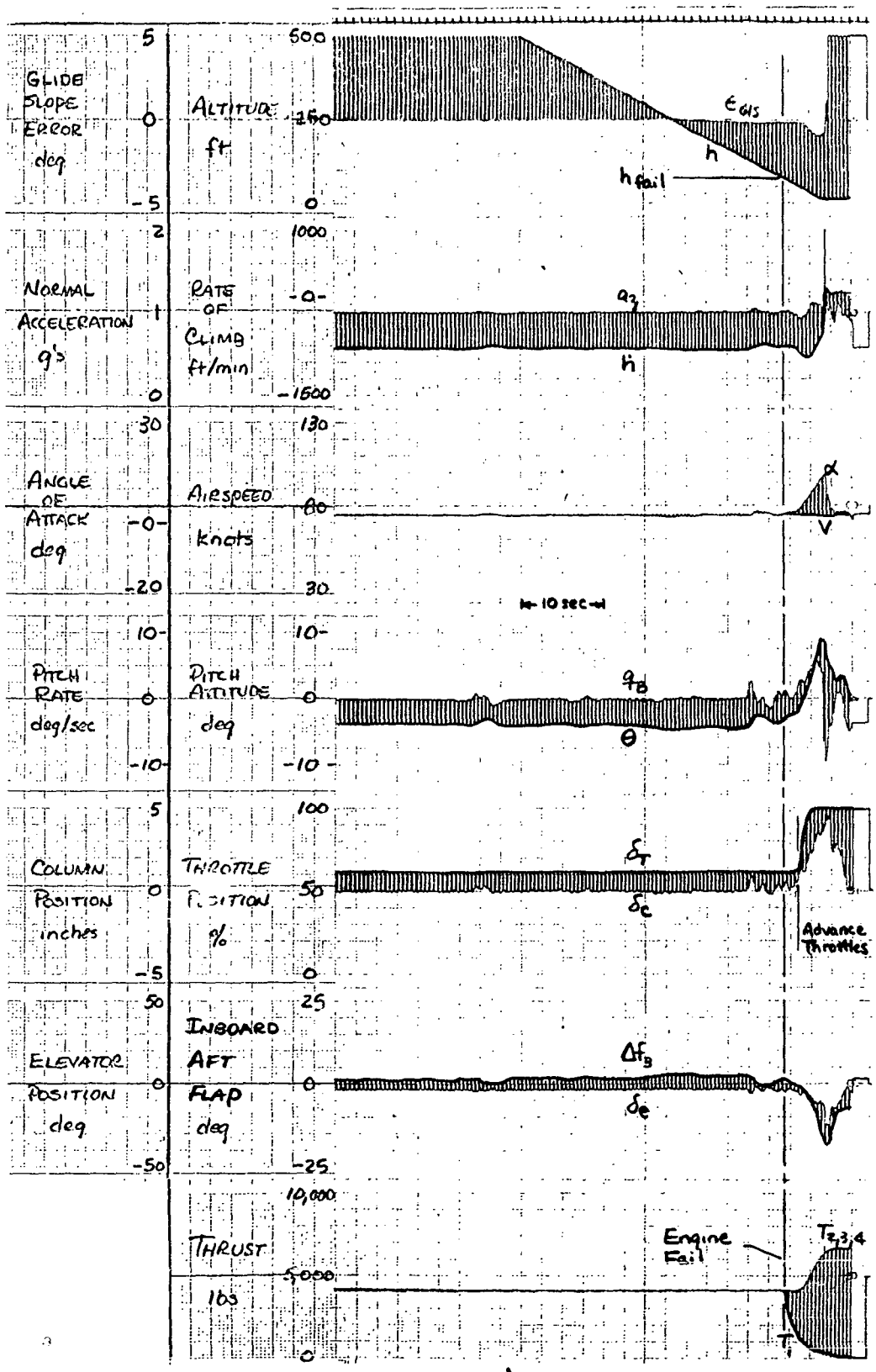

(b)

Figure 35 Continued - Engine Failed at 73 Feet

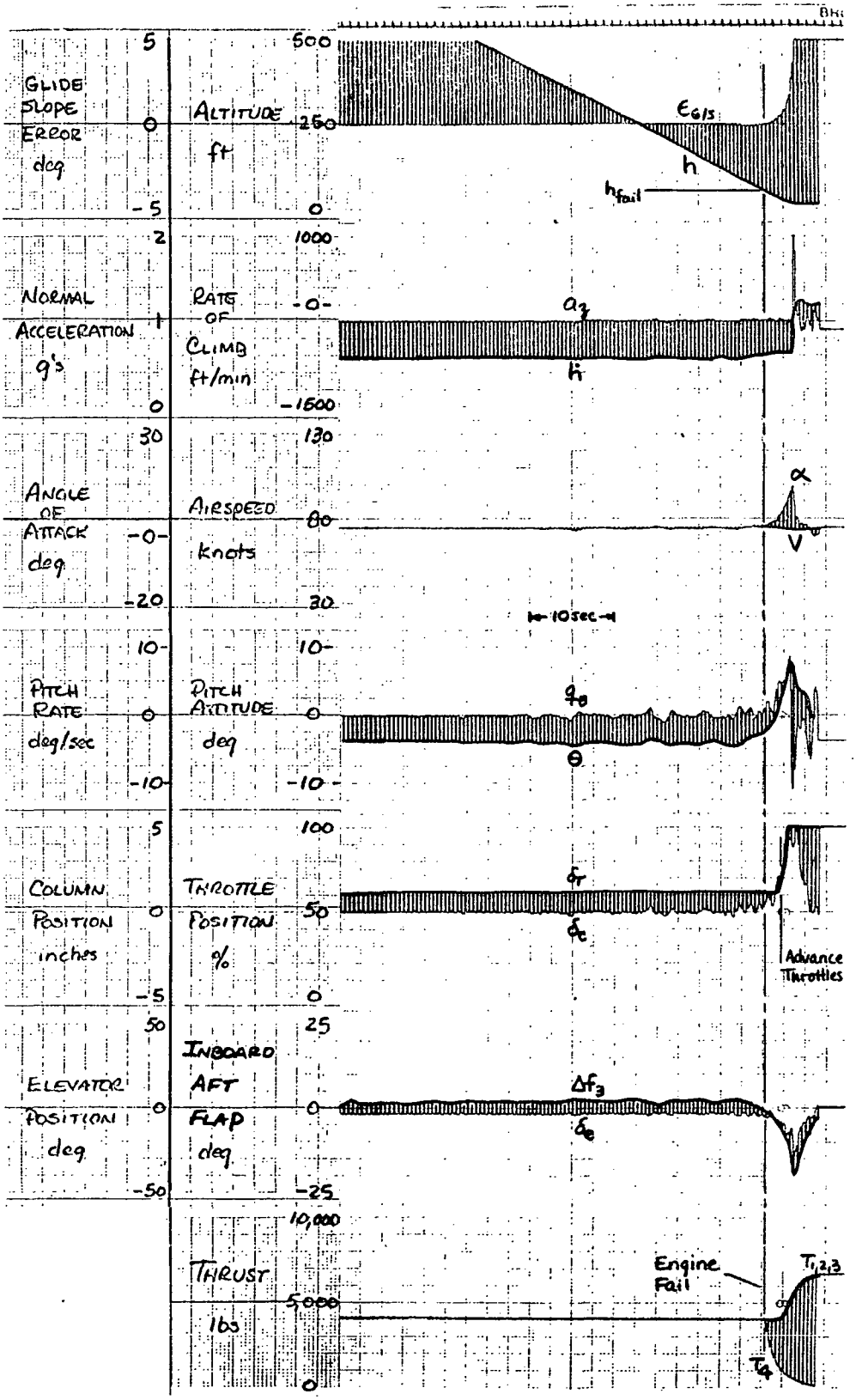

(C)

Figure 35 Continued - Engine Failed at 50 Feet

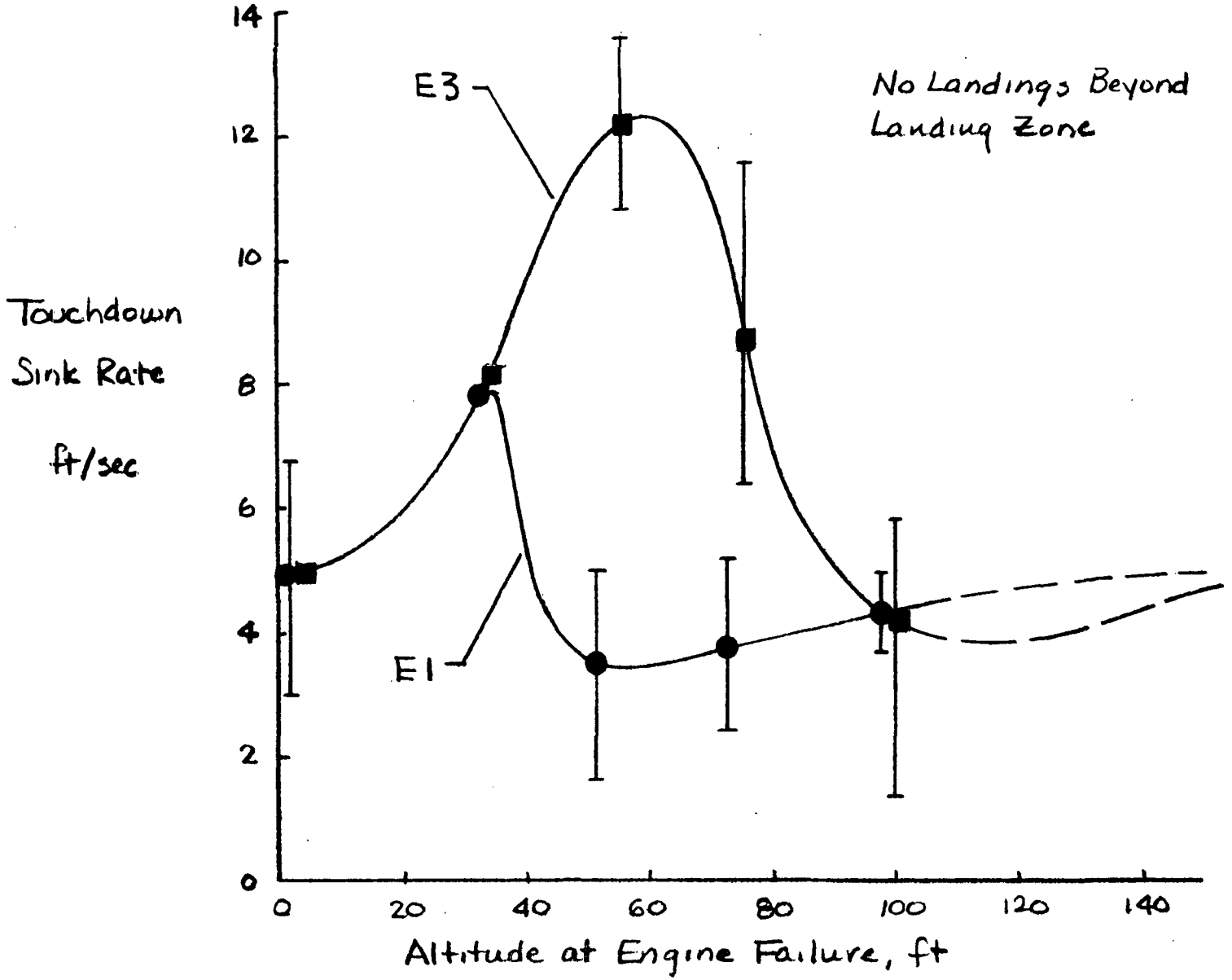

Figure 36 Trends of Engine-Out Touchdown Sink Rate with Altitude at Engine Failure for Fast and Slow Engine Response

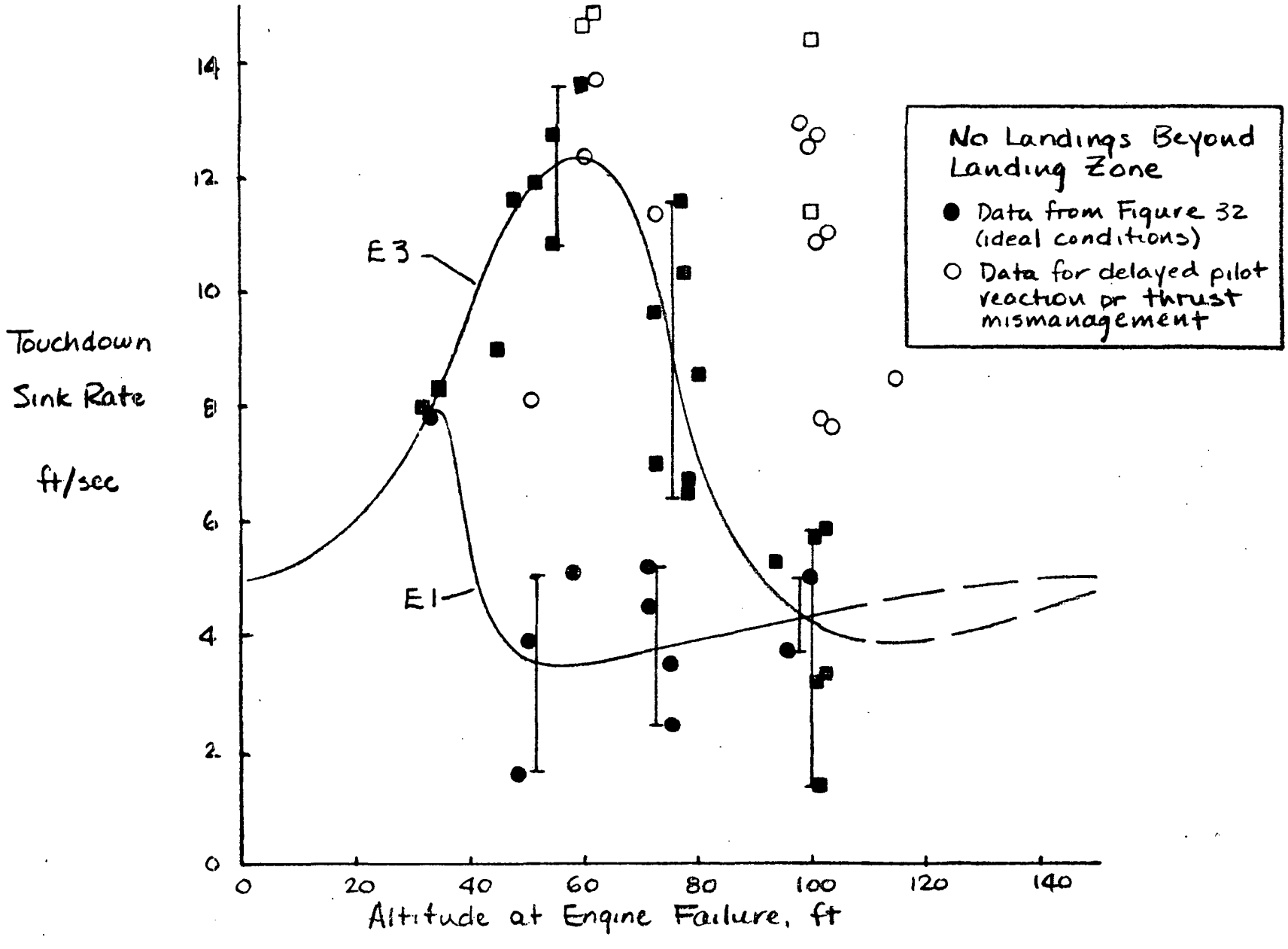

Figure 37 Collection of All Data for Engine-Out Touchdown Sink Rate for Fast and Slow Engines

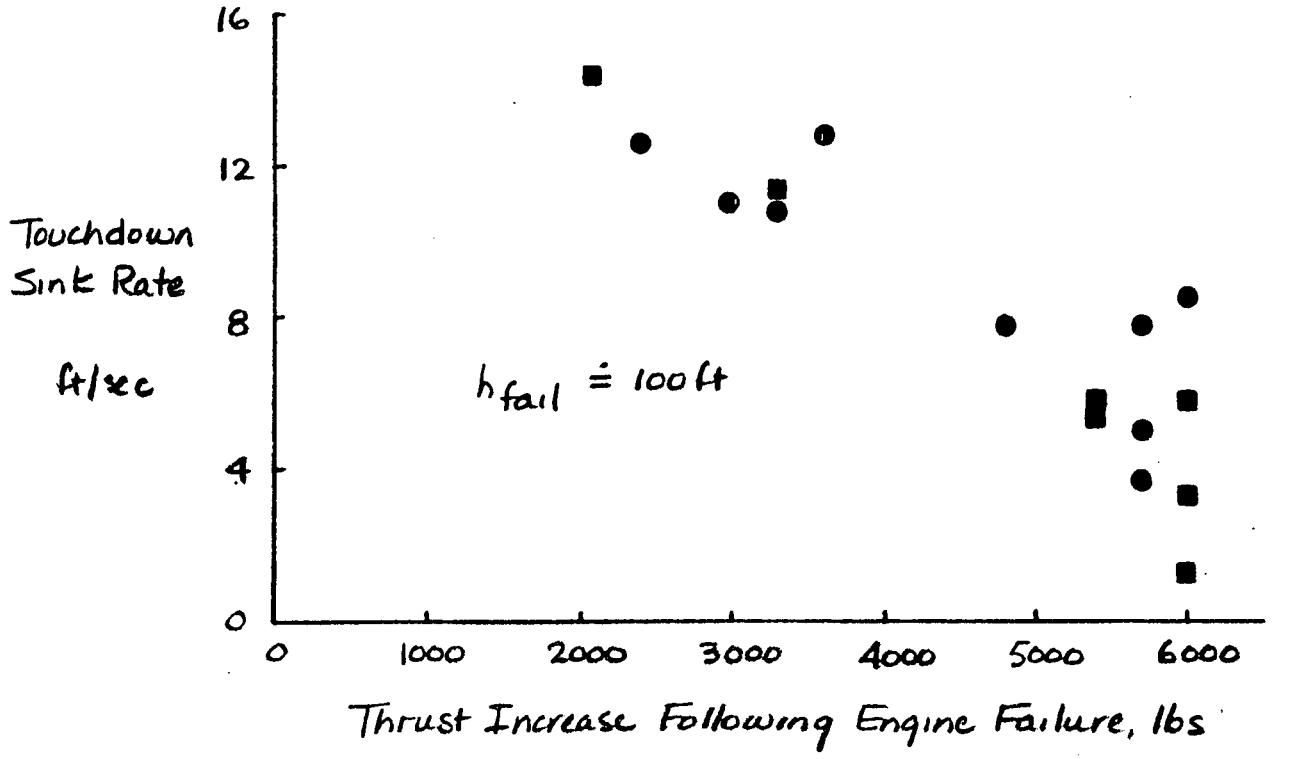

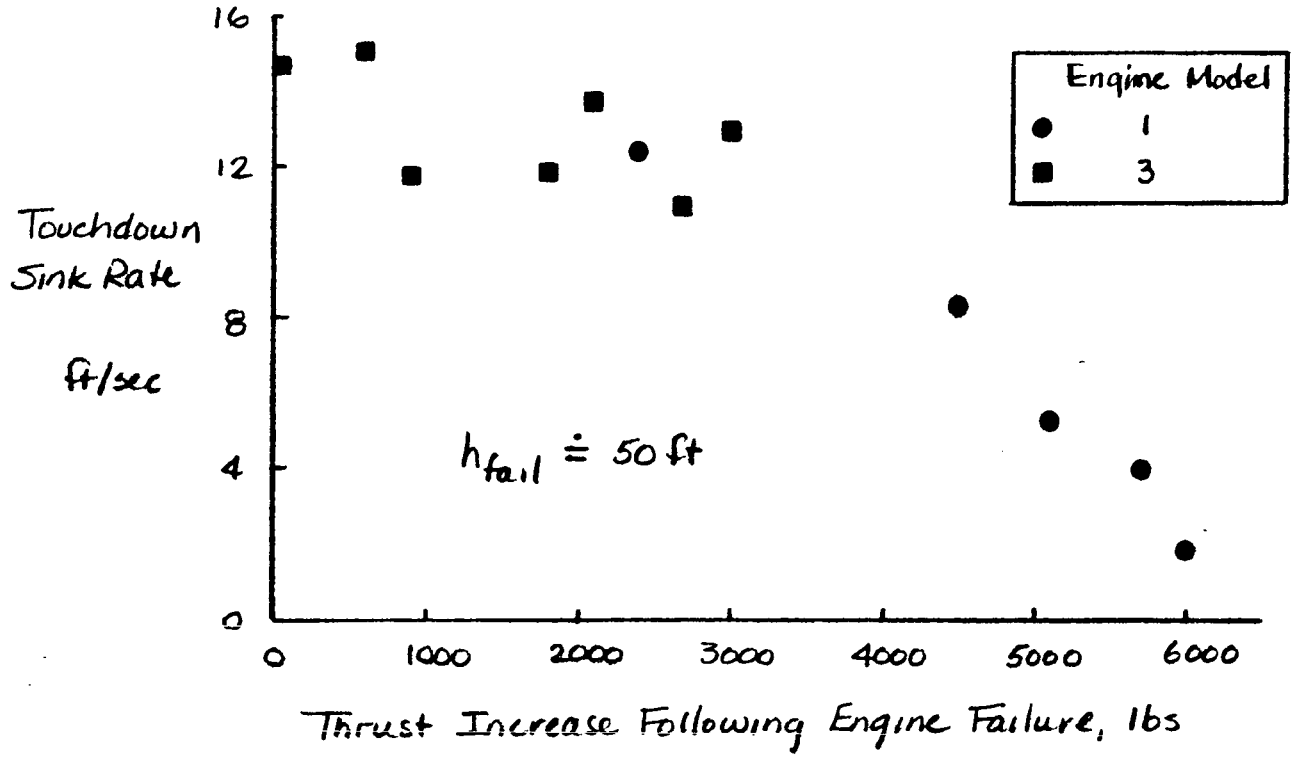

Figure 38 Trend of Engine-Out Touchdown Sink Rate with Magnitude of Thrust Increase Following Engine Failure

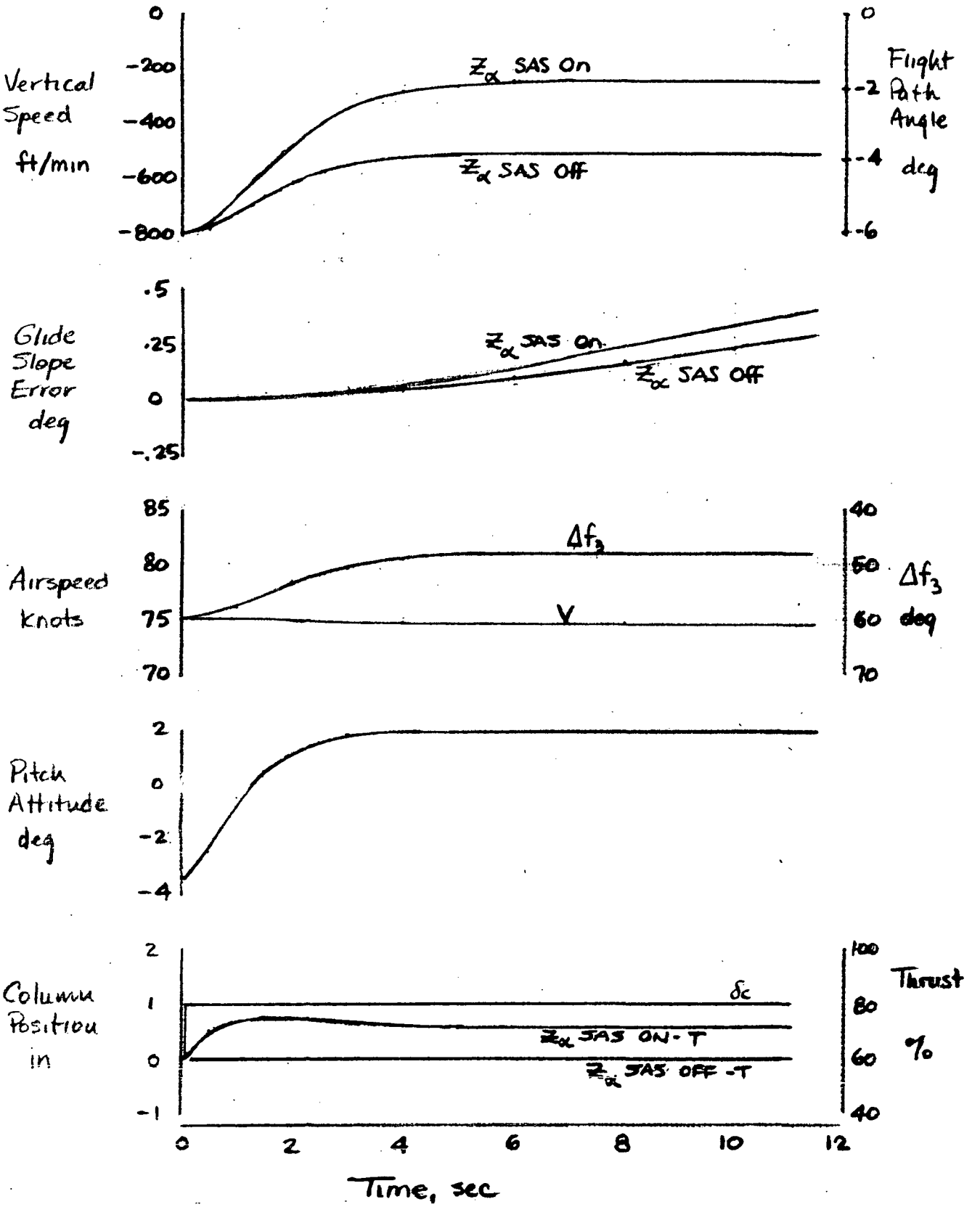

Figure 39 Comparison of Aircraft Response to a Step Column Input with and without Z_α Augmentation

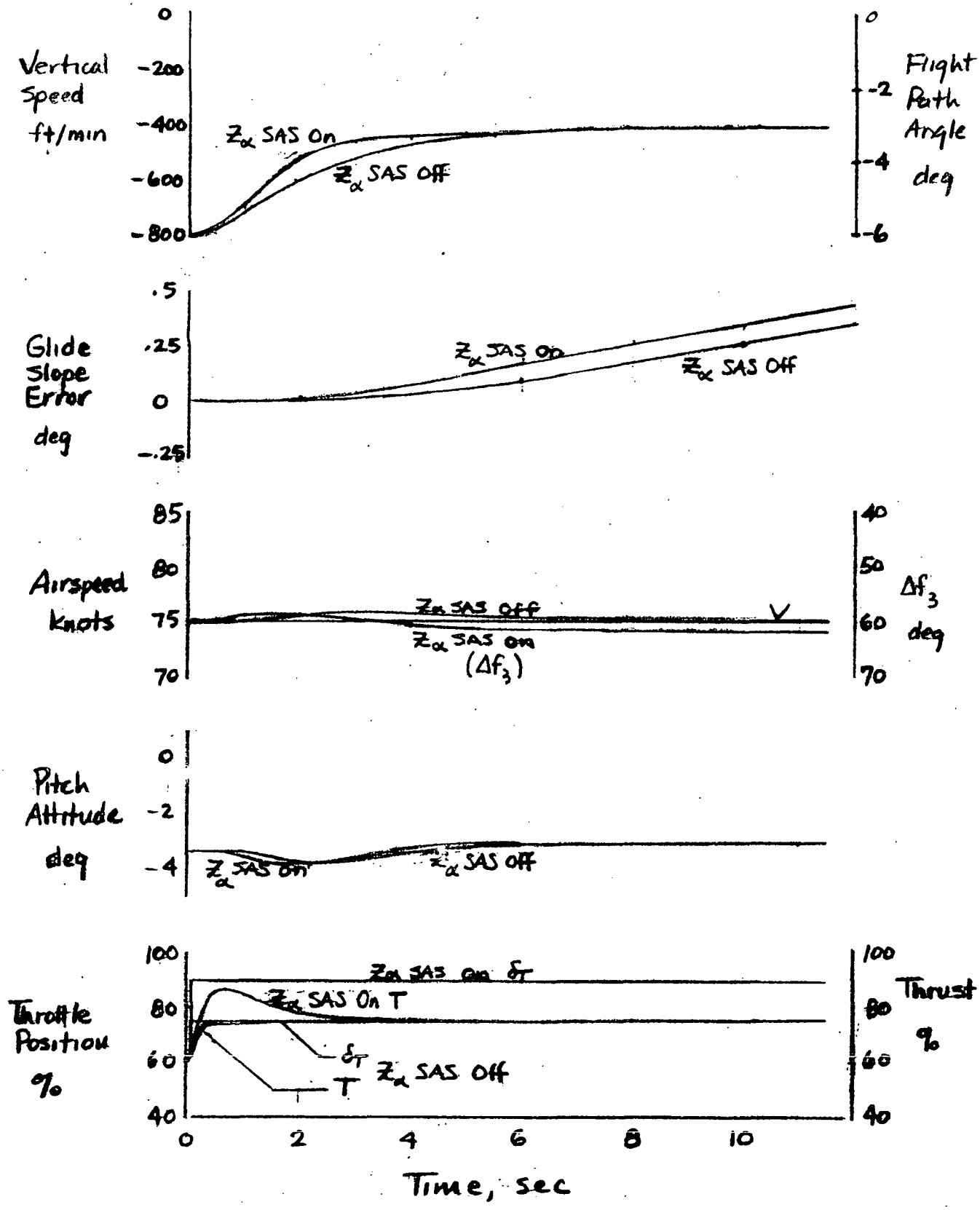

Figure 40 Comparison of Aircraft Response to a Step Throttle Input with and without Z_α Augmentation

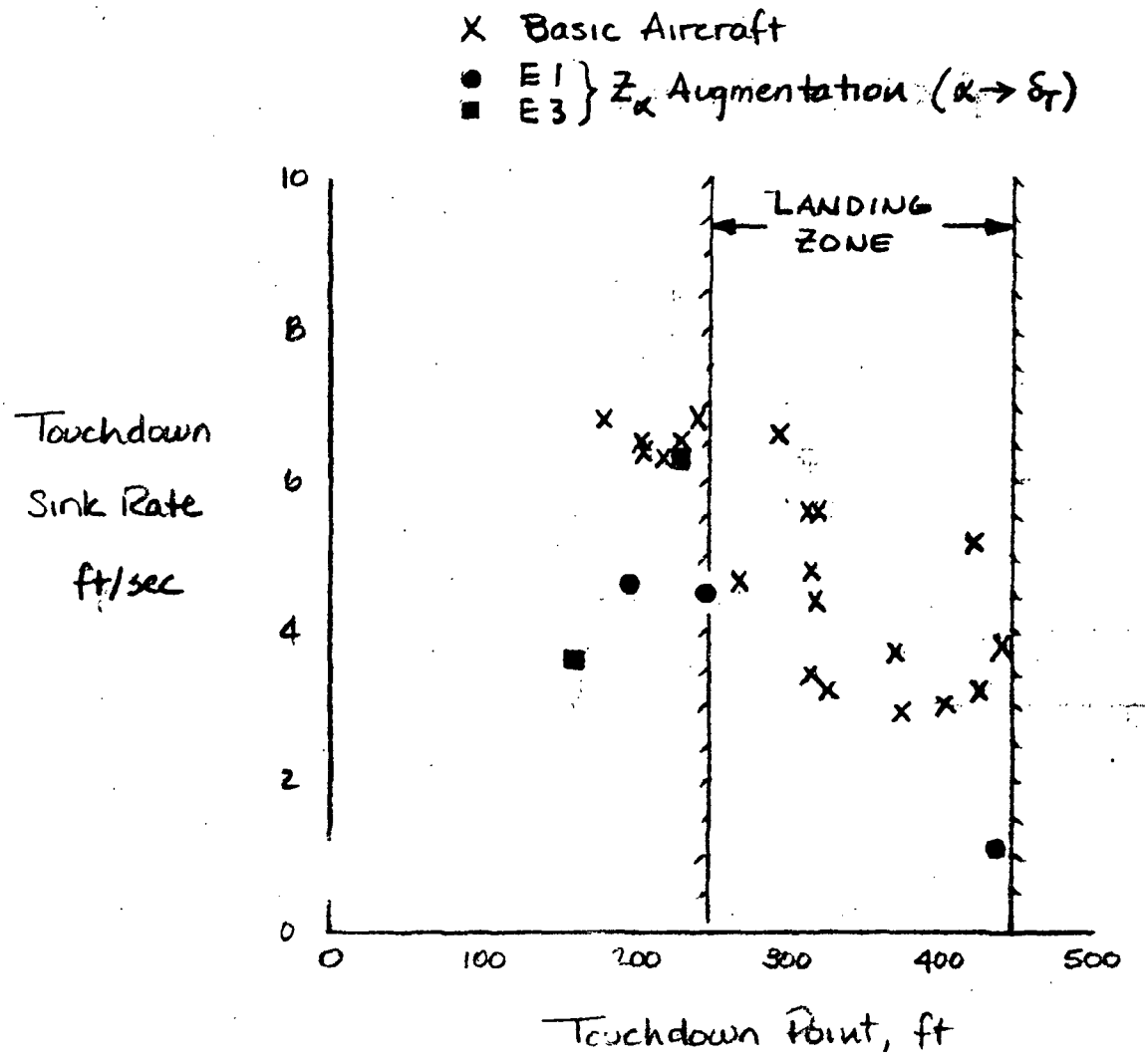

Figure 41 Comparison of Landing Precision of Basic Aircraft with Z_α Augmentation Configuration

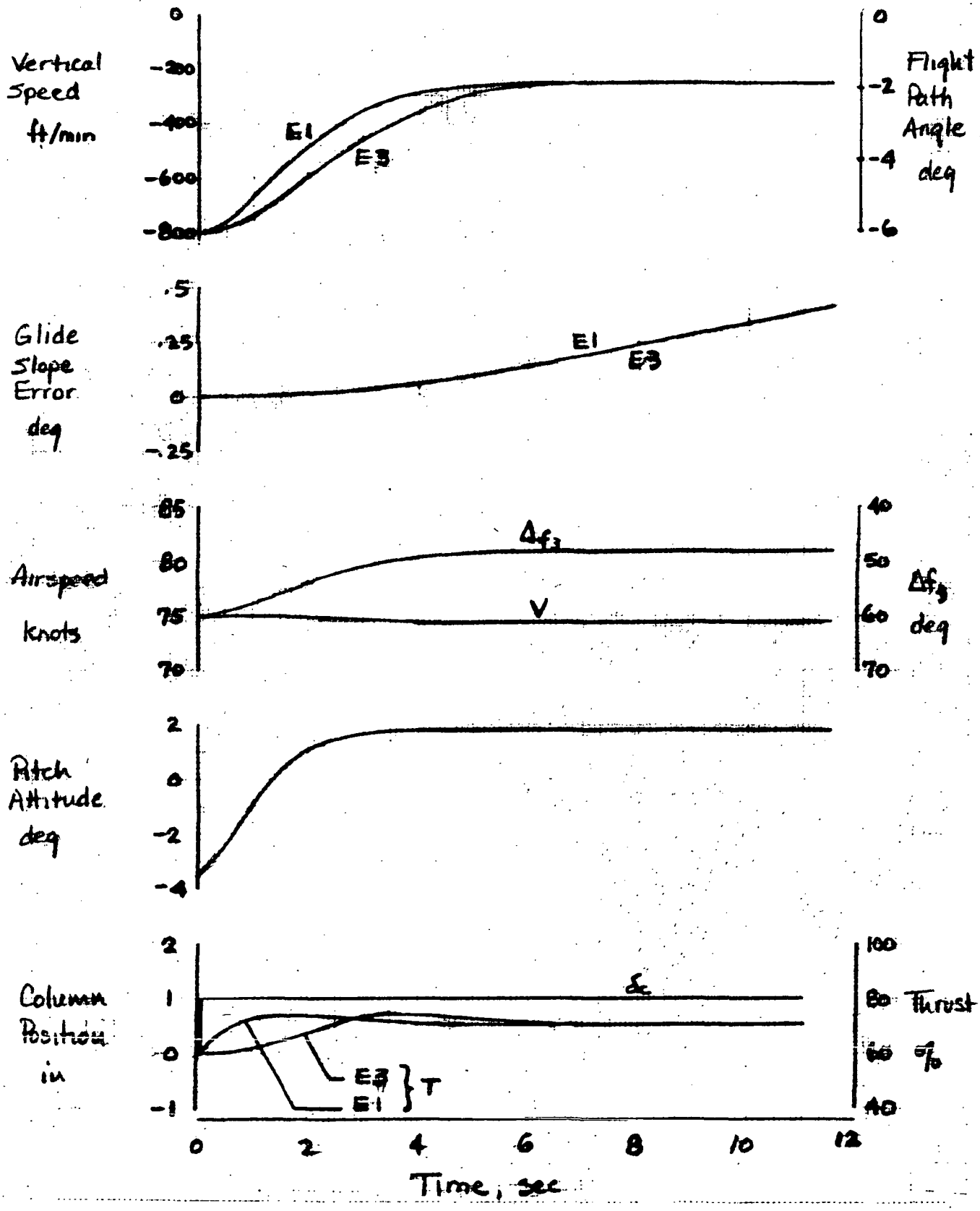

Figure 42 Comparison of Aircraft Response to a Step Column Input for Fast and Slow Engine Response - Z_α Augmentation On